

**DEVELOPMENT OF NOVEL NANOPARTICLE BASED  
PLK1, EGFR, AND PD-L1 TARGETED THERAPIES  
FOR LUNG CANCER**

By

Moataz Reda

A DISSERTATION

Presented to the Department of Biomedical Engineering  
and the Oregon Health & Science University School of Medicine  
in partial fulfillment of the requirements for the degree of

Doctor of Philosophy

June 2019

School of Medicine  
Oregon Health & Science University

---

CERTIFICATE OF APPROVAL

---

This is to certify that the PhD Dissertation of

Moataz Reda

has been approved

---

Mentor/ Wassana Yantasee, PhD, MBA

---

Committee Chair/ Monica Hinds, PhD

---

Committee Member/ Sudarshan Anand, PhD

---

Committee Member/ Joe Gray, PhD

---

Committee Member/ Jerry Jaboin, MD, PhD

# Table of Contents

List of Figures.....	v
List of Tables.....	vi
List of Abbreviations.....	vii
Acknowledgements.....	xi
Abstract.....	xiii
<b>Chapter 1: Introduction and Background .....</b>	<b>1</b>
<b>1.1 Medical needs for lung cancer treatment.....</b>	<b>1</b>
<b>1.2 Overview of radiation therapy and radiation sensitizers .....</b>	<b>3</b>
<b>1.3 Overview of immunotherapy .....</b>	<b>14</b>
<b>1.4 PLK1: a strong therapeutic target in cancer treatment.....</b>	<b>20</b>
<b>1.5 Nanoparticles in cancer treatment.....</b>	<b>26</b>
1.5.1 Nanoparticles as radiation sensitizers .....	27
1.5.2 Nanoparticles for immunotherapy .....	30
1.5.3 Translation of nanoparticle delivery platforms for cancer.....	33
<b>1.6 Novel mesoporous silica nanoparticles for cancer.....</b>	<b>34</b>
<b>Chapter 2: PLK1 and EGFR targeted nanoparticle as a radiation sensitizer for non-small cell lung cancer.....</b>	<b>37</b>
<b>2.1 Introduction.....</b>	<b>37</b>
<b>2.2 Material and Methods.....</b>	<b>39</b>
2.2.1 Nanoparticle synthesis and characterization.....	39
2.2.2 Cell culture and reagents.....	40
2.2.3 Nanoparticle cellular internalization.....	41
2.2.4 Western blot.....	41
2.2.5 RNA isolation and RT-PCR.....	42
2.2.6 Cell cycle arrest.....	42
2.2.7 Cell viability.....	43
2.2.8 Clonogenic survival.....	43
2.2.9 $\gamma$ H2ax staining.....	44
2.2.10 Apoptosis.....	44
2.2.11 Animal Studies.....	45
2.2.12 Statistical analysis.....	46
<b>2.3 Results.....</b>	<b>46</b>

2.3.1 Nanoparticle characteristics.....	46
2.3.2 Cetuximab conjugated nanoparticles are internalized in EGFR+ cells.....	51
2.3.3 Efficacy of PLK1 knockdown with C-siPLK1-NP.....	53
2.3.4 C-siPLK1-NP enhances radiation damage <i>in vitro</i> .....	55
2.3.5 C-siPLK1-NP enhances radiation sensitivity <i>in vivo</i> .....	59
2.3.6 Efficacy of C-siPLK1-NP in orthotopic lung tumor model.....	61
<b>2.4 Discussion.....</b>	<b>63</b>
<b>Chapter 3: Combination of PLK1 inhibition and PD-L1 blockade for treatment of lung cancer.....</b>	<b>67</b>
<b>3.1 Introduction.....</b>	<b>67</b>
<b>3.2 Material and Methods.....</b>	<b>69</b>
3.2.1 Cell lines and reagents.....	69
3.2.2 Nanoparticle synthesis and characterization.....	69
3.2.3 Flow cytometry.....	70
3.2.4 Cell viability after treatments.....	71
3.2.5 RT-qPCR to assess PLK1 gene knock down.....	71
3.2.6 Syngenic tumor models and treatments.....	71
3.2.7 Statistical analysis.....	72
<b>3.3 Results.....</b>	<b>73</b>
3.3.1 PLK1 knock-down induces expression of PD-L1.....	73
3.3.2 Combination of PLK1 inhibition with PD-L1 blockade enhances tumor control.....	74
3.3.3 Nanoparticle delivery of PLK1 inhibitor Volasertib (iPLK1-NP).....	75
3.3.4 PD-L1 targeted nanoparticle for iPLK1 delivery (p-iPLK1-NP).....	77
3.3.5 Local delivery of p-iPLK1-NP reduces local and distant tumor growth.....	79
3.3.6 Systemic administration of p-iPLK1-NP prolongs survival of mice with experimental metastatic tumors.....	81
<b>3.4 Discussion.....</b>	<b>83</b>
<b>Chapter 4: Summary, conclusions, and future directions.....</b>	<b>86</b>
4.1 Summary and conclusions.....	86
4.2 Future directions .....	89
<b>References.....</b>	<b>94</b>

## List of Figures

Figure 1.1 Increasing therapeutic window of radiation. ....	7
Figure 1.2 PLK1's role with cancer regulators.....	21
Figure 2.1. EGFR-targeted (cetuximab) mesoporous silica nanoparticle (NP) platform for PLK1 siRNA (siPLK1) delivery or C-siPLK1-NP.....	48
Figure 2.2. Reproducibility of nanoparticle synthesis.....	50
Figure 2.3. Specific cellular uptake of C-siRNA-NP to EGFR+ cells.....	52
Figure 2.4. Effects of C-siPLK1-NP treatment on NSCLC (A549, H460) cell lines.....	54
Figure 2.5. NP dose response and cell cycle arrest.....	55
Figure 2.6. C-siPLK1-NP sensitizes A549 lung cancer cells to radiation.....	57
Figure 2.7. C-siPLK1-NP sensitizes H460 NSCLC cells to radiation.....	58
Figure 2.8. C-siPLK1-NP enhances radiation effects <i>in vivo</i> .....	60
Figure 2.9. C-siPLK1-NP reduces orthotopic lung tumor growth.....	62
Figure 3.1. PLK1 siRNA knock-down induces PD-L1 expression.....	73
Figure 3.2. PD-L1 blockade potentiates the effect of PLK1 inhibition in syngenic lung tumors...74	
Figure 3.3. Nanoparticle delivery of PLK1 inhibitor volasertib (iPLK1-NP).....	76
Figure 3.4. PD-L1 targeted nanoparticle for iPLK1 delivery (p-iPLK1-NP).....	78
Figure 3.5. p-iPLK1-NP elicits anti-tumor immune effects.....	80
Figure 3.6. p-iPLK1-NP improves survival of mice bearing metastatic lung tumors.....	82
Figure 4.1. siRNA knock-down with iPLK1-NP.....	91
Figure 4.2. Adding CpG to p-iPLK1-NP enhances therapeutic benefit.....	92

## List of Tables

Table 1.1. Molecularly targeted therapies in clinical trials with radiation therapy.....	13
Table 1.2. FDA approved immunotherapies for NSCLC.....	17
Table 2.1. Characterization of C-siRNA-NP.....	48

## List of Abbreviations

5-FU	Fluorouracil
AKT	RAC-alpha serine/threonine-protein kinase
ALK	Anaplastic lymphoma kinase
ANOVA	Analysis of variance
APCs	Antigen presenting cells
APE1	DNA-(apurinic or apyrimidinic site) lyase
ATCC	American type culture collection
ATM	Ataxia telangiectasia and Rad3-related
ATR	Ataxia-telangiectasia mutated
$\beta$ -actin	Beta-actin
BCA	Bicinchoninic acid
BRCA1	Breast cancer type 1 susceptibility protein
CD3	Cluster of differentiation 3
CD4	Cluster of differentiation 4
CD8	Cluster of differentiation 8
CD80	Cluster of differentiation 80
CD86	Cluster of differentiation 86
CDK4/6	Cyclin-dependent kinase 4/6
CpG	CpG oligodeoxynucleotides
CRC	Colorectal cancer
CRT	chemoradiotherapy
Cs	Cesium
CSCs	Cancer stem cells
CT	computed tomography
CTG	CellTiter-Glo
CTLA-4	Cytotoxic T-lymphocyte-associated protein 4
DAMPs	damage-associated molecular patterns
DNA	Deoxyribonucleic acid
DNA-PKcs	DNA-dependent protein kinase, catalytic subunit
DSPE	1,2-Distearoyl-sn-glycero-3-phosphoethanolamine
EGFR	epidermal growth factor receptor
EPR	enhanced permeability and retention
FBS	Fetal bovine serum
FDA	Food and drug administration
FOXM1	forkhead box M1
GBM	glioblastoma
$\gamma$ H2ax	Gamma-H2A histone family member X
GSH	Glutathione
Gy	Gray

H <sub>2</sub> O <sub>2</sub>	Hydrogen peroxide
HDAC	Histone deacetylases
HER2	Human epidermal growth factor receptor 2
HLA	Human leukocyte antigen
HNC	Head and neck cancer
HPRT	Hypoxanthine-guanine phosphoribosyltransferase
HR	Homologous recombination
hr	Hour
i.p.	Intraperitoneal
i.v.	Intravenous
IACUC	Institutional Animal Care and Use Committee
IDO	Indoleamine 2,3-dioxygenase
IFN	Interferon
IL-10	Interleukin-10
IL-6	Interleukin-6
IMRT	Intensity modulated radiation therapy
irAEs	Immune-related adverse effects
IRDye	Infrared Fluorescent Dyes
IVIS	<i>In vivo</i> imaging system
kg	Kilogram
KRAS	KRAS proto-oncogene, GTPase
LLC	Lewis Lung Carcinoma
Luc	Luciferase
MAVS	Mitochondrial antiviral signaling protein
mg	Milligram
MHC	Major histocompatibility complex
min	Minutes
μg	Micrograms
μl	Microliters
mm	Millimeter
MNS	Mediastinal nodal sterilization
mRNA	Messenger RNA
MSNP	Mesoporous silica nanoparticle
mTOR	mammalian target of rapamycin
MW	Molecular weight
MYC	MYC Proto-Oncogene
NaCl	Sodium chloride
NCI	National Cancer Institute
NHS	N-Hydroxysuccinimide
ng	nanogram
NK	Natural killer
nm	nanometer



nM	nanomolar
nmol	nanomoles
NP	nanoparticle
NSCLC	non-small cell lung cancer
OS	overall survival
OX40	Tumor necrosis factor receptor superfamily 4
p53	Tumor protein p53
PARP	Poly(ADP-ribose) polymerase
PBS	Phosphate buffered saline
PD-1	Programmed cell death protein 1
PDI	Polydispersity Index
PD-L1	Programmed death-ligand 1
PEG	Polyethylene glycol
PEI	Polyethylene imine
PFS	Progression free survival
PGE	Prostaglandin E
PI	Propidium Iodide
PI3K	Phosphoinositide 3-kinases
PLGA	Poly(lactic-co-glycolic acid)
PLGH	Poly(DL-lactide-co-glycolide)
PLK1	Polo-like kinase 1
PRR	Pattern recognition receptors
PTEN	Phosphatase and tensin homolog
PVDF-FL	Polyvinylidene fluoride
RAD51	RAD51 recombinase
RGD	Arginylglycylaspartic acid
RISC	RNA-induced silencing complex
RNA	Ribonucleic acid
ROS	Reactive oxygen species
rpm	Revolutions per minute
RT	Radiation therapy
RTOG	Radiation therapy oncology group
RT-qPCR	Quantitative reverse transcription PCR
SBRT	Stereotactic body radiotherapy
SCID	Severe compromised immune deficiency
SD	Standard deviation
SEM	Standard error of the mean
shRNA	short hairpin RNA
siRNA	Small interfering RNA
SSBs	Single strand breaks
STAT3	Signal transducer and activator of transcription 3
T790M	Thr790Met
TBS-T	Tris-buffered saline-Tween 20

TEM	Transmission electron microscopy
TGA	Thermogravimetric analysis
TGF- $\beta$	Transforming growth factor beta 1
TILs	Tumor infiltrating lymphocytes
TLR	Toll-like receptor
TME	Tumor microenvironment
TNBC	Triple negative breast cancer
Tregs	Regulatory T cell
VEGF	Vascular endothelial growth factor
Z	Atomic number

## Acknowledgements

I would like to express my sincerest gratitude to the following individuals who have made my time as a PhD student at OHSU so valuable and memorable.

First and foremost, I would like to thank my mentor Dr. Wassana Yantasee for welcoming me into her lab and introducing me to the concepts of nanoparticle development and cancer research. Under her guidance and encouragement, I developed my passion for the field and for that I am very grateful. She trained me to be an effective researcher and to think critically and independently. She is very supportive and understanding, and has always provided superb advice on my academic research as well as my future career plans. Most of all, she is very caring and wants best for all of her students. It has been an honor for me to work with such a brilliant scientist and great person. I could not have asked for a better mentor for my PhD studies.

I also thank all of my committee members who have all helped immensely in guiding my PhD studies. I thank Dr. Monica Hinds for providing outstanding scientific guidance for my research and for always making sure that I am meeting deadlines and on track to graduate. Thanks to Dr. Sudarshan Anand for providing valuable and critical feedback on my studies. His expertise in cancer cell biology and radiation therapy helped me a great deal in appropriately setting up my experiments to test hypotheses. Thanks to Dr. Jerry Jaboin for his many insightful suggestions on my research strategies and for providing clinical perspective that helped to formulate my experiments. I thank Dr. Joe Gray for his continued support for our lab and my PhD studies. I am grateful for the sincere interest my committee members have shown in my research and in my personal development, I am very fortunate to have them on my committee.

I would also like to thank Dr. Owen McCarty for his continued support throughout my PhD and for always being available if I needed anything. Thanks to Virginia Howard and Rochelle Ntsasa for their help in placing orders for my experiments. I also thank Amy Koski for taking the time to show

me the intratracheal procedure which enabled me to develop lung tumor model. I would also like to extend my appreciation to Dr. Charles Thomas for his support and feedback for my radiation project and for getting me involved with the radiation medicine department events, as well as the Radiation Research Society meeting. It was a great experience for me to present my research, get feedback, and learn about other various efforts in the field.

I would like to acknowledge all the current and former members in Yantasee lab. Thanks to Dr. Worapol (Boom) Ngamcherdtrakul for spending many hours training me on methods of nanoparticle synthesis and characterization when I started, and for always setting a good example on how to conduct effective and efficient research. I thank Dr. Shenda Gu for training me on cell culture procedures and assisting with many assays including western blot and flow cytometry. Thanks to Dr. Jingga Morry and Dr. David Castro for getting me started on working with mice. Thanks to Daniel Bejan for his help in maintaining the lab and being there whenever I needed help with anything. Thanks to Dr. Natnaree (Ploy) Siriwon for all her help and advice for my immunotherapy project. I am very lucky to have worked with such an amazing group of scientists and fun people to be around. They always made coming to lab an enjoyable experience.

I would also like express my appreciation to my friends and family for their encouragement and motivation throughout my PhD. I thank my mom and dad for their unconditional love and for always being there for me through the good and hard times. Their care and guidance throughout my life have prepared me to take on any challenge. I would not be here today without their extraordinary support and endless contributions to my well-being. Thanks to my brother, Sherif, for being my rock and always looking out for me. He has constantly challenged and motivated me to be the best version of myself. I'm very fortunate to have him as my brother.

## ABSTRACT

Non-small cell lung cancer (NSCLC) is the deadliest form of cancer and represents nearly a fourth of all cancer related deaths worldwide. Identifying molecular targets and developing effective therapeutic regimens to improve NSCLC treatments and patient quality of life is needed. Nanoparticles possess unique properties to enhance treatment efficacy and reduce toxic side effects of traditional therapies. In my dissertation, I exploited versatile mesoporous silica nanoparticles (MSNP) to improve radiation therapy and immunotherapy, which are two key treatments for NSCLC patients.

For radiation therapy, I developed the MSNP as a radiation sensitizer by linking it to an antibody against the epidermal growth factor receptor (EGFR; overexpressed in 50% of lung cancer patients and a mediator of DNA repair) and delivering small interfering RNA (siRNA) against polo-like kinase (PLK1; a key mitotic regulator whose inhibition enhances radiation sensitivity). I showed that the nanoparticle platform targets EGFR+ cells and reduces PLK1 expression, leading to cell cycle arrest, reduced DNA repair capacity, and cell death in NSCLC cells. Furthermore, I found that the combination of the nanoparticles and radiation was synergistic and significantly reduced cell survival, which was confirmed *in vivo* in A549 NSCLC flank tumors. I also demonstrated the translational potential of the platform as a systemic lung cancer therapeutic in an orthotopic lung tumor model, where administration of NP reduced tumor growth and led to prolonged survival of mice.

Additionally, the effects of PLK1 on anti-tumor immunity were elucidated. I found that PLK1 knockdown or inhibition results in significant increase in the expression of the immune checkpoint programmed death ligand 1 (PD-L1; which exhausts cytotoxic T cell

function) in mouse and human lung cancer cells. In clinics, PD-L1 blockade with antibodies has provided promising results for some patients, however, the majority of patients do not respond to immune checkpoint blockade. Thus, I investigated the combination of PLK1 inhibition and PD-L1 blockade in order to augment their individual therapeutic effects. A PLK1 small molecule inhibitor was loaded in the nanoparticle core, and the PD-L1 antibody was conjugated to the nanoparticle surface. The combination was significantly more effective than the single drug counterparts in reducing tumor growth and prolonging survival of mice. Furthermore, in a metastatic lung tumor model, systemic administration of the nanoparticles was found to be as effective in improving survival as the free drugs delivered at a 5-fold higher dose, which highlights the potential to reduce side effects.

In conclusion, I developed MSNP to serve as a: 1) targeted therapeutic that is applicable to over 50% of NSCLC patients and is a radiation sensitizer, and 2) immuno-nanoparticle to improve immune checkpoint blockade responses. My findings suggest that clinical trials with PLK1 inhibitors should be conducted with radiation and/or immunotherapy to capitalize on the potential of targeting PLK1. Furthermore, our nanoparticle platform is a promising drug delivery vehicle, which is able to maximize therapeutic effects and warrants further investigation for NSCLC.

# Chapter 1: Introduction and background

## 1.1 Medical needs for lung cancer treatment

Non-small cell lung cancer (NSCLC) makes up 85% of lung cancers and is the leading cause of cancer mortality, representing nearly a fourth of total related cancer deaths worldwide.<sup>1</sup> Care of patients with NSCLC relies on a variety of treatments depending on which stage the cancer is diagnosed, molecular profiling, and overall patient health at the time of diagnosis.

For early stage NSCLC (stage I, stage II), surgical resection of tumors is preferred for patients who are medically fit to undergo surgery. In addition to surgery, patients may undergo radiation therapy before or after tumor resection as an adjuvant therapy. For patients who are not fit for surgery, radiation is the primary treatment. For locally advanced stage III NSCLC, which comprises about 30% of total diagnoses, radiation therapy usually in combination with platinum based chemotherapy is the first line therapy. For stage IV metastatic NSCLC, a tumor biopsy to obtain the molecular nature of the cancer is used to determine treatment. Patients with known mutations (e.g. EGFR mutation or ALK translocation) are administered targeted therapies against these mutations. For patients who do not harbor EGFR or ALK mutations and have high PD-L1 expression (over 50% of tumor cells are PD-L1+), immune checkpoint blockade is the first line therapy. For patients who do not harbor an identified druggable mutation or have high PD-L1, platinum based chemotherapy regimens are administered.

While targeted therapies against EGFR or ALK have dramatically improved treatments and reduced side effects compared with platinum based chemotherapy, these therapies

are ultimately prone to resistance. Moreover, only a minority of patients (15-20%) harbor EGFR or ALK mutations and can benefit from these therapies.<sup>2</sup> Similarly, immune checkpoint blockade has provided very promising results for some patients; however, the majority of patients will not respond to checkpoint blockade and many initial responders eventually relapse. In all, despite advancements in NSCLC treatments, the overall five year survival remains just 18%.<sup>1</sup> There is a need to develop more effective therapies to improve NSCLC patient outcomes.

In the era of precision medicine, identifying molecular targets to enhance existing therapies is crucial to improve survival of difficult to treat cancers such as lung cancer. One such target that has been investigated is the key mitotic regulator polo-like kinase 1 (PLK1). Previous studies have shown that PLK1 is upregulated in lung cancers and high PLK1 expression is correlated with worse prognosis.<sup>3,4</sup> In addition to its role in initiating and regulating mitosis, PLK1 has been shown to mediate other key signaling pathways in cancer progression.<sup>4-7</sup> For this reason, PLK1 is a strong molecular target to improve NSCLC therapies. However, despite the promise, specific inhibition of PLK1 in tumors has been elusive in clinics. Numerous PLK1 inhibitors have reached clinical trials but many were terminated due to unmanageable toxicities and none have reached FDA approval.

To improve traditional therapies, nanotechnology has garnered great attention in recent years. In particular, nanoparticle drug delivery vehicles can improve cancer treatment by localizing therapeutic effects to tumors which reduces doses and side effects, and enabling novel combination strategies. Mesoporous silica nanoparticles (MSNP) are a promising drug delivery vehicle owing to their biological safety,<sup>8-10</sup> ease of manufacturing



and scalability,<sup>11,12</sup> and high surface area to volume ratio that allows for delivery of high therapeutic payloads.<sup>12</sup> The focus of this dissertation is on the development of MSNP platforms to improve radiation therapy and immunotherapy for NSCLC. Radiation therapy remains a backbone of NSCLC treatment being administered to patients in both early and late stage disease, while immunotherapy is a promising new approach which warrants further investigation to improve clinical responses.

## **1.2 Overview of radiation therapy and radiation sensitizers**

Radiation therapy is foundational in the treatment of cancer, with over 60% of cancer patients receiving radiation. Radiation therapy is administered by delivering ionizing radiation to the tumor site. Ionizing radiation acts by two mechanisms to damage cells – 1) direct action: which create double strand breaks in DNA and 2) indirect action: which create reactive oxygen species (ROS) which in turn damage the DNA.<sup>13</sup> Both methods ultimately compromise the DNA of the cell and lead to cell death. The ultimate goal of radiation therapy is to maximize tumor damage and minimize normal tissue toxicity. This is referred to as therapeutic ratio. Our understanding of radiation biology has led to radiation schemes and methods that serve to enhance the therapeutic ratio. This includes: 1) the use of imaging and radiation technologies to accurately deliver doses to the tumor site, 2) delivering radiation doses in fractions, and 3) administering drugs (i.e. radiation sensitizers) which enhance radiation effects to cancer cells.

Advances in medical imaging and radiation delivery have improved our ability to localize radiation to the tumor site. Techniques such as 3D conformal radiation therapy, intensity modulated radiation therapy (IMRT), and stereotactic body radiation therapy (SBRT) have

allowed maximizing the radiation delivered to tumor and minimizing radiation to the surrounding normal tissue.<sup>14</sup> However, normal tissue toxicity cannot be entirely avoided. Ultimately, the amount of normal tissue exposure to radiation limits the dose that can be administered to the tumor. For instance, in the clinical trial RTOG 0617, dose escalation from 60 Gy to 74 Gy in locally advanced unresectable NSCLC did not improve patient outcomes, but rather increased toxicity and reduced overall survival.<sup>15</sup>

The clinical standard in delivering radiation for NSCLC is delivery of fractions of small doses (e.g. 2 Gy), rather than in large single doses of radiation, to reach the desired biological effect. Conventional radiotherapy regimens for NSCLC consist of 60 Gy radiation delivered in 30 fractions of 2 Gy.<sup>15</sup> The basis of fractioning radiation doses to improve therapeutic ratio relies on the 4R's of radiation biology principles as described by H.R. Withers in 1975. The 4Rs of radiation biology are repair, repopulation, reassortment, and reoxygenation.<sup>16</sup> Differences between normal tissue and tumors in regards to the 4Rs lead to an increase in therapeutic ratio with fractionation. By fractioning the dose, normal tissue are allowed to repair sub-lethal damage and repopulate more efficiently than cancer cells and thus can survive while the cancer cells do not. On the other hand, reoxygenation and reassortment potentiate the effects of fractioned radiation on cancer cells. Reoxygenation is the introduction of oxygenated regions in tumor as the number of cancer cells are reduced, and reassortment refers to the cycling of cancer cells to more sensitize phases of the cell cycle, in particular G2/M which is the most radiation sensitize cell cycle phase. Aside from the 4Rs of radiobiology, a 5<sup>th</sup> R is now appreciated as the intrinsic radiation resistance of cancer cells.<sup>17</sup> In particular, cancer stem cells are known to be radiation resistant and are the culprits of relapse following radiation therapy.<sup>18</sup>

As the same way fractionation enhances the therapeutic ratio due to the 4Rs, we can also enhance the therapeutic ratio by manipulating the cancer cell by any one of the 4Rs. For example, some of the first efforts to enhance radiation sensitivity were aimed at increasing oxygen in tumor tissue – in other words, reoxygenate the tumor. Another class of radiation sensitizers are chemotherapies, which can enhance radiation by affecting DNA repair or inducing cell cycle arrest (reassortment). More recently, efforts in precision medicine have motivated the use of molecularly targeted therapies to improve radiation response of cancer. Radiation sensitizers are reviewed in these three classes as follows, with a focus on molecularly targeted therapeutics.

Oxygen/oxygen mimics: Oxygen enhances radiation damage by reacting with free radicals to 'fix' (make permanent) damaged DNA.<sup>19</sup> Initially, to augment radiation with oxygen, the use of hyperbaric chambers was introduced. However, hyperbaric chambers are cumbersome and difficult to transfer in clinical setting, thus efforts here have subsided. The use of hydrogen peroxide ( $H_2O_2$ ) to produce oxygen in the tumor has also been investigated<sup>20</sup> and intratumoral injection of  $H_2O_2$  is currently under evaluation in phase I/II breast cancer clinical trial. An alternative strategy in this area has been the use of oxygen mimics rather than increasing oxygen in tumors directly. Oxygen mimics are compounds that contain nitrogen groups that act in the same manner as oxygen by fixing the damage induced by free radicals.<sup>21</sup> Misonidazole and nimorazole are two such agents that have been evaluated in preclinical and clinical settings. Misonidazole showed promising radiation sensitizing effects in preclinical studies in many solid tumors, however, the results in clinical trials were not promising.<sup>21</sup> Likewise, nimorazole showed promising preclinical results but its use in clinics is now limited to head and neck cancers,

where it is recommended for use with radiation in Denmark.<sup>21</sup> In all, despite the efforts made in this area, adverse effects of compounds and lack of tumor specificity limit the clinical translation of this strategy.

Chemotherapy: Another class of radiation sensitizers are chemotherapies which can enhance radiation by affecting mechanisms of DNA repair or inducing cell cycle arrest. For example, taxanes are mitotic arrest agents that can induce G2/M arrest and have been used in combination with radiation in hopes of garnering synergistic effects.<sup>22</sup> Other chemotherapies such as 5-FU, gemcitabine, and cisplatin interfere with DNA damage response and have been shown to sensitize cells to radiation.<sup>23</sup> As such, chemotherapy and radiation regimens have become routinely administered in several settings and have demonstrated an overall improvement in survival and cure rates. However, the toxicity associated with chemoradiotherapy is of great concern and ultimately limits the therapeutic benefit garnered.<sup>24</sup> In contrast, molecular targeted therapeutics which can act specifically on cancer cells provide an avenue to improve the tumor response of radiation while not increasing toxicity to normal cells. This has motivated efforts to develop targeted therapeutics to selectively enhance radiation effects to cancer cells only.<sup>25,26</sup>

Molecularly targeted radiation sensitizers: In the current era of precision medicine, efforts to utilize molecularly targeted therapeutics to enhance radiation effects are being investigated. By targeting a number of pathways associated with radiation response at the molecular level we can ultimately improve the therapeutic ratio of radiation leading to better outcomes (Figure 1). The most promising targets that are under investigation in clinical trials are reviewed (Table 1.1).

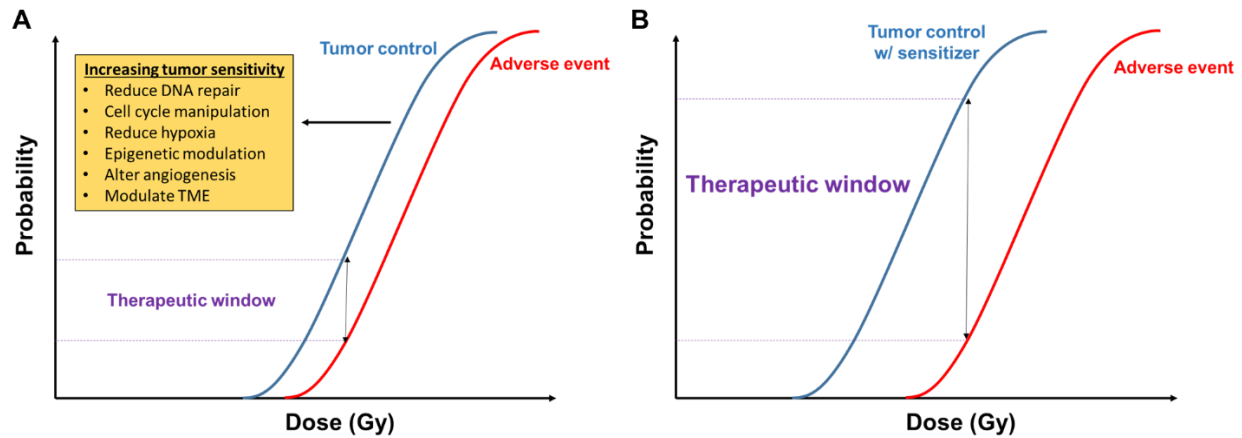


**Figure 1. Increasing therapeutic window of radiation.** At any given dose, there is a probability of tumor control or adverse event, the separation between tumor control and adverse event is therapeutic ratio (window). (A) Narrow therapeutic window can be increased by sensitizing tumors to radiation via various mechanisms, shifting tumor control curve to the left. (B) Increased therapeutic window after treatment with sensitizing drug.

**EGFR:** The epidermal growth factor receptor (EGFR) is a cell survival/growth signaling receptor that is overexpressed in several cancers.<sup>27</sup> Activation of EGFR following radiation has been reported and leads to downstream signaling contributing to cancer cell survival following radiation.<sup>28</sup> Moreover, EGFR has been shown to participate in mediating DNA repair following radiation. After radiation damage, EGFR is phosphorylated and translocated to the nucleus where it has been shown to interact with DNA-dependent protein kinase, catalytic subunit (DNA-PKcs) and repair the damaged DNA.<sup>29</sup> Clinical trials investigating EGFR inhibition to enhance radiation sensitivity have been investigated in a variety of cancer types using both EGFR monoclonal antibodies and small molecule inhibitors. The most promising results were in head and neck cancer where cetuximab, the EGFR monoclonal antibody, improved outcomes when combined with radiation therapy compared with radiation therapy alone.<sup>30</sup> In NSCLC, the addition of cetuximab to chemoradiation regimen did not show benefit.<sup>31</sup> However, retrospective analysis showed that improved survival was limited to the patients with high expression

of EGFR.<sup>31</sup> To date, cetuximab remains the only FDA approved targeted therapy for combination with radiation (for head and neck cancers).<sup>25</sup>

**PARP:** Poly(ADP-ribose) polymerase (PARP) proteins represent another strong target to interfere with the DNA damage response post radiation. PARP inhibitors function as radiation sensitizers by blocking repair of single strand breaks (SSBs) in DNA following radiation, resulting in complex lesions that cells are unable to repair.<sup>32</sup> Inhibition of PARP has shown to be radiosensitizing in a variety of cancers in pre-clinical studies<sup>32</sup> and the combination of radiation and PARP inhibitors (olaparib or veliparib) are ongoing in clinical trials in several cancers including breast, glioblastoma, NSCLC, and head and neck cancers.<sup>32,33</sup> Importantly, PARP inhibitors induce synthetic lethality in cancers with DNA repair mutations such as cancers harboring BRCA1/2 mutations, and have recently been granted FDA approval as single agent therapeutic for ovarian and metastatic breast cancer patients with BRCA mutation.<sup>34</sup> Not surprisingly, it has been shown that PARP inhibitors are more effective radiation sensitizers in BRCA-deficient tumors than BRCA-proficient tumors.<sup>35</sup> Thus, it is likely that the role of PARP inhibitors as radiation sensitizers will be most beneficial for patients with deficiencies in DNA repair such as BRCA mutant cancers. If germline DNA repair mutations are present, however, then systemic distribution of PARP inhibitors would also sensitize normal cells to radiation which raises toxicity concerns.

**HDAC:** Histone deacetylases (HDAC) are epigenetic regulators that alter chromatin by removing acetyl groups and in turn alter gene expression. Abnormal activity of HDAC has been demonstrated in cancer development and progression, resulting in transcriptional alteration of oncogenes and tumor suppressor genes.<sup>36</sup> Hence, inhibitors of HDAC are

studied to control the epigenetic programming of cancer cells. In the context of radiation therapy, inhibitors of HDAC have shown promise in pre-clinical studies<sup>37-39</sup> and have advanced to clinical trials in various cancer types. Although the exact mechanism of how targeting HDAC improves radiation response is not entirely understood, studies have shown that inhibiting HDAC reduces expression of several DNA repair genes.<sup>40-43</sup> Moreover, inhibiting HDAC relaxes chromatin and can result in more DNA damage following radiation.<sup>44,45</sup> The most promising HDAC inhibitors, vorinostat, panobinostat, and valproic acid have entered clinical trials in glioblastoma, NSCLC, and pancreatic cancers. However, attributed to a lack of specificity, HDAC inhibitors have shown limited efficacy in clinical trials,<sup>46</sup> and off-target effects on normal cells remain a concern.<sup>47</sup> This lack of specificity ultimately compromises their potential benefit as radiation sensitizers.

**ATM/ATR:** The ataxia-telangiectasia mutated (*ATM*) and ataxia telangiectasia and Rad3-related (*ATR*) proteins are two key mediators of DNA damage response. These proteins work together to facilitate DNA repair in response to cellular stress.<sup>48</sup> As such, inhibitors of these proteins have been developed in an effort to impair DNA repair after radiation and hence increase radiation sensitivity.<sup>49</sup> This is highlighted by the finding that ATM-deficient patients are the most sensitive patients to radiation.<sup>50</sup> Preclinical findings using ATM or ATR inhibitors have supported targeting these regulators to enhance radiation effects,<sup>51,52</sup> which has led to initiation of clinical trials in glioblastoma, lung cancer brain metastasis, and head and neck cancer. Results of these trials have not been reported.

**PI3K/AKT/mTOR:** The PI3K/AKT pathway is a key signaling pathway promoting cancer cell survival and proliferation.<sup>53</sup> Previous studies have reported that activation of this pathway following radiation results in radiation resistance.<sup>54,55</sup> This has led to efforts to

target this pathway to enhance radiation sensitivity. Nelfinavir was originally developed to treat HIV infection but was also found to inhibit PI3K/AKT,<sup>56</sup> and has been investigated in combination with radiation in NSCLC, glioblastoma, pancreatic, cervical and rectal cancer clinical trials. Results of nelfinavir with chemoradiation in locally advanced NSCLC showed median progression-free survival and overall survival of 12 months and 40 months, respectively.<sup>57</sup> This is a promising result, albeit with a low population size (35 patients), and warrants further investigation. Another target in the pathway is mammalian target of rapamycin (mTOR) which is a downstream protein kinase of PI3K/AKT. Specifically, PI3K activates AKT which in turn can activate mTOR.<sup>58</sup> As with PI3K/AKT inhibition, inhibitors of mTOR have shown radiation sensitizing properties in preclinical investigations.<sup>59,60</sup> Everolimus, mTOR inhibitor, has been tested in clinical trials in several cancers. However, results from phase I clinical trial in NSCLC indicated that the combination is associated with increase in pulmonary toxicity, where 5 out of 26 patients experienced grade 3-4 interstitial pneumonitis.<sup>61</sup>

**VEGF:** Vascular endothelial growth factor (VEGF) is another target thought to enhance radiation therapy by affecting the angiogenesis of the tumors. Indeed, cancer cells secrete high levels of VEGF to promote irregular vascularity in the tumor microenvironment.<sup>62</sup> This irregular vascular network may result in hypoxic regions harboring radiation resistant cells. Based on this, combining anti-angiogenesis agents with radiation has been investigated.<sup>63</sup> Bevacizumab, a monoclonal antibody targeting VEGF-A, is the most advanced anti-angiogenic drug and has been evaluated with radiation in large clinical studies.<sup>64</sup> While encouraging results have been reported in some settings, toxicity is a concern as adverse events are higher with the combination of bevacizumab and



radiation.<sup>65,66</sup> Furthermore, the concept that vascular normalization reduces tumor hypoxia has been challenged as prolonged exposure of anti-angiogenic agents may cause reduction of tumor vascularity that would result in an increase in tumor hypoxia.<sup>67</sup> This would reduce the efficacy of radiation therapy as previously discussed. Further studies are needed to evaluate the effects of VEGF inhibition on tumor hypoxia. Timing and duration of anti-angiogenic agents may be key to garnering clinical benefit with radiation therapy.

**Immune checkpoints (PD-1, PD-L1, CTLA-4):** Recently, the targeting of immune checkpoints has transformed treatments of NSCLC and other cancer types. Immune checkpoints serve to dampen the immune response leading to avoiding anti-tumor immune effects and cancer survival. Specifically, three targets have provided motivating results in various cancers. PD-1 which is expressed on cytotoxic T cells and binds to PD-L1 on cancer cells to exhaust T cells and avoid immune mediated death.<sup>68</sup> CTLA-4 is expressed on T cells and negates activation by dendritic cells.<sup>69</sup> Antibodies targeting PD-1, PD-L1, and CTLA-4 have received FDA approval and are now considered crucial in the treatment of cancers. The application of these therapies with radiation has been studied since radiation leads to the release of damage-associated molecular patterns (DAMPs) and induces cancer cell death to release antigens. DAMPs and antigens can then prime immune cells to stimulate an anti-tumor response.<sup>70</sup> Implementation of immunotherapy with radiation was motivated with the observance of the abscopal effect, which describes a tumor response that is outside the irradiated field indicating that an immune response was generated. Clinical trials in almost all solid tumors including NSCLC are currently evaluating immune checkpoint antibodies with radiation in both

sequential and concurrent formats.<sup>71</sup> Optimization of timing and schedule, identification of potential responders, and minimization of adverse events will be required. Ultimately, as our understanding of the intricate interplay between tumor cells and immune cells in the tumor microenvironment improves, we can identify appropriate strategies to capitalize on this combination. In the following section, the role of immunotherapy in the management of NSCLC is discussed in more detail. Table 1.1 summarizes molecularly targeted therapies that have been in clinical trials with radiation therapy for various cancer types.

**Table 1.1: Molecularly targeted therapies in clinical trials with radiation therapy**

Target	Drug	Mechanism of Action	Cancers investigated	Result in NSCLC
<b>EGFR</b>	*cetuximab, panitumumab, nimotuzumab, erlotinib, gefitinib	DNA damage response/Cell survival signaling	NSCLC, HNC, CRC, GBM, pancreatic, prostate, skin, esophageal	Cetuximab + CRT in stage III: no benefit in overall survival. Higher rate of grade 3 or worse toxic effects (86% vs. 70%). 2-year OS benefit in patients with high EGFR (544 patients) [NCT00533949]. Panitumumab + CRT in stage III: MNS rates were 68.2% and 50.0%, for CRT and CRT + panitumumab. Higher toxicity in experimental arm (60 patients) [NCT00979212]. Erlotinib + CRT in stage III: median time to progression was 14.0 months. 1-, 2-, and 5-year OS rates were 82.6%, 67.4%, and 35.9%. Acceptable toxicity (0 grade 4-5, 11 grade 3 adverse events. 12 patients had no progression and 34 had local and/or distant failure (46 patients) [NCT00563784].
<b>PARP</b>	olaparib, veliparib	DNA damage response	NSCLC, HNC, breast, GBM, ovarian	Olaparib Dose Escalating Trial + Concurrent RT with or without Cisplatin in locally advanced NSCLC (Recruiting) [NCT01562210].
<b>ATM</b>	AZD1390	DNA damage response	GBM	NA
<b>ATR</b>	AZD6738, M6620	DNA damage response	NSCLC brain metastasis, HNC, solid tumors	M6620 and whole brain RT for brain metastases from NSCLC, SCLC, or neuroendocrine tumors (Recruiting) [NCT02589522].
<b>PI3K/AKT</b>	nelfinavir	cell survival signaling	NSCLC, GBM, CRC, pancreatic, cervical	Combination CRT and nelfinavir in stage III NSCLC: PFS 12 month, OS 40 month, 5 year OS was 37 % (35 patients) [NCT00589056].
<b>mTOR</b>	everolimus	cell survival signaling	NSCLC, HNC, prostate, GBM	Everolimus + RT followed by consolidation chemotherapy in locally advanced or oligometastatic untreated NSCLC: 24% of patients experienced grade 3-4 pneumonitis (26 patients) [NCT01167530].
<b>VEGF</b>	bevacizumab	angiogenesis	NSCLC, CRC, GBM, pancreatic	(1) Terminated (toxicity) [NCT00531076]. (2) Combination CRT and bevacizumab in unresectable stage III NSCLC. Of 29 patients, 17 did not complete study (5 due to adverse events, 2 treatment related death) [NCT00334815].
<b>HDAC</b>	vorinostat, panobinostat, valproic acid	chromatin modification	NSCLC, GBM, HNC, pancreatic, prostate	Palliative radiotherapy with vorinostat in advanced or metastatic NSCLC phase I: maximum tolerated dose of vorinostat given concurrently with thoracic radiotherapy is 400 mg per fraction (17 patients) [NCT00821951].
<b>PD-1</b>	pembrolizumab, nivolumab	immune checkpoint blockade	NSCLC, HNC, CRC, GBM, breast, cervical, pancreatic, prostate, melanoma, esophageal	Consolidation pembrolizumab following CRT in stage III: median PFS was 15.4 months. 16 (17.2%) patients developed grade $\geq 2$ pneumonitis, 5 (5.4%) had grade 3-4 pneumonitis. 1 pneumonitis-related death. Improvement over historical controls (92 patients) [NCT02343952].
<b>PD-L1</b>	atezolizumab, durvalumab	immune checkpoint blockade	NSCLC, HNC, CRC, GBM, breast, cervical, pancreatic, prostate, melanoma, esophageal	Durvalumab consolidation post CRT: (473 patients received durvalumab and 236 received placebo). 24-month OS rate of 66.3% in durvalumab group vs. 55.6 in the placebo group. Median PFS 17.2 months vs. 5.6 months in placebo group. Median time to death or distant metastasis was 28.3 months vs. 16.2 months in placebo group. Grade 3-4 adverse events 30.5% vs. 26.1% in placebo group; 15.4% and 9.8% of the patients, respectively, discontinued due to adverse events [NCT02125461].
<b>CTLA-4</b>	ipilimumab	immune checkpoint blockade	NSCLC, HNC, CRC, cervical, pancreatic, prostate, melanoma, esophageal	Two patients experienced dose-limiting toxicity and 12 (34%) grade 3 toxicity. Response outside the radiation field was assessable in 31 patients. Three patients (10%) exhibited partial response outside irradiated field and 7 (23%) experienced clinical benefit (i.e. partial response or stable disease lasting $\geq 6$ months) (35 patients) [NCT02239900].

\*FDA approved with radiation, CRC: colorectal cancer, CRT: chemoradiotherapy, GBM: glioblastoma, HNC: head and neck cancer, MNS: Mediastinal nodal sterilization, NSCLC: non-small cell lung cancer, OS: overall survival, PFS: progression free survival, RT: radiation therapy.

### **1.3 Overview of immunotherapy**

In recent years, the interplay of immune system and tumor development has garnered great attention and some mechanisms of how cancer cells avoid immune destruction have been elucidated.

#### The immune response

Our body fights off infections and diseases by mechanisms of innate (non-specific) immunity and adaptive (specific) immunity. Innate immunity is the initial rapid response while adaptive immunity is the progressive and sustained response. The key cells in innate immunity are neutrophils, macrophages, and NK cells. These natural defensive cells are triggered by sensing inflammation and respond by clearing out the pathogen/invader via distinct mechanisms, such as phagocytosis or release of perforins. The innate immunity functions to clear the invader whereas the adaptive immunity is triggered to provide the sustained immune response. In adaptive immunity, foreign (non-self) antigens are recognized and prime antigen presenting cells (APCs, e.g. dendritic cells, B cells, macrophages) which in turn activate helper CD4+ T cells or cytotoxic CD8+ T cells. Cytotoxic CD8+ T cells bind to MHC class I on target cells expressing the antigens to initiate cell death. Helper CD4+ T cells aid the APCs in priming naive CD8+ T cell by direct activation or by releasing T cell cytokines (e.g., IL-2). CD4+ T cells also activate B cell proliferation to generate antigen-specific antibodies. Importantly, recognition of non-self antigens is also accompanied by the sensing of damage associated molecular patterns (DAMPs), which stimulate pattern recognition receptors (PRR) on APCs. It is believed that both non-self antigens and DAMPs must be sensed for priming and activation of T cells. Activated CD4+ or CD8+ T cells (effector T cells) then proliferate to

generate more effector T cells or memory T cells. Effector T cells carry out the same tasks as the parental cells, while memory T cells remain dormant until reactivated by its distinguished antigens. In this way, an immune response loop is generated to clear the infection. In order to avoid attack against normal tissues, host cells utilize checkpoints (e.g. CTLA-4, PD-1/PD-L1 axis) to inhibit an over-activation of immune response. CTLA-4 is expressed on T cells and receives an inhibitory signal from CD80/86 ligands on APCs. PD-1 is also expressed on T cells and receives inhibitory signal from PD-L1 ligands. This tightly controlled regulation of the immune response is required to clear invaders while maintaining normal tissue functions.

### Cancer immune evasion

It is now appreciated that one of the hallmark characteristics of cancers is their ability to evade the immune response.<sup>72</sup> A cancer that has progressed has established mechanisms of immuno-editing to evade recognition by host immune system. For example, cancer cells can reduce their antigen presentation by downregulating MHC class I on their surface.<sup>70</sup> Cancer cells can also alter their tumor microenvironment by secretion of cytokines to promote pro-tumor immune cells (e.g. M2 macrophages, myeloid derived suppressor cells (MDSCs), and regulatory T cells (Tregs)) that protect from immune destruction.<sup>73</sup> For instance, IL-6, IL-10, TGF- $\beta$ , PGE, and IDO are cytokines in the TME that promote immune evasion and cancer progression.<sup>74-77</sup> Interestingly, DAMPs released by dying or stressed cancer cells can also promote immunosuppression,<sup>73</sup> rather than stimulate APCs, in the TME. Furthermore, cancer cells can hijack immune checkpoints such as the PD-1/PD-L1 axis. Cancer cells upregulate PD-L1 on their cell

surface that binds to PD-1 receptors on cytotoxic T cells to exhaust them and inhibit their cytotoxic function.<sup>68,78,79</sup>

### Cancer immunotherapy

Strategies of immunotherapy to treat cancer have focused on altering the described mechanisms of cancer immune evasion. Until recently, little success had been achieved; however, the discovery of the key immune checkpoints in the last decade (CTLA-4 and PD-1 on T cells, and PD-L1 on cancer cells) have shown what the promise of immunotherapy for cancer treatment can hold and have reinvigorated the efforts in this field.

Indeed, immune checkpoint blockade with CTLA-4, PD-1, or PD-L1 antibodies has led to robust and durable responses for patients in a variety of cancers, and are now considered one of the key treatments in the management of cancers. In NSCLC, the PD-1 antibody nivolumab was the first to receive FDA approval in 2015 as second line therapy after tumor progression following platinum-based chemo or EGFR/ALK targeted therapy. Following promising results in clinical trials compared with standard platinum chemotherapy,<sup>80</sup> another PD-1 antibody pembrolizumab received FDA approval as first line therapy for metastatic NSCLC patients who do not harbor ALK or EGFR mutation, and whose tumors express over 50% PD-L1 expression. Two PD-L1 antibodies (atezolizumab and durvalumab) were also granted FDA approval for NSCLC. Durvalumab became the first immunotherapy approved for unresectable stage III NSCLC for patients whose tumors have not progressed following chemoradiotherapy regardless of their PD-L1 expression status.<sup>81</sup> Current FDA approved immunotherapies for NSCLC and their indications are listed in Table 1.2.

**Table 1.2 – FDA approved immunotherapies for NSCLC**

Target	Drug	PD-L1 status	Indication	FDA approval
PD-1	Pembrolizumab	>1%	Metastatic NSCLC whose tumors express PD-L1 (TPS $\geq$ 1%) with disease progression on or after platinum-based chemotherapy	10/2015
		>50%	First-line treatment of patients with metastatic NSCLC, with PD-L1 expression (tumor proportion score $\geq$ 50%, with no EGFR or ALK genomic tumor aberrations	10/2016
		NA	First line treatment in combination with pemetrexed and platinum-based chemotherapy for metastatic nonsquamous NSCLC, with no EGFR or ALK genomic tumor aberrations.	03/2017
	Nivolumab	NA	Metastatic NSCLC with progression on or after platinum-based chemotherapy. Patients with EGFR or ALK genomic tumor aberrations and disease progression on FDA-approved therapy for these aberrations	10/2015
PD-L1	Atezolizumab	NA	Metastatic NSCLC whose disease progressed during or following platinum-based chemotherapy. Patients with EGFR or ALK genomic tumor aberrations and disease progression on FDA-approved therapy for these aberrations	10/2016
	Durvalumab	NA	Unresectable stage III non-small cell lung cancer (NSCLC) whose disease has not progressed following concurrent platinum-based chemotherapy and radiation therapy.	02/2018

Limitations of immune checkpoint blockade

While patients who respond to immune checkpoint blockade may show robust and durable responses, only a minority of total patients respond, and even for patients with high PD-L1 expression, response rates remain under 50%.<sup>80</sup> Furthermore, many initial responders will develop resistance and ultimately relapse.<sup>82</sup> Another limitation is the identification of potential responders to immune checkpoint blockade. PD-L1 high expression does suggest a response to PD blockade; however it is far from definitive as PD-L1 negative tumors have also shown response to PD blockade.<sup>68,83</sup> This may be due

to PD-L1 having dynamic and inducible expression, changing in response to therapies. Sampling for PD-L1 expression is another issue as PD-L1 is heterogeneously expressed in tumor microenvironment and in various cell types.

While in general immune checkpoint blockade has less severe and distinct toxicity from chemotherapy, autoimmune disorders caused by immunotherapy is a concern. Systemic distribution of these antibodies can cause aberrant and uncontrolled immune response, leading to immune-related adverse effects (irAEs).<sup>84</sup> While generally manageable, discontinuation of treatment due to irAEs have occurred and in some instances irAEs can be fatal.<sup>84</sup>

Thus, based on these limitations, strategies to improve the response, therapeutic efficacy, and manage toxicities of immune checkpoint blockade are highly warranted for NSCLC and other cancers. Consequently, research efforts have been directed towards improving immunotherapy by combination strategies with other therapies.

#### Immune checkpoint blockade combination strategies

As previously discussed, the combination of immunotherapy and radiation was motivated due to the immunogenic alteration caused by radiation. Likewise, chemotherapies are being investigated in combination with immune checkpoint blockade in clinical trials in NSCLC and other cancers. In NSCLC, the majority of these trials are investigating PD-1 or PD-L1 antibodies with platinum based chemotherapies since they remain the standard of care for majority patients. Other preclinical efforts have aimed at identifying chemotherapies that cause immunogenic cell death to combine with immune checkpoint blockade.



Several molecularly targeted therapies are also being investigated in combination with either PD-1 or PD-L1 blockade in clinical trials, including inhibitors of CDK4/6, PARP, HDAC, and VEGF, which have all shown promise in preclinical studies.<sup>70</sup> Moreover, for patients with known mutations (EGFR mutation or ALK translocation), combination of immune checkpoint blockade with inhibitors against those mutations are also being explored.<sup>85</sup> Lastly, combination with dual immunotherapies is also under investigation such as administering antibodies against both PD-1 and CTLA-4, or inhibiting cytokines such as IDO with immune checkpoint blockade.<sup>70</sup>

Ultimately, as with radiation therapy and chemotherapy, the goal of these combinations will be to improve cancer cell killing but not increase systemic toxicity. Furthermore, higher response rates and more durable responses for NSCLC patients are desired. In the next section, the potential of PLK1 as a therapeutic target to improve existing therapies is discussed.

## **1.4 The mitotic regulator PLK1: a strong therapeutic target in cancer treatment**

PLK1 is a highly conserved mitotic protein which plays a role in nearly every aspect of cell division including mitotic entry, centrosome maturation, bipolar spindle formation, chromosome segregation, cytokinesis, and mitotic exit.<sup>86</sup> PLK1 is only expressed in rapidly dividing cells making it a potential target for cancer therapy.<sup>5</sup> Indeed, lung and other cancers overexpress PLK1, and high PLK1 expression is correlated with reduced survival for lung cancer patients.<sup>3</sup> Importantly, PLK1 signaling also mediates many molecular mechanisms associated with cancer. Previous studies have shown PLK1 interacts with both tumor oncogenes and tumor suppressor genes, resulting in cancer progression and therapeutic resistance.<sup>4-7</sup> In fact, PLK1 inhibition has been shown to mediate resistance of cancer to a variety of drugs including chemotherapies and targeted therapies.<sup>87</sup> For example, in NSCLC cells, PLK1 inhibition was found to overcome T790M mutation of EGFR which is induced following treatment with EGFR small molecule inhibitors in clinics and leads to resistance.<sup>88</sup> Moreover, PLK1 has been identified as a target to kill various cancer stem cells,<sup>89-91</sup> which are intrinsically resistant to standard therapies and lead to relapse.

The role of PLK1 with critical oncogenes and tumor suppressor genes are outlined in Figure 1.2 and reviewed below. The potential of PLK1 as a target to augment radiation therapy and immunotherapy is also discussed.

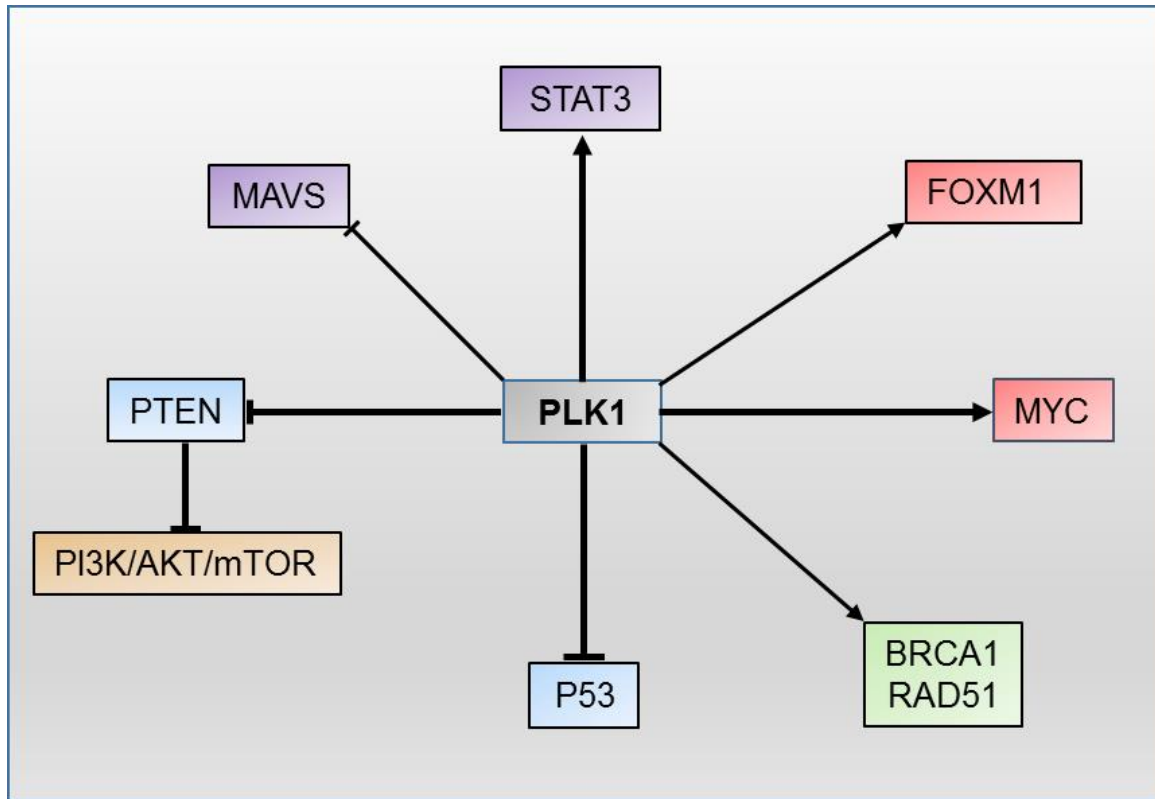


**Figure 1.2.** Summary of PLK1's role with tumor oncogenes (red), tumor suppressors (blue), immune regulators (purple), and DNA repair genes (green).

**PLK1 inactivation of tumor suppressors (e.g., p53, PTEN):** Perhaps the most well-known tumor suppressor gene is p53. P53 keeps rogue cells from becoming cancerous by maintaining genomic stability and initiating apoptosis when needed. Several studies have shown that PLK1 and p53 are negative regulators of each other.<sup>92,93</sup> Thus, PLK1 inhibition can lead to functional p53 activity which can promote cancer suppressive effects. Similarly, PLK1 has also been linked to PTEN tumor suppressor and acts as a negative regulator by phosphorylating PTEN to inhibit its suppressive functions.<sup>94,95</sup> PTEN acts as a tumor suppressor by blocking the activation of PI3K/AKT/mTOR pathway, which is a key pathway in cancer proliferation and survival as discussed previously.

**PLK1 and oncogenic transcriptional regulators (e.g., MYC, FOXM1):** The MYC oncogene is a master transcriptional regulator of various processes including cell growth, proliferation, metabolism, cell cycle progression, and apoptosis.<sup>96</sup> Aberrant MYC regulation has been found in the majority of cancers and developing effective therapeutics to effectively target MYC has long been sought after.<sup>97</sup> Several studies have reported PLK1 to directly phosphorylate MYC,<sup>98,99</sup> thus PLK1 is a target to kill MYC-dependent tumors. Another transcription factor tied to PLK1 is FOXM1. The role of FOXM1 in promoting tumorigenesis have been described,<sup>100</sup> and overexpression of FOXM1 correlates with worse prognosis for cancer patients.<sup>101</sup> Phosphorylation of FOXM1 regulates transcriptional activity leading to cell proliferation and PLK1 was found to phosphorylate FOXM1, which in turn transcribes PLK1.<sup>102</sup> Thus, PLK1 and FOXM1 create a positive feedback loop to allow for mitotic progression and expression of tumor promoting genes.

**PLK1 in DNA damage response:** PLK1 has been shown to play a role in DNA damage response, particularly in homologous recombination (HR), which is the predominant mechanism of DNA repair during mitosis. For instance, Chabalier-Taste et al. showed that PLK1 phosphorylated and recruited BRCA1 for DNA repair.<sup>103</sup> Yata et al. reported that PLK1 also phosphorylates RAD51, another participant in HR DNA repair, to increase their concentration and mediate HR.<sup>104</sup>

**PLK1 and cancer stem cells:** Cancer stem cells are a subpopulation of cancer cells that possess stem cell properties such as self renewal and ability to differentiate to varying cell types with altered gene expression.<sup>105</sup> Studies have shown that CSCs are resistant to standard therapies such as radiation and chemotherapy, and ultimately are the culprits

of cancer relapse following therapy.<sup>106,107</sup> Intriguingly, PLK1 has been identified as a potential target in cancer stem cells in various cancers including colon,<sup>89</sup> glioblastoma,<sup>90</sup> and breast cancers.<sup>91</sup>

**PLK1 for radiation therapy:** As discussed, PLK1 inhibition results in mitotic arrest where cells are most sensitized to radiation. Previous reports have shown this in preclinical studies in several cancer types. Furthermore, studies have shown that due to PLK1's role in DNA damage, inhibiting PLK1 also reduces DNA repair capacity and may also increase radiation sensitivity in this way.<sup>108</sup> Lastly, PLK1 inhibitors have been shown to target cancer stem cells, which cause relapse after radiation therapy as discussed above. Consequently, these observations suggest that PLK1 is a very promising target to improve radiation responses. However, to date, no PLK1 therapies have been investigated in clinical trials with radiation therapy.

**PLK1 and immune regulation:** Several studies have indicated that PLK1 may have a role in regulating tumor immunity. Li et al. assessed PLK1 expression with tumor immunity in various cancer types. The authors found that high PLK1 expression in various tumor tissues correlated with lower HLA (encode MHC proteins) expression, and decreased B cells, NK cells, and tumor infiltrating lymphocytes.<sup>109</sup> Furthermore, PLK1 inhibition in cancer cells was found to increase HLA mRNA and MHC class I protein.<sup>109</sup> Studies have also shown that PLK1 regulates STAT3 activation. STAT3 is expressed in both tumor and immune cells and its activation promotes production of immunosuppressive factors to promote a pro-tumor environment and immune evasion.<sup>110</sup> PLK1 and STAT3 were shown to control each other's activation in esophageal squamous cell carcinoma, and PLK1 inhibition led to reduced STAT3 and phosphorylated STAT3 expression.<sup>111</sup> In NSCLC

cells, Yi et al. showed that inhibiting PLK1 reduced STAT3 phosphorylation, but not total STAT3.<sup>112</sup> PLK1 has also been found to regulate type I interferon (IFN) production.<sup>113,114</sup> Specifically, PLK1 associates with the mitochondrial antiviral-signaling protein (MAVS) and negatively controls its activity in inducing IFN. Arresting cells in G2/M with nocodazole inhibited IFN induction, which was partially restored with PLK1 depletion.<sup>114</sup> This suggests that PLK1 may promote tumorigenesis through inhibition of innate immune responses.

Collectively the many roles of PLK1 suggest that it is a strong molecular target for cancer treatment and to improve existing therapies. However, effective PLK1 inhibition remains a clinical challenge.

#### Limitation of current PLK1 therapies

Based on the promise of targeting PLK1, several PLK1 small molecule inhibitors have been developed and reached clinical trials. However, the majority of trials were terminated early due to adverse toxicities, in particular hematological toxicities.<sup>115</sup> To achieve sufficient tumor bioavailability, PLK1 inhibitors have been designed to have long half-lives. This results in long exposure times with hematopoietic precursor cells in blood and bone marrow, and ultimately leads to dose-limiting toxicity of neutropenia (low neutrophils) and thrombocytopenia (low platelets). Additionally, PLK1 inhibitors can also have off-target effects and inhibit other PLK family members, namely PLK2 and PLK3, whose roles are not entirely understood.<sup>116</sup> Of all PLK1 inhibitors, volasertib (BI6727) was the most advanced and reached phase III clinical trial for acute myeloid leukemia (blood cancer),<sup>115</sup> but eventually failed to meet primary endpoint of objective response.<sup>117</sup> For lung cancer, volasertib was terminated as a monotherapy early in a clinical trial due to

lack of response at the determined maximum tolerated dose.<sup>118</sup> Inhibition of PLK1 with small molecule inhibitors remains a clinical challenge.

An alternative to PLK inhibition with small molecules is the use of small interfering RNA (siRNA) to knockdown PLK1 at the mRNA level. SiRNA are short synthetic nucleic acids that can specifically target any mRNA sequence and cleave the mRNA, halting the production of the associated protein. SiRNA gene therapy has been extensively researched for cancer treatment since its Nobel prized discovery in 2006, with the motivation that the technology can be harnessed to inhibit any oncogene with great specificity. It is also advantageous over antibodies and inhibitors as it orchestrates its effect at the mRNA levels instead of at the protein levels. As a result, we have previously reported that siRNA can overcome both intrinsic and acquired resistance of cancer cells to the antibody and inhibitor that target the same protein (e.g., HER2),<sup>119</sup> and cancer was not as prone to develop resistance to siRNA as they were to the protein targeting therapies.<sup>120</sup> However, siRNA requires a delivery vehicle to allow long blood circulation, intracellular delivery, and release in cytoplasm of the target cell. In this regard, nanoparticles are a very promising siRNA delivery vehicle supported by many preclinical studies, and various platforms have reached clinical trials for a variety of diseases including cancer. For targeting PLK1, TKM-PLK1, a liposomal nanoparticle delivering PLK1 siRNA, was evaluated in phase I/II clinical trial and showed promising results when used to treat liver cancer (stable disease in 51% of 43 patients),<sup>121</sup> but it was not as promising for cancer outside the liver.<sup>122</sup>

Collectively, these results suggest that alternative therapeutics targeting PLK1 are needed. Furthermore, as previous studies have elucidated the extensive interplay of

PLK1 with many genes that regulate cancer progression and immune evasion, this highlights that monotherapy with PLK1 inhibitors alone may be ineffective. Consequently, to illicit the full potential of targeting PLK1, combination with other therapeutic modalities is likely needed.

## **1.5 Nanoparticles in cancer treatment**

The application of nanotechnology in cancer has become a central focus in biomedical research. In particular, nanoparticles (NPs) possess unique properties to overcome the limitations associated with traditional cancer therapies, and they have been developed as drug delivery vehicles to provide tumor targeting and deliver therapeutics such as chemo drugs, inhibitors, and nucleic acids.<sup>123</sup> First, the increased size of NPs can eliminate fast renal clearance of small molecules. Nanoparticles can also mediate toxicity concerns of systemic distribution by localizing therapeutic effects in tumors due to the enhanced permeability and retention (EPR) effect. The EPR is enabled by the physiological nature of tumors which upregulate pro-angiogenic factors leading to formation of immature and leaky vasculature which can increase nanoparticle infiltration in tumors.<sup>124</sup> Moreover, poor lymphatic drainage increases nanoparticle retention within the tumors. This abnormal vasculature is known to allow for the accumulation of appropriately sized NPs (30-200 nm) in tumors compared with normal tissues.<sup>123</sup> Additionally, the use of polyethylene glycol (PEG) as a nanoparticle coating can avoid opsonization and rapid clearance by the mononuclear phagocytic system, which prolongs their half-life and tumor accumulation. To further enhance targeting and reduce systemic toxicity, nanoparticles can also be decorated with targeting agents (e.g., antibodies) to specifically target cancer cells.



Another feature of nanoscale materials is their high surface area to volume. This enables loading with high therapeutic payloads and/or imaging agents.<sup>125</sup> Furthermore, delivery of multiple therapeutics can be achieved on a single platform which may enhance potential synergistic effects of the therapeutics. Nanoparticles can also deliver agents that would otherwise be non-functional in physiological conditions. For instance, as aforementioned, siRNA hold great promise and they can be designed to target any oncogene with great specificity. In fact, most of cancer genetic aberrations identified are undruggable with current small molecule inhibitors or antibodies. Consequently, efficacious nanoparticles for siRNA delivery in cancer treatment are sought after. Lastly, in addition to serving a delivery vehicle, nanoparticles can also have intrinsic effects (e.g., photothermal, ROS scavenging, ROS generating) on cancer cells depending on the components of the nanomaterials. This versatility of nanoparticles have been utilized in various cancer treatment settings. Below examples of the use of nanoparticles as radiation sensitizers and for immunotherapy are reviewed.

### **1.5.1 Nanoparticles as radiation sensitizers**

#### Nanoparticle delivery of chemotherapies for radiation therapy

A number of studies have investigated delivery of chemotherapies with nanoparticles in combination with radiation. As discussed in section 1.2, certain chemotherapies can potentiate radiation effects and chemoradiation therapy has become a backbone in a variety of cancers. However, the combination of chemotherapy and radiation also results in significant toxicity which hinder potential synergistic benefits and may reduce patient quality of life. Thus, attempts to improve chemo delivery with nanoparticles has been explored. Abraxane, albumin bound paclitaxel, improves solubility of hydrophobic

paclitaxel and can reduce systemic toxicity of paclitaxel given with castor oil. Several clinical trials are ongoing to evaluate abraxane in combination with chemoradiotherapy for NSCLC, pancreatic, and head and neck cancers. CRXL101 is a cyclodextrin-PEG polymeric nanoparticle formulation with the chemo drug camptothecin. A phase I clinical trial of CRXL101 in combination with capecitabine and radiation therapy in rectal cancers has recently been initiated.

#### High atomic number nanoparticles for radiation therapy

Another strategy for nanoparticle radiosensitization is the use of high atomic number (Z) materials. High Z materials are promising material for use with radiation as they can enhance attenuation of x-rays and thus escalate the biological effects of radiation on DNA. The most studied metallic nanomaterial as radiation sensitizer is gold. Gold is a promising material in this setting due to its biological inertness, as well as its ease in manufacturing and scalability. For example, Zhang et al. reported on 2 nm gold nanoclusters covered with glutathione (GSH) shell that could accumulate in tumors via EPR effects and significantly enhanced radiation effects in U14 mouse cervical cancer model.<sup>126</sup> While this material relied on EPR to accumulate the gold particles in tumors, Liang et al. developed gold nanoclusters with cyclic RGD peptide shell to target  $\alpha_v\beta_3$  integrin positive cancer. The targeted nanoclusters with radiation were shown to improve tumor control compared with non-targeted nanoclusters with radiation, or radiation alone in a 4T1 mouse breast tumor model.<sup>127</sup> Another metal based nanoparticle is NBTXR3, which is hafnium oxide nanoformulation. As with gold, hafnium oxide enhances the absorption of ionizing radiation in cells. NBTXR3 showed promising preclinical results and is currently under clinical investigation for soft tissue sarcomas (phase II/III) and head and

neck cancers (phase I), where it is administered intratumorally in combination with radiation.<sup>128</sup>

### Molecularly targeted nanoparticles for radiation therapy

More recently, efforts have shifted to developing molecularly targeted nanoparticles as radiation sensitizers. Wang et al. delivered HDAC inhibitors, vorinostat and quisinostat, with nanoparticles consisting of PLGA/inhibitor core coated with layer of DSPE-PEG.<sup>47</sup> Nanoparticle delivery of each inhibitor was shown to be superior to the inhibitor alone and could enhance the radiation effects in colorectal and prostate cancers by enhancing gH2ax foci formation.<sup>47</sup> Similarly, Karve et al. utilized the same nanoparticle construct to deliver wortmannin, an inhibitor of PI3K pathway, which is highly toxic agent when delivered alone. Delivery of wortmannin on the NP was shown to provide radiation sensitivity while significantly enhancing the maximum tolerated dose of wortmannin.<sup>129</sup> As discussed above, siRNA based therapeutics hold great promise for cancer treatment. While several siRNAs have shown promise to combine with radiation *in vitro*, only a few studies have shown *in vivo* radiation sensitizing effects using siRNA due to limitations of *in vivo* delivery of siRNAs. In one study, an iron oxide nanoparticle coated with chitosan, PEI, and PEG polymers delivered siRNA against APE1, an enzyme involved in base excision repair of DNA, and was shown to be effective as a radiation sensitizer in glioblastoma mouse models.<sup>130</sup> To date, despite the promise of siRNA, no siRNA therapeutic has entered clinical trials in combination with radiation.

### **1.5.2 Nanoparticles for immunotherapy**

The promising clinical outcomes with immune checkpoint blockade have led to the emergence of several new strategies to induce immune responses using nanoparticles. In this area, nanoparticles provide tremendous benefits as they can enable co-delivery of immune regulating agents on a single platform. Indeed, in the last couple of years, nanoparticles have been designed to deliver antigens, adjuvants, TME modulators, and checkpoint blockade agents in preclinical studies with some very promising results. Strategies in this area are reviewed below.

#### Antigen/adjuvant delivery on NPs (cancer vaccines)

Nanoparticles can protect antigens from degradation and increase their circulation time leading to enhanced delivery to APCs. Kranz et al.<sup>131</sup> developed RNA-lipoplexes (RNA-LPX) to deliver RNA-based antigens to dendritic cells. The vaccine led to the generation of effector and memory T cells and IFN- $\alpha$  dependent tumor regression in mice. Results of the lipoplex vaccine delivering common tumor antigens in the first three melanoma patients in phase I clinical trial was also reported. Promisingly, induction of IFN- $\alpha$  and antigen-specific T cell responses were observed for each patient. Another advantage of nanoparticles is the ability to incorporate both antigen and adjuvant on the same construct to act as a vaccine and induce a potent immune response. Kuai et al.<sup>132</sup> reported on high density lipoprotein-mimicking nanodiscs that deliver antigen peptide and CpG adjuvant (stimulator of TLR9). The nanovaccine was shown to stimulate 47-fold more antigen-specific CD8+ T cells than vaccine without NP. When combined with checkpoint inhibitors (PD-1 and CTLA-4 antibodies), the vaccine led to complete tumor control in almost all of the mice with MC38 or B16F10 tumors.<sup>132</sup> In addition to delivering antigens and adjuvants,

other immune modulatory agents can also be incorporated. For example, Zhu et al.<sup>133</sup> developed L-glutamic acid polypeptide and PEG nanocapsules to deliver antigen, CpG, and shSTAT3. STAT3 signaling is immunosuppressive and can also reduce effectiveness of CpG immune stimulation. The vaccine induced 8-fold more antigen-specific CD8+ T cells than antigen and CpG alone, and resulted in reduction of antigen-specific colorectal tumors (in lungs of mice). While antigen delivery is a promising approach, a limitation remains in the identification of appropriate neoantigens which may be difficult to identify for each tumor type and also vary greatly for each patient.

#### Immune checkpoints on NPs

In addition to delivering antigens and adjuvants, nanoparticles have also been utilized to improve the existing therapies targeting immune checkpoints. Schmid et al.<sup>134</sup> reported on PLGA/PEG nanoparticles conjugated with PD-1 antibody to target T cells and deliver TGF- $\beta$  inhibitor to counter immune dampening. The platform improved tumor control and extended survival of mice bearing MC38 colon tumors compared with free drug administration at the same dose. Furthermore, delivery of TLR7/8 agonist (R848) with the PD-1 antibody conjugated NPs enhanced infiltrated CD8+ T cells in tumors and sensitized tumors to subsequent PD-1 blockade. Similarly, Mi et al.<sup>135</sup> developed PLGA/PEG nanoparticles conjugated with PD-1 and OX40 antibodies as a dual immunotherapy platform. Co-delivery of the antibodies on NP was shown to enhance T cell infiltration and resulted in improved tumor control than the free antibodies or single antibody NPs in B16F10 and 4T1 tumor models.<sup>135</sup>

Kosmides et al.<sup>136</sup> reported on iron oxide nanoparticles containing two antibody types that stimulate 4-1BB on T cells and block PD-L1 checkpoint on tumor cells. The nanoparticles

significantly delayed tumor growth and extended survival of mice bearing B16F10 or MC38 tumors, compared with free antibodies or single antibody nanoparticles. A similar approach by Chiang et al.<sup>137</sup> was to develop fucoidan polysaccharide–dextran iron oxide nanoparticle for delivery of CD3 and CD28 antibodies for T cell activation, and PD-L1 antibody for checkpoint blockade. In this study, the iron oxide core was also used to enable magnetic guided delivery to tumors to reduce off-target effects. The regimen enhanced tumor immunity, improved tumor control, and extended survival in 4T1 breast cancer model, while magnetic guidance could reduce organ accumulation of NPs. Meir et al.<sup>138</sup> utilized gold nanoparticles conjugated to PD-L1 antibodies to allow for prediction of response with CT imaging, and to improve tumor delivery of the antibody. As immune checkpoints currently only work for a subset of patients, early identification of responders would be beneficial in clinics as non-responsive patients could be switched to a different treatment regimen. Accumulation of anti-PD-L1 conjugated gold NPs in tumors was shown to predict response of the PD-L1 blockade as early as 48 hours post treatment. Delivery with gold NPs also reduced tumor growth with one fifth of the standard clinical dose. Other reports have aimed at delivering chemotherapy with PD-L1 targeted nanoparticles. Xu et al.<sup>139</sup> developed PEG-PCL NPs conjugated to PD-L1 antibody for targeted delivery of docetaxel. The PD-L1 targeted nanoparticles showed higher uptake in cells compared with non-targeted nanoparticles and could enhance G2/M arrest and apoptosis in gastric cancer cell lines. Emami et al.<sup>140</sup> developed polymeric (lipoic acid-PEG) gold nanoparticles to conjugate PD-L1 antibody for delivery of doxorubicin to colorectal cancer cells. Treatment of nanoparticles with NIR irradiation significantly increased apoptosis and cell cycle arrest in CT-26 colon cancer cells. *In vivo* data were

not reported for either nanoparticle delivering chemo with PD-L1 antibody. One clinical trial has investigated the combination of nab-paclitaxel (abraxane) with atezolizumab for metastatic TNBC.<sup>141</sup> Results of the clinical trial were promising and this combination has recently been granted FDA approval as the first line treatment for metastatic TNBC.

### **1.5.3 Translation of nanoparticle delivery platforms for cancer**

Overall, despite the promise and many efforts, the translation of nanoparticles for cancer treatment has not significantly progressed.<sup>128</sup> To date only four nanoparticles have been granted FDA approval for solid tumors. Abraxane (albumin bound paclitaxel nanoparticle) and Doxil (liposomal doxorubicin) were the first approved FDA nanoparticles for cancer, where they were shown to alleviate some systemic toxicity compared with the free chemotherapy counterpart in clinical trials. Eligard is a leuprolide acetate polymeric (PLGH) nanoparticle, a GnRH agonist, which is approved for advanced prostate cancer. Onivyde is a liposomal irinotecan which received FDA approval in 2015 for treatment of metastatic pancreatic cancer that has been previously treated with chemotherapy. For NSCLC, abraxane received FDA approval in 2012 as the first line treatment in combination with carboplatin for locally advanced or metastatic NSCLC who cannot undergo surgery or radiation. Abraxane remains the only approved nanoparticle therapeutic for NSCLC.

In regards to siRNA delivery, most nanoparticle carriers that have reached clinical trials are lipid based without stealth material (e.g., PEG) and targeting agent, thus they intrinsically home to the liver and are not effective at treating other solid tumors (such as TKM-PLK1 as aforementioned).<sup>142</sup> The only FDA approved siRNA therapeutic is patisiran

(approved in 2018) which targets transthyretin for the rare but fatal liver disease familial amyloid polyneuropathy. For cancer, no siRNA (or miRNA) therapeutic is FDA approved. Several issues in clinical trials have been observed<sup>143-145</sup> including toxicity to the liver and spleen (e.g., ALN-VSP02), immunogenicity (e.g., MRX34), immature destabilization (e.g., CALAA-01), non-specific uptake due to the lack of targeting agents (e.g., DCR-MYC, Atu027, TKM-PLK1, ALN-VSP02) and challenges in large-scale manufacturing. Superior nanoparticle delivery platforms are needed to meet the clinical demands of delivering therapeutics effectively to tumors.

## **1.6 Novel mesoporous silica nanoparticles for cancer**

Our group has extensively developed and optimized mesoporous silica nanoparticles for drug and siRNA delivery. As compared with other nanoparticle materials, MSNP provide several advantages. First, MSNP are highly scalable and reproducibly synthesized at a much cheaper cost than many alternative platforms such as gold. Moreover, MSNP is porous and can be loaded with imaging agents and drugs in the pores, while therapeutics such as siRNA and antibodies can be loaded on the exterior. We and others have also shown that MSNP degrades to benign silicic acid,<sup>146,147</sup> which is cleared by the kidneys in urine. Silica is the third most abundant trace element in the body after iron and zinc, implicating its intrinsic safety.<sup>148</sup> Systemic administration of MSNPs has been investigated in clinical trials for delivering an imaging agent<sup>149</sup> or as a coating of gold particles.<sup>150</sup> However, MSNP as a therapeutic carrier has yet to be investigated in clinical trials for cancer treatment.



To allow for *in vivo* delivery of therapeutics, our MSNP platform is assembled in a layer-by-layer fashion with: (1) cross-linked cationic polymer (polyethylenimine, PEI) allowing endosomal escape of siRNA and other nucleic acids, (2) PEG to prevent nucleic acids from enzymatic degradation and to make the nanoparticle stealth from the body's immune system, and (3) antibody for tumor targeting. PEI was chosen as the most effective endosomal-escape polymer. As high molecular weight (MW) PEI can be toxic, we cross-linked small MW PEI with a bio-reducible crosslinker to achieve the efficacy of high MW PEI while releasing small clearable PEI fragments afterward to mitigate toxicity. Moreover, small molecule inhibitors or chemotherapies can be loaded in the pores of MSNP prior to the polymer coating, while nucleic acids can be attached to the final construct (via electrostatic interaction with PEI) with just a few minutes mixing in saline. This versatility allows for practically any therapeutic to be integrated into the platform and novel combination therapy strategies to be evaluated. The multiple therapeutic delivery capability of the nanoparticles opens doors for future precision medicine approaches, where biomarkers can initiate facile development of patient-specific targeted nanoparticles. Figure 1.3 illustrates the layer-by-layer synthesis procedure of the MSNP platform.

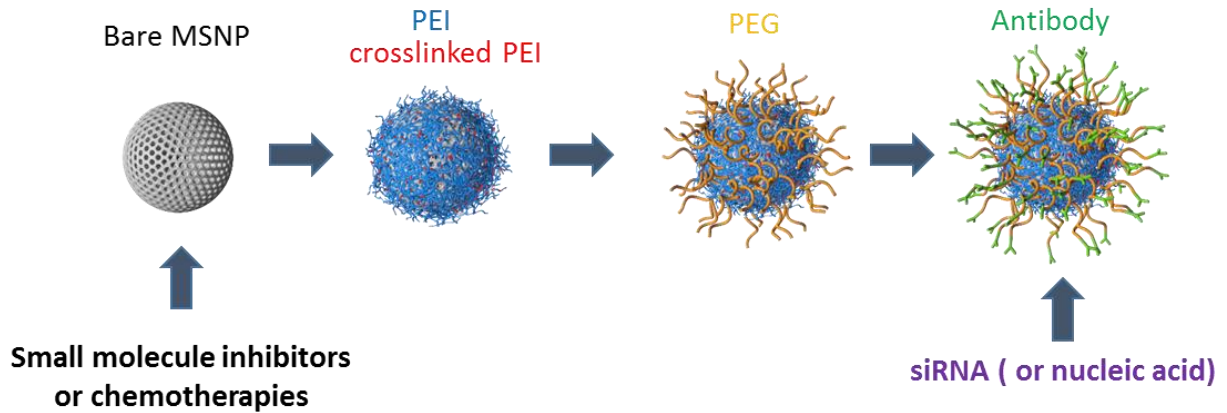


**Figure 1.3. Mesoporous silica nanoparticle platform.** Small molecule inhibitors or chemotherapies can be loaded in pores of MSNP. Following polymer surface modification with PEI and PEG, antibodies can be conjugated and nucleic acids (e.g. siRNAs) can be electrostatically bound.

The MSNP platform was originally developed as a HER2+ breast cancer targeted therapy, which has been under development with two fast-track phase I/II SBIR awards from the NCI. Under the awards, our group has shown (1) formulation optimization and stability after a long-term storage,<sup>151,152</sup> (2) siRNA, PEI and silica release mechanisms, body distribution and clearance,<sup>153</sup> and (3) safety of the platform in rodent models.<sup>153</sup> Overall, the platform has very favorable efficacy and safety profile, and all success indicates great clinical translational potential of the platform.

## **Chapter 2: PLK1 and EGFR targeted nanoparticle as a radiation sensitizer for non-small cell lung cancer**

### **2.1 INTRODUCTION**

Non-small cell lung cancer (NSCLC), which makes up 85% of lung cancers, is the leading cause of cancer mortality, resulting in more deaths than colon, breast, and prostate cancers combined, and represents nearly a fourth of total cancer deaths.<sup>1</sup> Radiation therapy remains a cornerstone in lung cancer treatment that is administered to over half of all patients as part of their treatment paradigm.<sup>154</sup> Advances in medical imaging and radiation technology have allowed for more precise and accurate radiation delivery; however, outcomes for lung cancer patients have not improved<sup>155</sup> as the five year survival remains 18%.<sup>1</sup> The radiation therapy oncology group clinical trial RTOG 0617 for stage III NSCLC, which aimed to improve local tumor control and prolong survival by increasing the radiation dose (from 60 Gy to 74 Gy) in a chemoradiation regimen, did not result in better outcomes but rather caused higher toxicity to patients leading to reduced survival.<sup>15</sup> In the same trial however, the addition of cetuximab (an EGFR-directed monoclonal antibody believed to inhibit DNA repair) led to modest improvements in patients with high EGFR expression.<sup>15</sup> This highlights the potential of molecularly targeted agents to improve the therapeutic ratio of radiation leading to better outcomes for patients. The goal of this research is to develop a targeted therapeutic to enhance radiation sensitivity of lung cancer. We previously reported on a human epidermal growth factor receptor 2 (HER2) antibody conjugated mesoporous silica nanoparticle (MSNP) that could target cancer cells in multiple HER2+ breast tumor mouse models and deliver small interfering

RNA (siRNA) to impart gene silencing efficacy.<sup>119,151,156</sup> Herein, I developed the MSNP platform for lung cancer, where effective targeted therapies are an urgent need. By conjugating an EGFR monoclonal antibody on MSNPs and delivering siRNA against polo-like kinase 1 (PLK1), I show that the nanoparticle is effective as both a single agent therapy and as a radiation sensitizer for NSCLC.

We target PLK1, a key mitotic regulator, which is overexpressed in lung cancer and other various types of cancer.<sup>4</sup> Previous studies have shown that high PLK1 expression is correlated with reduced survival for cancer patients.<sup>3,157,158</sup> Inhibition of PLK1 results in failure to complete mitosis, which leads to G2/M cell cycle arrest and apoptotic cell death. As G2/M is the most radiation sensitive cell cycle phase, PLK1 inhibition also sensitizes cancer cells to radiation.<sup>159</sup> Furthermore, PLK1 has been shown to contribute to resistance of cancer cells to several drugs including taxanes, doxorubicin, gemcitabine,<sup>87</sup> and EGFR inhibitors.<sup>88</sup> In addition, PLK1 has been identified as a target to kill various cancer stem cells,<sup>89-91</sup> which are resistant to standard therapies including radiation and chemotherapy, and therefore lead to cancer relapse. Collectively, these observations suggest that inhibition of PLK1 may have promising therapeutic potential for cancer treatment.

To deliver the nanoparticle platform specifically to lung cancer cells, the EGFR monoclonal antibody, cetuximab, was conjugated on MSNP. EGFR is overexpressed in several cancers, and its high expression correlates positively with poor prognosis.<sup>160-163</sup> In NSCLC, EGFR is overexpressed in about 50% of patients<sup>164</sup> with higher EGFR expression in more advanced stages.<sup>160,165</sup> Thus, the receptor is an appropriate homing target. Furthermore, following radiation damage, EGFR is phosphorylated and

translocates to the nucleus where it plays a role in mediating DNA repair.<sup>29</sup> In this regard, addition of cetuximab may have therapeutic benefit as it has been shown to block the translocation of EGFR to the nucleus following irradiation.<sup>166</sup> Indeed, cetuximab has shown promise in clinical trials as a radiation sensitizer in head and neck cancer<sup>167</sup> and EGFR+ lung cancer.<sup>168</sup> Therefore, cetuximab on the nanoparticle may also provide a therapeutic effect, in addition to mediating the targeting to EGFR+ lung cancer cells. I hypothesized that the combination of the EGFR antibody cetuximab and PLK1 siRNA on the nanoparticles (C-siPLK1-NP) would serve as potent radiation sensitizer for NSCLC, as illustrated in Fig. 1A. An effective radiation sensitizer would render cancer cells more susceptible to death by radiation, thereby improving treatment efficacy and reducing adverse effects of radiation therapy. Thus, this study highlights a novel strategy that may significantly improve the outcomes and quality of life for lung cancer patients.

## **2.2 MATERIALS AND METHODS**

### **2.2.1 Nanoparticle synthesis and characterization**

Sol-gel synthesis of bare MSNPs and layer-by-layer surface coating of MSNPs was carried out in the same manner as in our previous report.<sup>11,151</sup> For conjugation of cetuximab to PEG of the nanoparticles, cetuximab (2 mg/ml, Eli Lilly and Company) was buffer-exchanged to PBS pH 8 using Zeba Spin columns (Thermo Fisher Scientific) and thiolated with Traut's reagent (50-fold molar excess) for 2 hr (350 rpm). Thiolated cetuximab was then exchanged to buffer PBS pH 7.2 and added to MSNP-PEI-PEG at 10% w/w for shaking (300 rpm) overnight at 4°C. The next day, nanoparticles were

washed 2x with PBS pH 7.2. SiRNA is loaded last by quick mixing with NP (~5 minutes). Nanoparticles size and charge were determined by Zetasizer (Malvern). To quantify polymer loading, 1 mg nanoparticles (MSNP, MSNP-PEI, or MSNP-PEI-PEG) were heated to 950 °C (20 °C/min) with TGA Q50 (TA Instruments). Weight/temperature profiles of MSNP, MSNP-PEI, and MSNP-PEI-PEG were compared to determine percent loading of each polymer and final silica yield. Amount of antibody on NP was determined by Pierce BCA protein assay kit (Thermo Fisher Scientific). SiRNA loading extent on NP was determined by fluorescence using a fluorescent tagged siRNA (Dy677-siSCR), as in our previous report.<sup>151</sup>

### **2.2.2 Cell culture and reagents**

Non-small cell lung cancer cells A549 (CCL-185) and H460 (HTB-177) were obtained from ATCC and cultured in RPMI-1640 medium with 10% fetal bovine serum (FBS). A549 cells with stable expression of red-shifted firefly luciferase gene (Bioware® Brite Cell line A549-Red-Fluc) were purchased from Perkin Elmer and maintained under the same conditions as parental A549 cells. Normal lung epithelial cells NL20 (CRL-2503) were purchased from ATCC and maintained in the recommended complete growth medium. *In vivo* grade siRNA was purchased from Dharmacon. The siRNA sequences used were: PLK1 (antisense 5'-UAUUCAUUCUUCUUGAUCCGG-3'); scrambled SCR (antisense 5'-UUAGUCGACAUGUAAACCA-3'). Scrambled siRNA with dyes (DyLight 677 or Alexa Fluor 488) attached to the sense strand were purchased from Dharmacon.

### **2.2.3 Nanoparticle cellular internalization and EGFR surface expression**

Nanoparticle internalization in cells was performed in suspension as we have previously reported.<sup>151</sup> Briefly, cells ( $1 \times 10^6$ ) were harvested and incubated with Alexa Fluor 488 dye

tagged siSCR nanoparticles (100  $\mu\text{g}$  NP) for one hr. Cells were then washed 3x with FACS buffer and resuspended in 0.5 mL FACS buffer. Trypan blue (0.4% in PBS, 0.5 mL) was added to each suspension to exclude signal from non-internalized nanoparticles. Cells were analyzed on a Guava easyCyte (Millipore Sigma) flow cytometer (10,000 events per sample). For EGFR cell surface expression of cancer and normal cells, human EGFR antibody (cetuximab) was used as primary antibody followed by washing 3x with FACS buffer, before staining with anti-human Alexa Fluor 488 secondary antibody (Life Technologies) for one hr. Cells were then washed 3x with FACS and analyzed with flow cytometer. For EGFR cell surface expression post treatments, 1 million cells were treated with non-target NP, C-NP (3  $\mu\text{g}$  cetuximab), or cetuximab (100  $\mu\text{g}$ ) for two hr. Cells were washed with FACS buffer before staining with an Alexa Fluor 647 labeled EGFR antibody (BD Biosciences), washing, and analyzing with flow (10,000 events per sample, biological replicates).

#### **2.2.4 Western blot**

Cells were seeded in 6 well plates overnight and treated with PBS or C-NP with SCR or siPLK1 (50 nM – NP/siRNA = 50). Cell culture medium was changed one day after treatment. Three days post treatment, cells were lysed in RIPA buffer (50-100  $\mu\text{l}$  per well). Lysate was sonicated and centrifuged (15,000 RPM for 15 minutes) and supernatant was collected. Amount of total protein was quantified using BCA. 30  $\mu\text{g}$  of proteins (per sample) were mixed with 4X Novex NuPAGE LDS sample buffer and beta-mercaptoethanol (10% final concentration). Samples were denatured for 5 min at 95  $^{\circ}\text{C}$  and loaded onto gel (NuPAGE) for electrophoresis. Proteins were then transferred onto PVDF-FL membrane and blocked with LICOR blocking buffer. Membranes were

incubated with primary antibodies overnight (PLK1,  $\beta$ -actin) at 4°C. Next day, membranes were rinsed with TBS-T and IRDye conjugated secondary antibodies (LI-COR) were added for 1 hour under rocking at room temperature. Membranes were scanned on a LI-COR Odyssey CLx imaging system.

### **2.2.5 RNA isolation and RT-PCR**

RNA was isolated and purified from cells or tumors with GeneJet RNA purification kit (Thermo Fisher Scientific) according to manufacturer's instructions. Tumors were homogenized in lysis buffer using Bullet Blender 5E (Next Advance) prior to RNA isolation. One-Step qRT-PCR was performed using EXPRESS One-Step Superscript™ qRT-PCR Kit (Invitrogen). 20 ng RNA per reaction was used. Cycling conditions were 50 °C for 2 min, 95 °C for 10 min, 40 cycles of 95 °C for 15 s, and 60 °C for 1 min. TAQMAN gene expression primer Human HPRT mRNA (Hs99999909\_m1) was used as housekeeping gene and Human PLK1 mRNA (Hs00983225\_g1) was used to assess PLK1 gene knockdown in tumors and cell lines (PLK1 relative to HPRT). Data was analyzed using  $2^{-\Delta\Delta C(t)}$  method.

### **2.2.6 Cell cycle arrest**

Cells (50K/well) were seeded in 6 well plates overnight and treated with PBS, PLK1 inhibitor BI6727 (10 nM), C-siSCR-NP, or C- siPLK1-NP (50 nM – NP/siRNA = 50). Cell media was changed one day after treatments. At various time points, cells were collected, washed with FACS, and stained with Hoechst for 30 min at 37 °C before analyzing with flow cytometer. Percentage of cells in each phase was determined using FlowJo software.



### **2.2.7 Cell viability**

For cell viability without radiation, cells were seeded in 96 well plates overnight and treated with PBS, C-siSCR-NP, or C-siPLK1-NP (30-60 nM – NP/siRNA = 50). Cell media was changed one day after treatments. 4 days post treatment, CellTiter-Glo (CTG) assay (Promega) was performed according to manufacturer's instructions. Tecan plate reader was used to quantify luminescence. For cell viability following radiation, cells were treated with NP and radiation as in described for clonogenic survival. Following radiation, cells were plated in 96 well plate (1K cells/well) in quadruplicates. One week post radiation, CTG assay was performed.

### **2.2.8 Clonogenic survival**

Cells (50K/well) were seeded in 6 well plates overnight and treated with PBS, C-siSCR-NP, or C-siPLK1-NP (15-120 nM – NP/siRNA = 50). Cell media was changed one day after treatments. 72 hr post treatment, cells were irradiated using a Cs-137 irradiator (Sheperd Mark) with 0, 2, 4, 6 Gy. Cells were then harvested, counted, and re-plated in 6 well plates (50-100 cells for 0 Gy, 100-200 cells for 2 Gy, 200-400 for 4 Gy, 500-2000 for 6 Gy). Two weeks post radiation, colonies were fixed with methanol and stained with crystal violet (0.5% in 25% methanol) and counted. Colonies of >50 cells were scored. Survival fraction was calculated as described in literature <sup>169</sup>.

### **2.2.9 $\gamma$ H2ax staining**

Cells (1500/well) were seeded in 96 black well plates overnight and treated with PBS, siSCR-NP, siPLK1-NP, C-siSCR-NP, or C-siPLK1-NP (30 nM – NP/siRNA = 50). Cell media was changed one day after treatments. 72 hr post treatment, cells were irradiated with 0, 2, 6 Gy using Cs irradiator. 24 hr post irradiation, cells were fixed with methanol,

washed, and stained with phosphor-histone H2ax antibody (Cell Signaling #2577) for 1 hr. Cells were washed and stained with anti-rabbit Alexa Fluor 488 secondary antibody (Life Technologies) for 1 hr, followed by Hoechst 33342 (10 ug/ml) for 15 minutes. Cells were imaged on an EVOS FL Auto fluorescence microscope at 20X magnification.  $\gamma$ H2ax foci per nuclei was determined using Cell Profiler (Broad Institute).

### **2.2.10 Apoptosis**

Cells (50K/well) were seeded in 6 plates overnight and treated with PBS or C-siPLK1-NP (50 nM – NP/siRNA = 50) the next day. Cell media was changed 24 hr after treatments. 72 hr post treatment, cells were irradiated with 0 or 6 Gy. One day post radiation, cells were collected and washed with FACS buffer. Annexin V primary antibody (Abcam ab14196) was added for 30 minutes at room temperature, followed by Alexa Fluor 488 secondary antibody for 30 minutes at room temperature. Cells were then washed 2x with FACS buffer and propidium iodide (PI) was added at 10  $\mu$ g/ml for 5 minutes. Cells (10,000 events per sample) were analyzed with flow cytometer. Annexin-/PI- indicates healthy cells, Annexin-/PI+ indicates dead cells, Annexin+/PI- indicates early apoptotic cells, and Annexin+/PI+ indicates late apoptotic cells.

### **2.2.11 Animal Studies**

For evaluation of the therapeutic as a radiation sensitizer, A549 cells (5 million) were subcutaneously injected into left and right flank of 6-week old male SCID mice (NCI SCID/NCr; Charles River Laboratories) in matrigel (Corning). Tumor growth was monitored using a Vernier caliper and volume calculated by  $0.5 \times \text{length} \times \text{width}^2$ . When tumor sizes reached average of 120 mm<sup>3</sup>, mice were grouped to receive saline, C-siSCR-

NP, or C-siPLK1-NP intra-tumoral injections to both left and right tumors. Three days following each NP injection (0.3 nmol siRNA per tumor), the left tumors of mice were irradiated at 2 Gy using a small animal x-ray irradiator. Mice were anesthetized and a lead shield (Braintree Scientific) that exposes only the left flank of mice was used. NP and radiation were administered once a week for 6 consecutive weeks. Two weeks after last radiation dose, mice were sacrificed and all tumors were harvested, weighed, and prepared for RNA analysis.

To establish orthotopic tumors in lungs of mice, I adopted an intra-tracheal instillation procedure.<sup>170</sup> Mice were anesthetized using isoflurane, placed on intubation stand (BrainTree Scientific) angled at 60°, and held in place by hooking upper incisors over a small rubber band located at the top of the stand. A fiber optic light source was placed over from the neck of the mouse. The mouse's tongue was then retracted to one side to visualize trachea. Once the tracheal opening was visualized, the gavage catheter (2 mm round tip) is inserted with attached syringe containing 100 µl of sterile saline at the opposite end of the syringe. If in the trachea, motion of the saline occurs as the mouse breathes. The syringe containing saline was then removed, and a solution containing 5 million A549-Luc cells with 5 mM EDTA in cell media was pipetted in the gavage catheter, followed by 100 µl of air. Mice were monitored until recovery from anesthesia. Three weeks following intra-tracheal instillation, mice were injected intravenously with 300 µl of saline, C-siSCR-NP, or C-siPLK1-NP (0.5 mg siRNA/kg animal). Luminescence in lungs (tumor burden) was monitored with IVIS. For IVIS, mice were i.p. injected with 150 mg/kg luciferin (Gold Bio) 20 minutes prior to imaging. Tumor burden was determined by averaging photon flux of mice in prone and supine positions. Mice were monitored daily

and weighed once a week during the course of study. All studies were reviewed and approved by Institutional Animal Care and Use Committee (IACUC) at Oregon Health and Science University (OHSU).

### **2.2.12 Statistical analysis**

Comparison between two groups was performed with Student's *t* test. Comparisons among 3 or more groups were performed using one-way ANOVA with Bonferroni's correction for multiple comparisons, or two-way ANOVA with Tukey's correction when comparing treatments across radiation doses (i.e.  $\gamma$ H2ax). Tumor burden over the course of treatment was analyzed using two-way ANOVA with Tukey's correction for multiple comparisons. Kaplan Meier survival curve was analyzed using the log-rank (Mantel-Cox) method. Significance was set at  $p < 0.05$ . *In vitro* data are expressed as mean  $\pm$  SD; *in vivo* data are expressed as mean  $\pm$  SEM. GraphPad Prism 8.0 (GraphPad Software Inc.) was used for all statistical analysis.

## 2.3 RESULTS

### 2.3.1 Nanoparticle characteristics

In comparison to other nanoparticle drug carriers, MSNPs offer several advantages such as being biologically benign, having large surface area and high porosity, ease of controlling size and modifying surface chemistry, and high scalability. Fig. 2.1A depicts a schematic representation of the proposed combination effect of EGFR antibody and siPLK1 on our nanoparticle platform. Our platform consists of an MSNP core (~50 nm by TEM – Fig. 2.1B) coated layer-by-layer with: 1) bio-reducible crosslinked polyethylene imine (PEI) which allows the use of low MW PEI as a cationic polymer for siRNA binding and effective endosomal escape, 2) polyethylene glycol (PEG) to prevent aggregation, opsonization, and immune response, and 3) antibody to target specific cell type. To target EGFR+ cells, cetuximab was conjugated to the nanoparticle platform (Fig. 2.1C) to obtain a final particle size of 115 nm (Fig. 2.1D) with a slightly cationic charge of +13 mV in 10 mM NaCl (Table 1). I achieved excellent batch to batch nanoparticle synthesis as measured in terms of core particle size, final size after surface modification, siRNA loading, and knock-down efficacy using luciferase as a model gene as shown in Figure 2.2. The composition of the final construct contains 15% PEI and 10% PEG (quantified by thermal gravimetric analysis, TGA), and 2.7% antibody/MSNP (quantified by BCA assay) (Table 1). SiRNA (2 wt.% of MSNP) is loaded last onto the nanoparticle via electrostatic interactions between the negatively charged siRNA and the cationic polymer PEI. As the loading of siRNA on the nanoparticle is sequence non-specific, any siRNA (or a set of siRNAs) can be loaded in under 5 minutes.<sup>11</sup> This flexibility in changing siRNAs offers potential for future personalized medicine approaches.

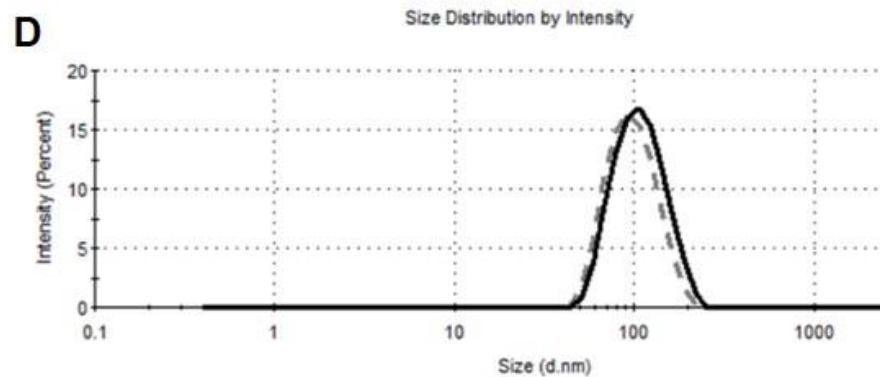
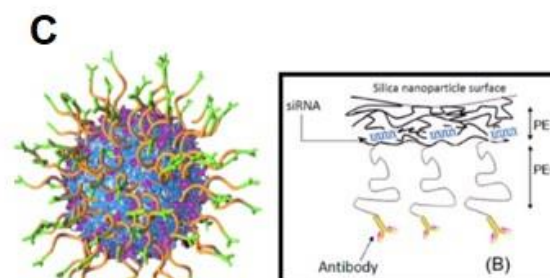
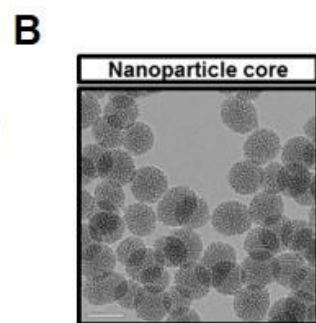
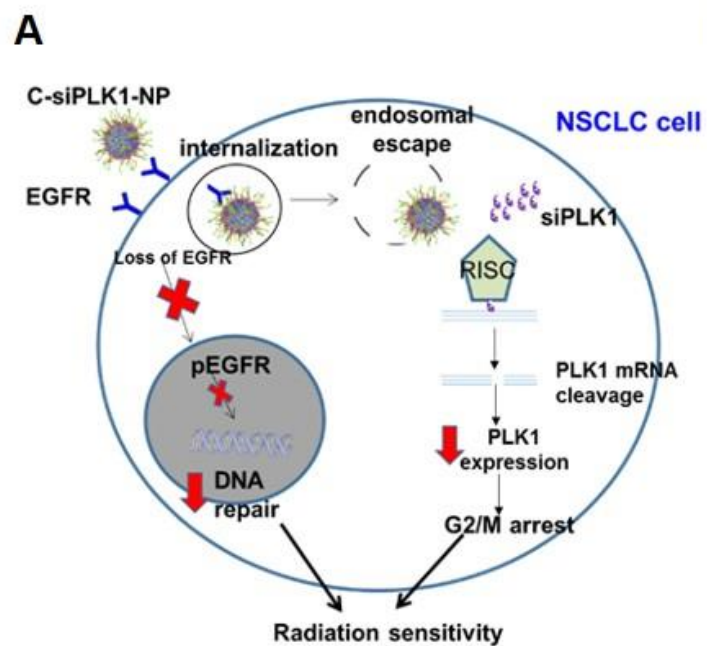
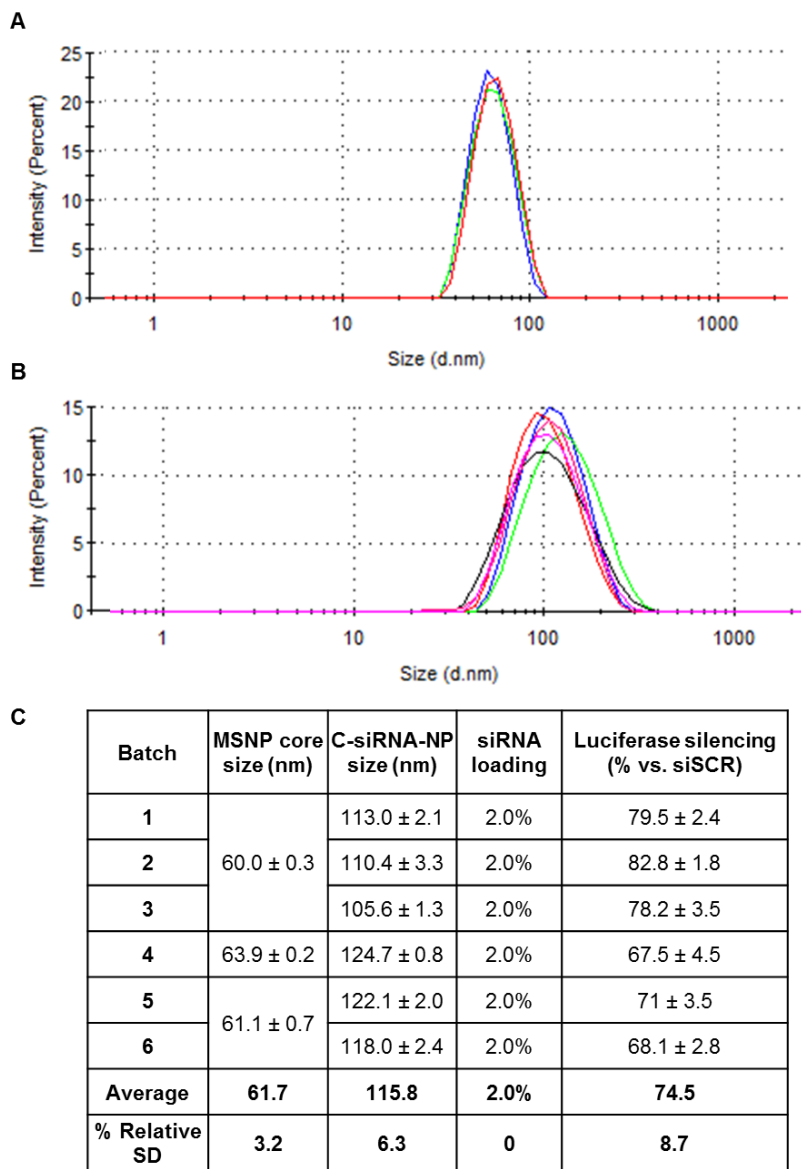


Table 2.1

MSNP size (nm)	Hydrodynamic size with modifications		Zeta potential (mV)	TGA		BCA	complete siRNA loading
	Size (nm)	PDI		%PEI	%PEG	%antibody/MSNP	
61.7 ± 2.0	115.8 ± 6.9	0.23 ± 0.02	13.4 ± 0.7	15.4	9.8	2.7	2-4%

**Figure 2.1. EGFR-targeted (cetuximab) mesoporous silica nanoparticle (NP) platform for PLK1 siRNA (siPLK1) delivery or C-siPLK1-NP.** (A) Scheme of central hypothesis illustrating the proposed combination effect of EGFR antibody and siPLK1 on our nanoparticle platform as a novel radiation sensitizer. C-siPLK1-NPs bind to EGFR receptors and are internalized, resulting in the loss of EGFR and phosphorylated EGFR, which can normally reach the nucleus to repair DNA. This reduces the cell's ability to repair the damage caused by radiation. Simultaneously, siPLK1 on the nanoparticles is released in the cytosol and incorporated in the RNA induced silencing complex (RISC) to mediate PLK1 mRNA cleavage, which reduces PLK1 protein expression and arrests the cells in G2/M where they are most sensitive to radiation damage. Therefore, the platform serves a dual role (by targeting PLK1 and EGFR) to sensitize NSCLC cells to radiation. (B) TEM image of 50-nm MSNP (scale bar = 50 nm). (C) Schematic of the nanoparticle construct with layer-by-layer surface modifications. (D) Representative hydrodynamic size of C-NP with (solid) and without siRNA (dotted) loading by Zetasizer.

**Table 2.1. Characterization of C-siRNA-NP.** Hydrodynamic size of bare MSNP and C-siRNA-NP determined by Zetasizer. Data expressed as mean  $\pm$  SD. Polymer loading (PEI and PEG) determined by thermal gravimetric analysis (TGA). Antibody (cetuximab) loading determined by BCA assay. Complete siRNA binding at 2 wt.% and 4 wt.% assessed by loading a fluorescent labeled siRNA (Dy677-siRNA) on C-NP.



**Figure 2.2 Reproducibility of nanoparticle synthesis.** (A) Hydrodynamic size of core MSNP (3 batches). (B) Hydrodynamic size of MSNP after polymer coating and siRNA binding (6 batches). (C) Summary of NP size before and after surface modifications, and luciferase silencing vs. siSCR at dose of 30 nM siRNA against luciferase. Data presented as mean ± SD.



### **2.3.2 Cetuximab conjugated nanoparticles are internalized in EGFR+ cancer cells.**

To determine whether cetuximab conjugated nanoparticles (C-NP) target EGFR+ cancer cells, I performed flow cytometry on EGFR+ cells incubated with siRNA-loaded C-NP. EGFR was chosen as the homing target for NSCLC due to its overexpression, as well as its role in DNA damage repair following radiation. Dye tagged (Alexa Fluor 488) siRNA was loaded to C-NP and incubated with two high EGFR expressing NSCLC cell lines (A549 and H460) and a low EGFR normal lung epithelial cell line, NL-20 (see EGFR expression in Fig. 2.3A). After quenching cells with Trypan blue (to exclude non-internalized particles), uptake in the cell lines was quantified by flow cytometry. The EGFR+ cancer cells internalized the nanoparticles more than 8-fold over the EGFR-low normal lung cell line, illustrating the preferential targeting of nanoparticles to EGFR+ cells (Fig. 2.3B). To confirm the engagement of C-NP to EGFR, cancer cells were treated with C-NP, non-targeted nanoparticles, or free cetuximab antibody. Following a two hr incubation, cells were washed and analyzed with flow cytometry for cell surface EGFR level. As shown in Fig. 2.3C-D, the targeted nanoparticles effectively reduced cell surface EGFR level by over 50% in both cell lines when compared with cells treated with non-targeted nanoparticles or non-treated cells. Moreover, C-NP was more effective than free cetuximab antibody despite much lower dose of cetuximab on the nanoparticles (3  $\mu\text{g}$  cetuximab) than free cetuximab (100  $\mu\text{g}$ ). This owes to the high density of cetuximab on the nanoparticles (i.e., at 2.7 wt.% and  $8.8 \times 10^{13}$  nanoparticles per gram, there are  $1.3 \times 10^3$  antibodies per one nanoparticle) that the cell surfaces were exposed to.

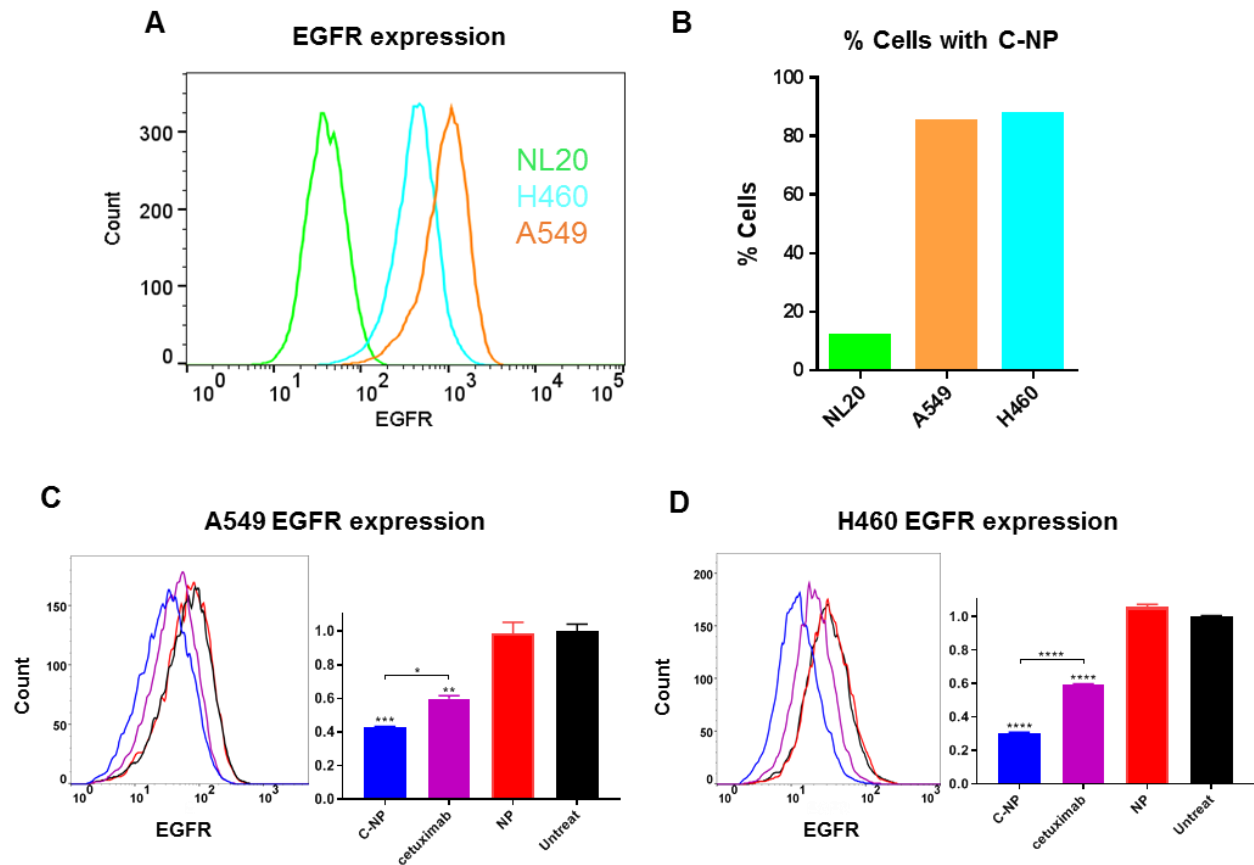


**Figure 2.3. Specific cellular uptake of C-siRNA-NP to EGFR+ cells.** (A) EGFR levels of NSCLC (A549, H460) and normal (NL20) cells by flow cytometry. (B) A fluorescent labeled siRNA (Dy677 siRNA) on C-NP shows higher internalization in EGFR+ NSCLC cells (A549, H460) over normal NL20 lung cells by 8-fold. EGFR surface labeling in (C) A549 and (D) H460 upon incubation with C-NP, cetuximab, or NP in NSCLC cell lines. 100  $\mu$ g NP or C-NP doses (2.7  $\mu$ g cetuximab), and 100  $\mu$ g free cetuximab, were treated; all with 2 hr contact time. Data presented as mean  $\pm$  SD from independent duplicates (10,000 events per sample); \* $P$ <0.05, \*\* $P$ <0.01, \*\*\* $P$ <0.001, \*\*\*\* $P$ <0.0001.

### 2.3.3 Efficacy of PLK1 knockdown with C-siPLK1-NP

PLK1 is a key target to treat lung cancer and other cancers.<sup>4</sup> However, effective PLK1 inhibition in the clinics remains elusive. To examine PLK1 silencing efficacy by C-NP *in vitro*, NSCLC cells were treated with C-NP loaded with siRNA against PLK1 (C-siPLK1-NP) or scrambled siRNA (C-siSCR-NP). The selected siPLK1 sequence was previously screened and identified to have the best PLK1 knockdown efficacy.<sup>156</sup> As shown in Fig. 2.4, C-siPLK1-NP effectively knocked down >80% of PLK1 mRNA (Fig. 2.4A) and reduced > 90% of PLK1 protein expression (Fig. 2.4B) in both EGFR+ lung cancer cells, while the scrambled siRNA nanoparticle had no effect. The consequence of PLK1 knockdown in the NSCLC cells resulted in significant loss of cell viability (Fig. 2.4C). Furthermore, PLK1 knockdown resulted in the accumulation of cells in G2/M phase of cell cycle, similar to the effect of the PLK1 inhibitor BI2536 (Fig. 2.4D-E). Inducing G2/M arrest increases the cell's sensitivity to radiation damage, as cells in the G2/M phase are more sensitive to radiation than cells in G1 or S phase.<sup>171</sup> Based on this, I determined the time point in which PLK1 knockdown resulted in the highest accumulation of cells in G2/M (Figure 2.5). G2/M arrest induced by PLK1 knockdown was first observed at 24 hr and increased up to 72 hr post treatment. I used the 72 hr time point in subsequent studies to assess the efficacy of C-siPLK1-NP as a radiation sensitizer.

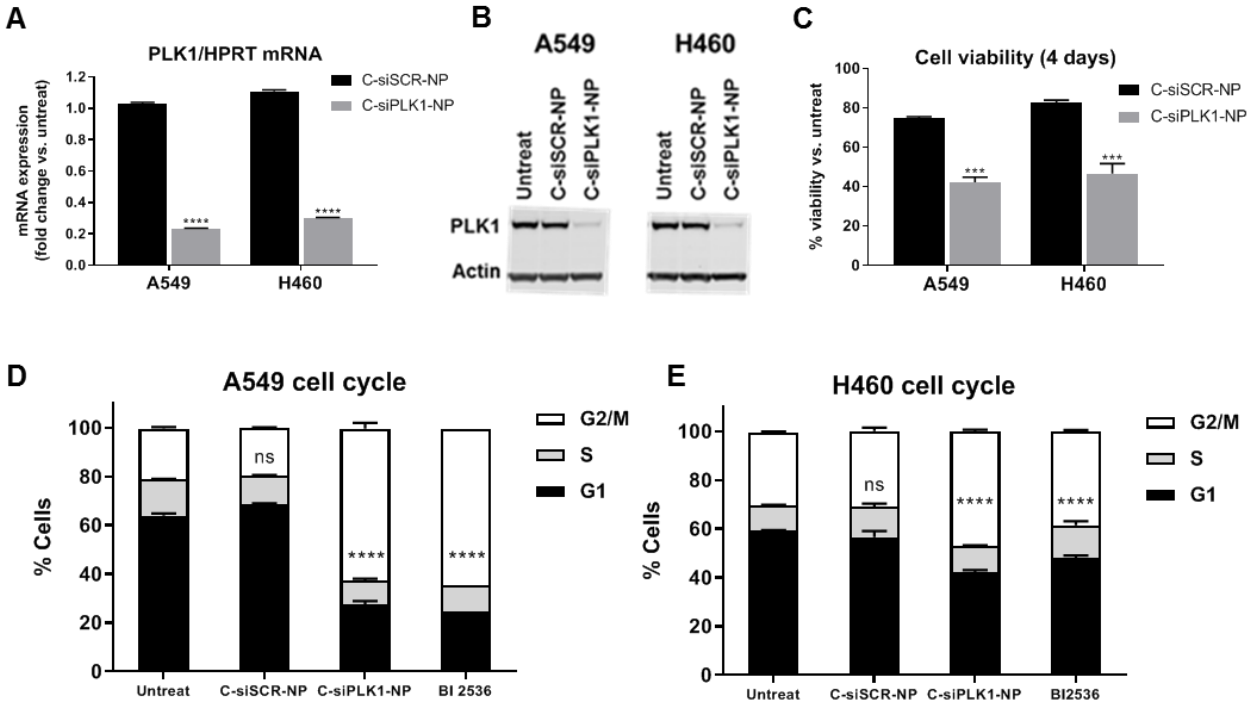


**Figure 2.4. Effects of C-siPLK1-NP treatment on NSCLC (A549, H460) cell lines.** (A) 48-hr PLK1 mRNA knockdown (HPRT used as house-keeping gene) and (B) 72-hr PLK1 protein reduction at 50 nM siRNA dose in A549 and H460. (C) 4-day cell viability at 30 nM siRNA dose in A549 and H460. Data presented as mean  $\pm$  SD from 3-4 independent samples; \*\*\* $P$ <0.001, \*\*\*\* $P$ <0.0001 vs. siSCR control. Cell cycle arrest increase in G2/M phase in (D) A549 and (E) H460 72 hr post treatment of C-siPLK1-NP (50 nM as siRNA) or BI2536 (PLK1 inhibitor, 10 nM). Data presented as mean  $\pm$  SD from independent duplicates (10,000 events per sample); \*\*\*\* $P$ <0.0001 vs. untreat control.

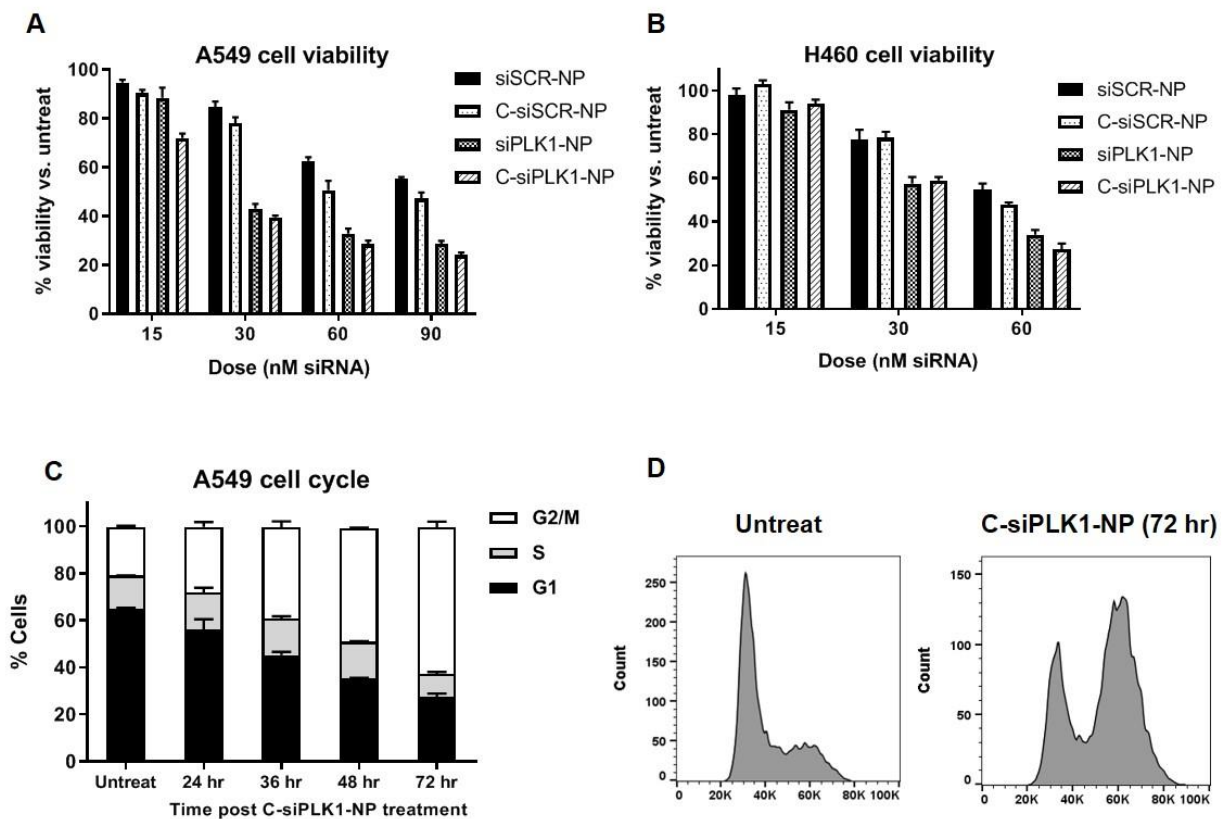


**Figure 2.5. NP dose response and cell cycle arrest.** Dose response of various NP treatments on NSCLC cell viability in (A) A549 and (B) H460. (C) Cell cycle arrest increase in G2/M phase at varying time points post treatment of C-siPLK1-NP. (D) Representative histogram of untreated and 72 hr post treatment of C-siPLK1-NP in A549 cells. Data presented as mean  $\pm$  SD.

### 2.3.4 Targeted nano-therapeutic enhances radiation damage *in vitro*

The efficacy of the nanoparticles as a radiation sensitizer was assessed *in vitro* by established assays: clonogenic survival, cell viability,  $\gamma$ H2ax induction, and apoptosis (Fig. 2.6). A549 and H460 cells were treated with C-siPLK1-NP, C-siSCR-NP, or PBS for 72 hr and irradiated at 2, 4, and 6 Gy. As shown in Fig. 2.6A, C-siPLK1-NP alone reduced colony formation by 60% and when combined with 2 Gy radiation was more effective than

2 Gy and 4 Gy radiation alone and resulted in just 10% survival. Complementary to the clonogenic survival, pre-treated cells were irradiated and plated for 7 days to assess cell viability by CellTiter-Glo (CTG) assay. Cells that received a combination of radiation and either nanoparticle (C-siSCR-NP or C-siPLK1-NP) were significantly less viable than those exposed to the single treatments (nanoparticles or radiation alone) (Fig. 2.6B). Similar results were obtained with H460 cell line (Figure 2.7). I also determined the synergy of the combination using the Chou-Talalay method<sup>172</sup>. The clonogenic survival dose response curves of C-siPLK1-NP alone, radiation alone, and their combination are shown in Fig. 2.6C-D. The combination index (CI) of C-siPLK1-NP (50 nM as siPLK1) and radiation indicates a strong synergistic effect (CI ranged from 0.3-0.5) at all radiation doses tested (2-6 Gy) (Fig. 2.6E). Additionally, I assessed  $\gamma$ H2ax foci induction and apoptosis (24 hr post irradiation - 4 days post NP treatment). H2ax is phosphorylated in response to DNA damaging agents (e.g. chemo or radiation) and thus can be used as a marker to assess DNA damage caused by treatments, in particular double strand breaks.<sup>173</sup> As shown in Fig. 2.6F, radiation or PLK1 knockdown alone induced  $\gamma$ H2ax foci and foci increased significantly after treatment with C-NP than with non-targeted NP. This illustrates the therapeutic benefit of cetuximab (reducing DNA repair capacity) on the nanoparticles in addition to its targeting to EGFR+ cells (shown in Fig. 2.3B). In addition, Annexin V/PI staining was used to confirm apoptotic cell death in response to treatment. The combination of C-siPLK1-NP and radiation resulted in over 50% of cells in late apoptosis (Annexin+/PI+), compared with 33% and 7% for C-siPLK1-NP or radiation alone, respectively (Fig. 2.6G).

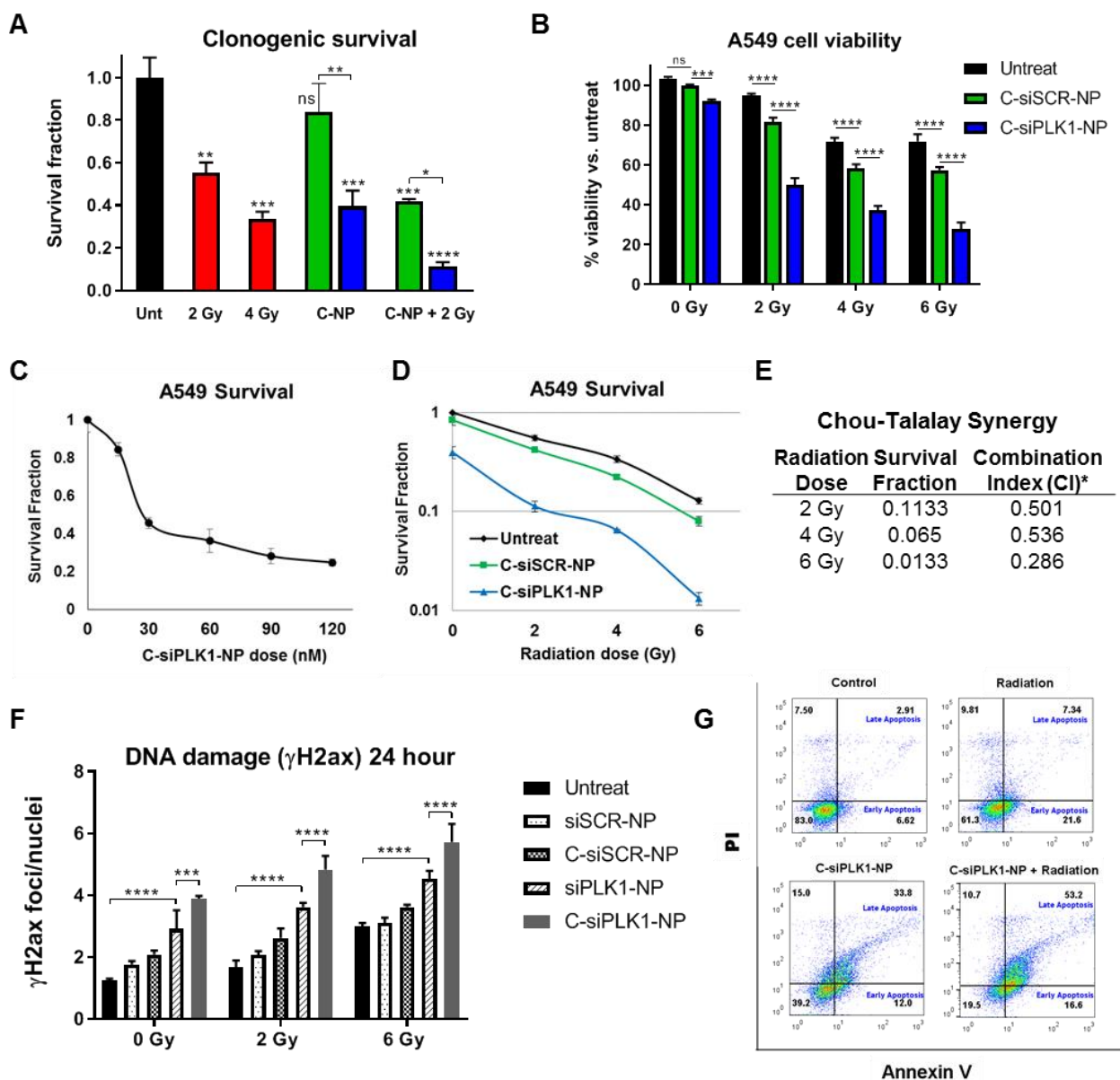


**Figure 2.6. C-siPLK1-NP sensitizes A549 lung cancer cells to radiation.** Cells were treated with C-NP (50 nM as siRNA) for 72 hrs followed by 2-6 Gy irradiation and re-plated for (A) 2-week clonogenic survival or (B) one-week cell viability by CTG assay (B). (C and D) Survival dose response of A549 treated with C-NP (15-120 nM, C), radiation (2-6 Gy, D), and the combination (50 nM C-NP, 2-6 Gy radiation, D). Data presented as mean  $\pm$  SD from 2-3 independent samples; \* $P$ <0.05, \*\* $P$ <0.01, \*\*\* $P$ <0.001, \*\*\*\* $P$ <0.0001. (E) Chou-Talalay synergy analysis reveals synergistic combination at all radiation doses tested. (F)  $\gamma$ H2ax foci induction 24 hr post irradiation (0, 2, or 6 Gy). Non-target NP or C-NP (30 nM) were treated 72 hr prior to irradiation. Data presented as mean  $\pm$  SD from 3-4 independent samples (9 images per sample); \* $P$ <0.05, \*\* $P$ <0.01, \*\*\* $P$ <0.001, \*\*\*\* $P$ <0.0001. (G) Annexin/PI staining 24 hr post 6 Gy irradiation (10,000 events per sample).

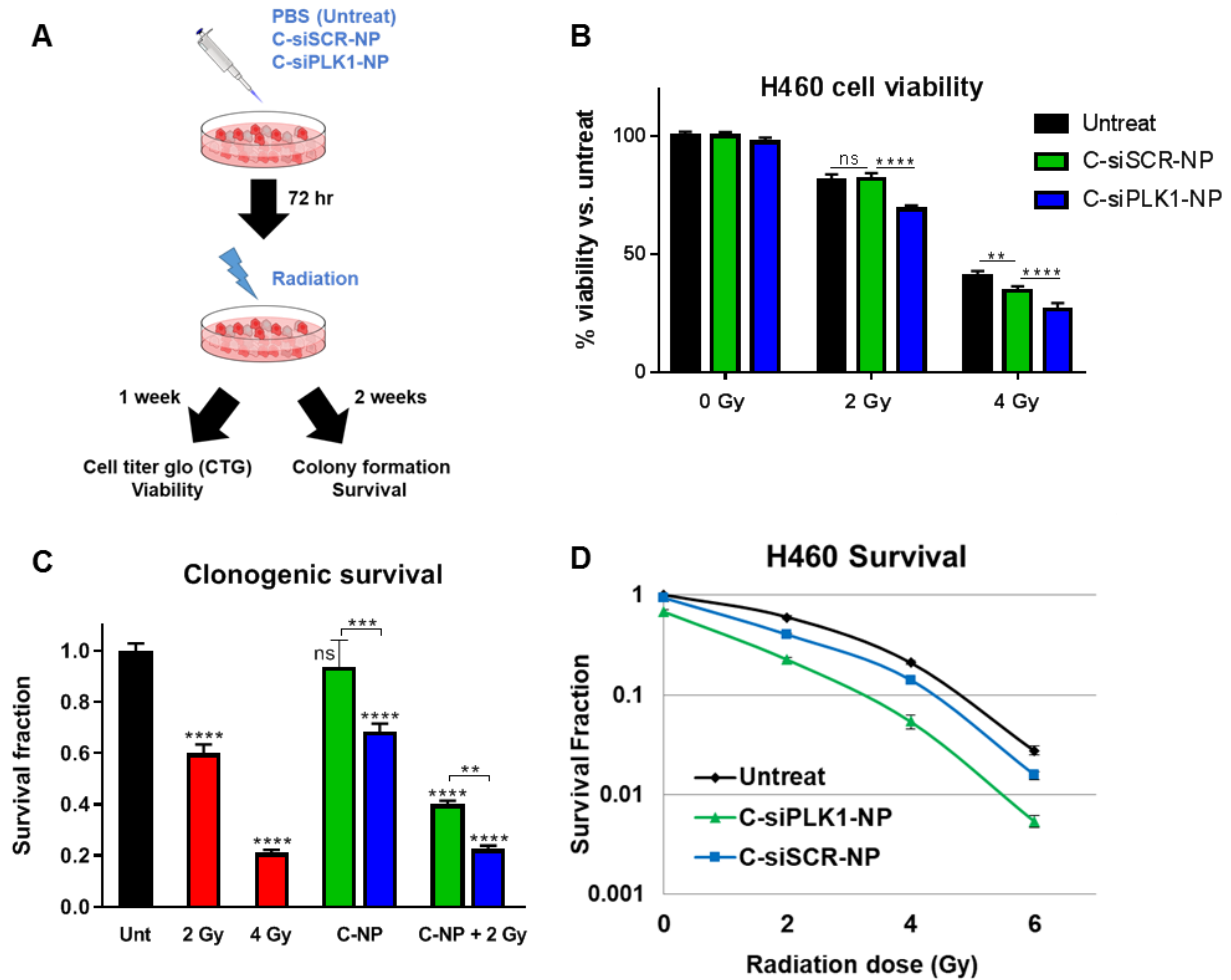


**Figure 2.7. C-siPLK1-NP sensitizes H460 NSCLC cells to radiation.** Cells were treated with C-siPLK1-NP (50 nM) for 72 hrs followed by 2-6 Gy irradiation and re-plated for one week cell viability by CTG assay or 2-week clonogenic survival (A). (B) H460 cell viability (1K cells plated post radiation). (C, D) Clonogenic Survival of C-siPLK1-NP (50 nM), radiation (2-6 Gy), and the combination (50 nM C-NP, 2-6 Gy radiation). Data presented as mean  $\pm$  SD from 2-3 independent samples; \*\* $P < 0.01$ , \*\*\* $P < 0.001$ , \*\*\*\* $P < 0.0001$ .



### 2.3.5 C-siPLK1-NP enhances radiation sensitivity *in vivo*

To investigate the combination of C-siPLK1-NP with radiation *in vivo*, I chose a well-controlled easy-to-irradiate mouse model in which A549 lung cancer cells (5 million) were inoculated in both flanks of Nude SCID mice (two tumors per mouse). When tumors reached  $\sim 120 \text{ mm}^3$ , I intratumorally injected saline, C-siSCR-NP, or C-siPLK1-NP to both tumors on each mouse (at 0.3 nmol siRNA per tumor, once a week). At 72 hr post treatment, 2 Gy radiation was administered to the left tumor (see Fig. 2.8A) using a small animal x-ray irradiator with a lead shield that exposes only the left flank of the mouse. The treatments were administered for 6 consecutive weeks. As shown in Fig. 5, treatments with C-siPLK1-NP (Fig. 2.8B) or radiation alone (Fig. 2.8C) slowed down the tumor growth after multiple doses of NP or radiation, while the combination of radiation and C-siPLK1-NP (Fig. 2.8C) resulted in immediate tumor control and eventual regression of the tumors. Furthermore, tumors that received the combination of C-siSCR-NP and radiation had superior tumor control than radiation alone (Fig. 2.8B-C), owing to the radiation sensitizing effects of cetuximab, as previously discussed. Two weeks after the last radiation dose, mice were sacrificed and tumors were weighed and harvested for mRNA analysis. A significant reduction in tumor weight was observed for mice treated with either nanoparticle (C-siSCR-NP or C-siPLK1-NP) in combination with radiation (Fig. 2.8D). As shown in Fig. 2.8E, tumors treated with C-siPLK1-NP and radiation had significantly less PLK1 mRNA than saline treated or radiation treated tumors, confirming that tumor reduction was correlated to PLK1 knockdown. Although C-siPLK1-NP alone slowed down tumor growth during treatments, there was no reduction of PLK1 mRNA in C-siPLK1-NP treated mice 2 weeks post last dose, which may have been too long to see the siPLK1

effect alone. In all, my *in vitro* and *in vivo* findings demonstrate the potential of the nano-therapeutic as a radiosensitizer.

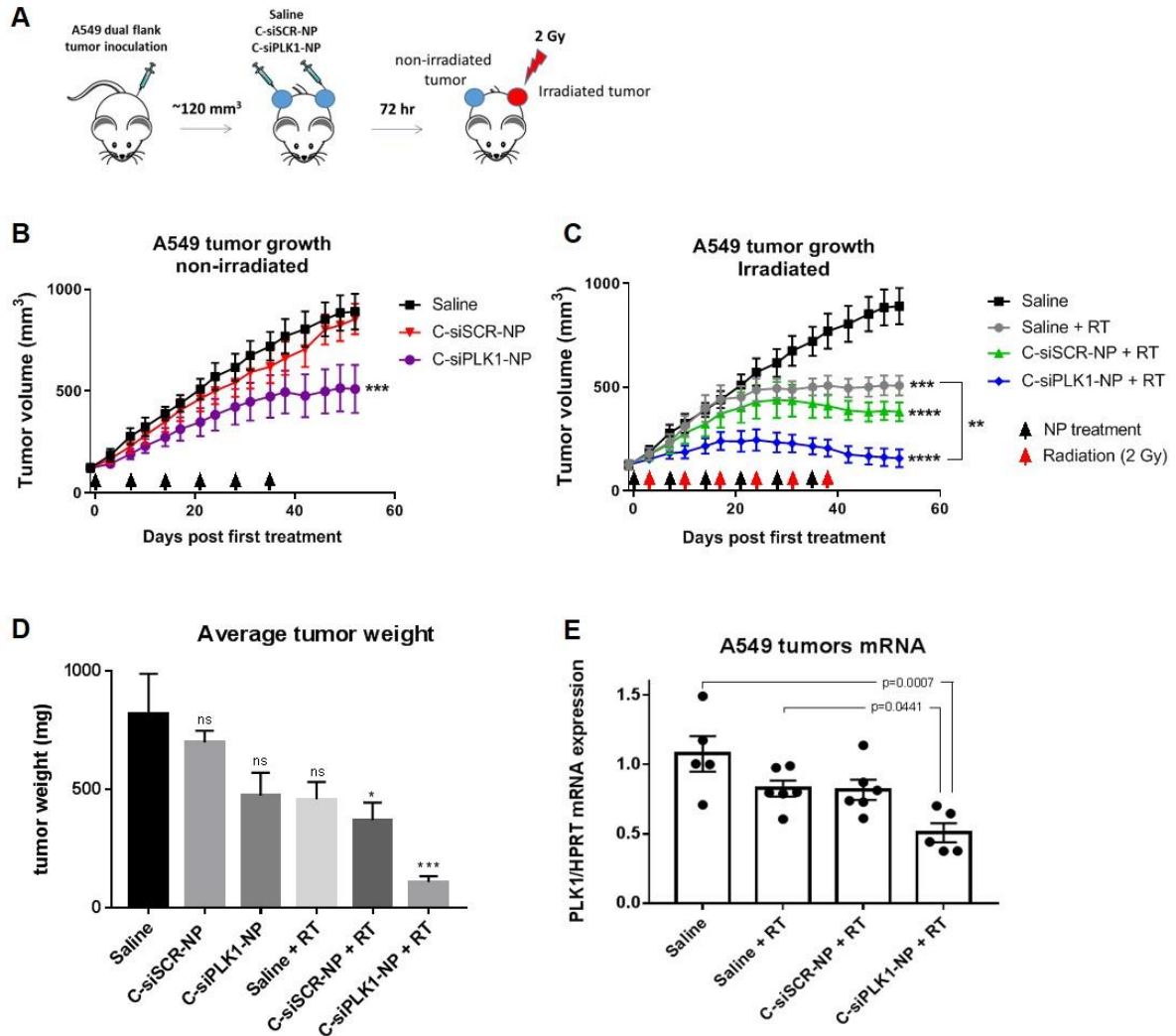


**Figure 2.8. C-siPLK1-NP enhances radiation effects *in vivo*.** (A) 5 million A549 tumor cells were inoculated in both flanks of SCID mice. Treatments (0.3 nmol siRNA per tumor, once a week) and radiation (2 Gy to the left tumor only; 72 hrs post treatments with nanoparticles) were administered for 6 weeks (n=7). Growth of (B) non-irradiated tumors and (C) irradiated tumors in A549 tumor bearing mice treated with saline, C-siSCR-NP, or C-siPLK1-NP. (D) Average tumor weight at sacrifice (day 52 post first treatment; two weeks post last radiation dose). (E) PLK1 mRNA expression of the tumors from (D). Arrows indicate treatment dates. Data presented as mean  $\pm$  SEM; \*P<0.05, \*\*P<0.01, \*\*\*P<0.001, \*\*\*\*P<0.0001.

### 2.3.6 Efficacy of C-siPLK1-NP in orthotopic lung tumor model

To assess the translational potential of the nano-therapeutic as a systemic therapy, I developed an orthotopic lung tumor model using a non-surgical intratracheal instillation procedure (Fig. 2.9). A549 cancer cells expressing luciferase (5 million) were injected through the trachea in anesthetized mice using gavage needles with rounded tips. Tumor growth signal was monitored by bioluminescence using *in vivo* imaging system (IVIS), and upon sacrifice, large tumor nodes are macroscopically visible confirming the presence of tumor in lungs (Fig. 2.9A). Three weeks after tumor inoculation, mice were grouped and injected weekly with saline, C-siSCR-NP, or C-siPLK1-NP intravenously (Fig. 2.9B). Tumor growth was monitored weekly by luminescent signal of mice in prone and supine positions using IVIS. As shown in Fig. 2.9C-D, C-siPLK1-NP significantly reduced the growth of the orthotopic tumors after 8 administrations at a dose of 0.5 mg siRNA/kg animal once per week. Furthermore, mice exhibited no weight loss during treatments (Fig. 2.9E), indicating the safety of the nanoparticle platform, which is in agreement with our prior work. Extended tumor control after the last treatment was also observed for mice treated with C-siPLK1-NP (Fig. 2.9F), which led to prolonged survival compared with mice treated with C-siSCR-NP or saline (Fig. 2.9G). This confirms my *in vitro* findings that C-siPLK1-NP is effective as a single agent therapeutic for NSCLC, and demonstrates the safety and efficacy of the platform, and its potential to serve as a targeted therapy for lung cancer. As previously demonstrated, such efficacy is expected to significantly increase when combining with radiation therapy.

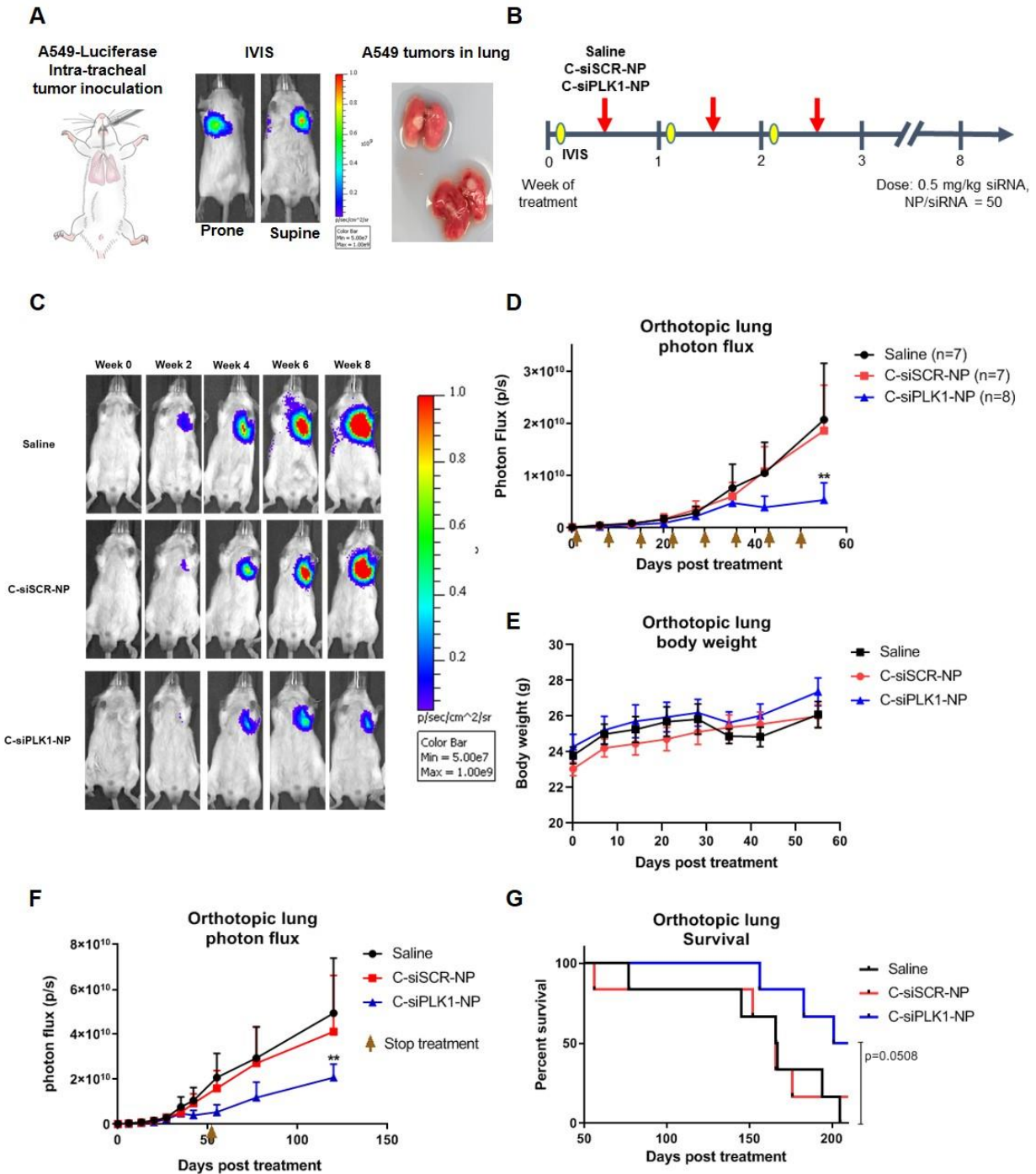


**Figure 2.9. C-siPLK1-NP reduces orthotopic lung tumor growth.** (A) *In vivo* images showing luminescent signal of A549-Luc tumors from intratracheal inoculation, which was confirmed with the presence of tumor nodes in the lungs. (B) Once tumors were established (3 weeks post inoculation), mice were treated with saline, C-siSCR-NP, or C-siPLK1-NP once per week at 0.5 mg/kg siRNA dose for 8 weeks. (C) IVIS imaging for C-siPLK1-NP, C-siSCR-NP, or saline treated

mouse in supine position over the course of treatment. (D) Lung tumor growth determined by average photon flux of prone and supine position for each mouse (n=7-8). Arrows indicate treatment days. (E) Body weight of mice during NP treatment administration. (F) Orthotopic lung tumor growth during and after completion of treatments (marked by arrow). Data presented as mean + SEM, \*P<0.05, \*\*P<0.01 vs. saline. (G) Kaplan-Meier Survival curve showing extended survival for mice treated with C-siPLK1-NP (n=6), P=0.0508 vs. saline. Copyright permission obtained from Encapsula NanoSciences for mouse cartoon in (A).

## 2.4 DISCUSSION

Molecularly targeted therapeutics that can enhance the effects of radiation have potential to benefit millions of cancer patients who receive radiation therapy. In contrast to traditional approaches used to enhance radiation sensitivity (e.g. chemotherapy, oxygen mimics, metallic nanoparticles),<sup>174</sup> targeted therapies provide the opportunity to preferentially act on cancer cells. Despite this promise, the only FDA approved targeted therapy for combination with radiation is cetuximab for head and neck cancer.<sup>175</sup> Identifying targeted therapy and radiation combinations to improve treatment is needed. Herein, I have developed a novel radiation sensitizer based on a mesoporous silica nanoparticle (MSNP) platform. By conjugating an EGFR-antibody to MSNP and delivering PLK1 siRNA, I show that the nano-therapeutic can effectively target NSCLC cells to initiate cell death and sensitize tumor cells to radiation.

The majority of lung cancer patients are diagnosed at advanced disease stages and require systemic therapy to relieve symptoms and prolong survival.<sup>154</sup> Platinum based chemotherapeutics remain the standard of care, but have limited efficacy and carry significant side effects.<sup>176</sup> For patients who harbor a mutated epidermal growth factor receptor (EGFR) or anaplastic lymphoma kinase (ALK) translocation, targeted therapy

with EGFR or ALK inhibitors may be administered. While such targeted therapies have dramatically improved outcomes for some patients, one drawback is that they are prone to resistance.<sup>177</sup> Furthermore, most NSCLC patients do not harbor EGFR or ALK abnormalities and there are no targeted therapies for KRAS and many other identified or unknown oncogenic drivers. Immunotherapy, targeting programmed cell death protein 1 (PD-1) or programmed death ligand 1 (PD-L1), has shown promising results but still benefits just a minority of patients.<sup>2,178</sup> Effective systemic therapy with minimal side effects is consequently an area of unmet clinical need.

In this research, I focused on wild type EGFR and KRAS mutant NSCLC (e.g. A549, H460) since there are no current targeted therapies for this patient subgroup (over 30% of lung adenocarcinomas).<sup>179</sup> However, it is anticipated that the therapeutic can be applicable to any cancer patient whose tumors have high EGFR expression such as lung, breast, colon, glioblastoma, and head and neck cancers,<sup>180</sup> and in particular for patients receiving radiation therapy. Radiation is currently administered to the majority of lung cancer patients in various stages of disease. For unresectable locally advanced NSCLC, the standard of care consists of conventional external beam radiation (30 fractions of 2 Gy each) with concurrent or sequential chemotherapy – which carries significant toxicity. Furthermore, the role of radiation therapy for lung cancer patients continues to expand with new technologies and techniques. For example, stereotactic body radiotherapy, which allows for the delivery of high doses of radiation per fraction (e.g. 4 fractions of 15 Gy each), has shown promise as an alternative approach to surgical resection for early stage lung cancer patients.<sup>181</sup> Thus, the targeted radiation sensitizer I have developed here will potentially benefit lung cancer patients in all disease stages.

While EGFR antibodies and inhibitors are established drugs for patients with EGFR mutations, PLK1 inhibitors have been plagued in clinics. A major limitation is that current PLK1 small molecule inhibitors are ineffective for solid tumors due to their low tumor bioavailability and toxic side effects to healthy cells. PLK1 inhibitors must have long half-lives to achieve sufficient intra-tumor concentrations, but this results in sustained exposure to hematopoietic precursor cells in blood and bone marrow, leading to hematologic dose-limiting toxicities (neutropenia and thrombocytopenia).<sup>182-185</sup> Of all PLK1 inhibitors, volasertib has shown the most promise having reached phase III clinical trial but only for acute myeloid leukemia (blood cancer).<sup>115</sup> For lung cancer, volasertib was terminated as a monotherapy early in a phase II clinical trial due to a lack of response.<sup>118</sup> As an alternative approach, a PLK1 siRNA nanoparticle (TKM-PLK1) was developed and showed promising results with stable disease observed in 51% of patients with hepatocellular carcinoma (HCC) in a phase I/II clinical trial.<sup>121</sup> However, the material has a low therapeutic window (0.6-0.75 mg/kg) and is lipid based; thus, it is only effective at treating liver cancers. Therefore, an effective PLK1 therapeutic remains an unmet clinical need for other solid tumors, including lung cancers. We expect that C-siPLK1-NP can circumvent the issues associated with low tumor bioavailability and toxic side effects of current PLK1 inhibitors in clinical trials. SiRNA knockdown of PLK1 may be advantageous over antibodies and inhibitors because it orchestrates its effect at the mRNA level instead of the protein level, which may overcome certain resistance mechanisms. For instance, we have previously reported that siRNA can overcome both intrinsic and acquired resistance of HER2+ cancer cells to small molecules or antibodies targeting the same protein.<sup>119</sup> In addition we also found that cancer was not prone to

develop resistance to siRNA as they would to small molecule inhibitors or antibodies.<sup>120</sup> The nanoparticle construct can also improve tumor bioavailability via the enhanced permeability and retention effect.<sup>186</sup> Furthermore, cancer cell targeting by cetuximab on the nanoparticles would reduce off-target effects to healthy cells.

Ultimately, we envision that the application of EGFR-antibody conjugated nanoparticle for delivering siPLK1 will be impactful as a lung cancer treatment in 1) patients with KRAS or other mutations for which there are currently no targeted therapies, 2) combination with radiation therapy to increase sensitivity and as a result, reduce doses and toxic side effects, and 3) overcoming cancer resistance and relapse by effectively targeting PLK1 of cancer stem cells as shown in previous reports.<sup>89-91</sup> In our prior work, we reported on the MSNP platform's overall safety, biocompatibility, long-term storage and stability,<sup>11</sup> as well as efficacy in multiple breast cancer models.<sup>119,151,156</sup> Thus, the platform is already well positioned to advance to clinical trials. My findings herein illustrate that C-siPLK1-NP has great potential to serve as a potent radiation sensitizer and to meet the clinical need of an effective therapeutic against PLK1, which is a key target to defeat cancer. In addition, I show that co-targeting both EGFR and PLK1 is a highly effective strategy to enhance radiation sensitivity, which warrants further investigation for all high EGFR expressing cancers as aforementioned.



## **Chapter 3: Combination of PLK1 inhibition and PD-L1 blockade for treatment of lung cancer**

### **3.1 INTRODUCTION**

Polo-like kinase 1 (PLK1) is a critical mitotic kinase that is overexpressed in various cancers and provokes oncogenic properties.<sup>4</sup> Previous studies have illustrated the potential of PLK1 inhibition as a therapeutic strategy and several PLK1 small molecule inhibitors have reached clinical trials.<sup>187</sup> However, PLK1 inhibitors as a monotherapy have not advanced beyond clinical trials due to poor efficacy and dose-limiting toxicities.<sup>182-185</sup> The most advanced PLK1 inhibitor, volasertib (BI6727), reached phase III clinical trial for acute myeloid leukemia (blood cancer),<sup>115</sup> but eventually failed to meet primary endpoint of objective response.<sup>117</sup> For lung cancer, volasertib was terminated as a monotherapy early in a phase II clinical trial due to lack of response at the given dose limiting toxicity (300 mg once every 3 weeks).<sup>118</sup> These results suggest that alternative therapeutic strategies are needed to elicit the full potential of inhibiting PLK1.

The recent emergence of immune checkpoint blockade targeting the PD-L1/PD-1 axis have provided promising results for NSCLC patients. PD-L1 expression on tumor cells inhibits tumor directed cytotoxic CD8+ T cell activity by binding to PD-1 receptor of the T cells and suppressing their function.<sup>68,78,79</sup> Recently, checkpoint inhibitors for PD-1 and PD-L1 (e.g., pembrolizumab, nivolumab, atezolizumab, and durvalumab) received FDA approval for treatment of NSCLC, either as first line (pembrolizumab) or second line therapy.<sup>81</sup> However, while patients who respond may show robust and durable responses, only a minority of total patients respond, and many initial responders eventually

relapse.<sup>80,85,188</sup> Furthermore, systemic distribution of antibodies against immune checkpoints can cause aberrant and uncontrolled immune responses, leading to immune-related adverse effects (irAEs) that damage normal tissues.<sup>84</sup> These toxicities can result in discontinuation of treatment and in some instances irAEs can be fatal. Thus, strategies to improve the response and therapeutic efficacy of immune checkpoint blockade are of great interest.<sup>189</sup>

A recent study showed that PD-L1 protein abundance fluctuated during cell cycle progression in multiple human cancer cell lines, peaking in M and early G1 phase.<sup>190</sup> Accordingly, increased PD-L1 protein abundance was observed in multiple mouse tumor-derived cell lines arrested in M phase by nocodazole or taxol.<sup>190</sup> In my previous study (Chapter 2), I identified that reduction of PLK1 induces a strong mitotic arrest that can be sustained for several days post treatment. Collectively, these observations led me to hypothesize that combining PD-L1 antibodies with mitotic kinase inhibitors, such as PLK1 inhibitors, can increase cancer cell killing owing to the apoptotic effect of the PLK1 inhibitors and the anti-tumor immune effect that would be provoked by PD-L1 checkpoint blockade.

Herein, we developed a PLK1 inhibitor loaded mesoporous silica nanoparticle platform (MSNP) conjugated to PD-L1 antibody to synergize combination effects of targeting both PLK1 and PD-L1. By utilizing the nanoparticle construct to deliver these agents, we can effectively co-localize therapeutic effects to the tumor and reduce toxic concerns associated with systemic treatment of the drugs. Our study highlights a rationale combination strategy to augment existing therapies without increasing toxicity by utilizing our MSNP platform as a delivery carrier.

## 3.2 MATERIALS AND METHODS

### 3.2.1 Cell lines and reagents

A549 NSCLC were purchased from ATCC (CCL-185) and maintained in RPMI media with 10% fetal bovine serum (FBS). Lewis Lung Carcinoma (LLC) metastatic variant, LLC-JSP cells, and fluorescent labeled LLC-JSP cells were gift from Dr. Don Gibbons lab (MD Anderson Cancer Center), and were cultured in RPMI + 10% FBS. Antibodies used: Human PD-L1 antibody (eBioscience), mouse PD-L1 (PE, BD Biosciences), mouse CD3 (APC, eBioscience), mouse CD8a (Pacific Blue, Invitrogen), mouse CD4 (BV711, BD biosciences), mouse PD-1 (PE/Cy7, BioLegend). Alexa Fluor 488 secondary antibody was purchased from Life Technologies. *In vivo* grade mouse PD-L1 antibody was purchased from BioXcell (BE0101), and volasertib was purchased from Selleckchem. SiRNA sequences: PLK1 (antisense 5'-UAAUUCAUUCUUCUUGAUCCGG-3'); scrambled SCR (antisense 5'-UUAGUCGACAUGUAAACCA-3') were purchased from Dharmacon.

### 3.2.2 Nanoparticle synthesis and characterization

Bare MSNPs were synthesized as we have previously reported.<sup>151</sup> For PLK1 inhibitor loading, volasertib was dissolved in DMSO and diluted in ethanol solution and mixed with MSNPs in ethanol for overnight shaking at room temperature (350 RPM). The next day, nanoparticles were coated with PEI (Alfa Aesar) and mal-PEG-NHS (Jenkem) following our previous studies.<sup>11,151</sup> For PD-L1 antibody conjugation, *in vivo* grade mouse PD-L1 antibody (BioXcell) was buffer exchanged to PBS pH 8 (Zeba spin column, Thermo Fisher) and thiolated using Traut's reagent (Thermo Fisher) following manufacturer's protocol. Thiolated antibody was added to NP at 20 wt.% and shaken overnight at 4°C (300 RPM). Nanoparticles were washed with PBS pH 7.2 before characterization.

Nanoparticle size was 90 nm, determined using Malvern Zetasizer. Antibody loading was 4 wt.%, determined by protein quantification of NP supernatant with BCA assay. To quantify PLK1 inhibitor loading, nanoparticles were shaken in DMSO solution to release the drug and supernatant was collected. Absorbance of supernatant was measured with Tecan plate reader to determine loading extent to be 0.5 wt.%. The p-iPLK1-NP is nanoparticle loaded with both PLK1 inhibitor and PD-L1 antibody, p-NP is nanoparticle loaded with PD-L1 antibody, and iPLK1-NP is nanoparticle loaded with PLK1 inhibitor.

### **3.2.3 Flow cytometry**

Cells (100K cells/well) were plated in 6 well plates overnight and treated with indicated treatments the next day. Following treatments, cells were collected and aliquoted to 1 million cells per sample before washing in FACs buffer and staining. Primary and secondary antibodies were stained for 30 mins and 1 hour, respectively, under rocking on ice. After staining, cells were washed in FACs buffer before flow analysis with Guava easyCyte (Millipore Sigma) flow cytometer (10,000 events per sample). For tumors, tumors were harvested, minced, and incubated with 1 mg/ml DNase for 30 minutes before smashing through 70 um filter to obtain single cell suspension. RBC lysis buffer was incubated with cells for 5 minutes, and washed with PBS. 1 million cells per sample were blocked with Fc-shield before staining with dye conjugated antibodies for 30 minutes (in FACs buffer). Cells were then washed with FACs buffer and analyzed with Guava (50,000 events per sample).

### **3.2.4 Cell viability after treatments**

Cells (1500/well) were plated in white flat bottom 96 well plate overnight. The following day, cells were treated with drug loaded nanoparticles and controls as indicated and

media was changed 24 hr post treatment. 4-5 day post treatment, cell viability was assessed using Cell Titer Glo assay (Promega) following manufacturer's instructions. Luminescence was read with Tecan plate reader.

### **3.2.5 RT-qPCR to assess PLK1 gene knock down**

RNA was isolated with GeneJet RNA purification kit (Thermo Fisher Scientific) following manufacturer's instructions. One-Step qRT-PCR was performed using EXPRESS One-Step Superscript™ qRT-PCR Kit (Invitrogen). Cycling conditions: 50 °C for 2 min, 95 °C for 10 min, 40 cycles of 95 °C for 15 s, and 60 °C for 1 min. TAQMAN gene expression primers Human *HPRT* mRNA (Hs99999909\_m1), Human *PLK1* mRNA (Hs00983225\_g1), and Human PDL1 (Hs00204257\_m1) were used. Data was analyzed using  $2^{-\Delta\Delta C(t)}$  method.

### **3.2.6 Syngenic tumor models and treatments**

For single tumor flank model, LLC-JSP murine lung cancer cells (200K) were inoculated in right flank of C57BL/6 female mice (6 weeks) (Charles River NCI colony). At 8 days post tumor inoculation, mice received intraperitoneal (i.p.) treatments of volasertib (20 mg/kg) and/or PD-L1 antibody (10 mg/kg) every 5 days for 3 doses total. Tumors were measured with Vernier Caliper and volume calculated by  $V = 0.5 \times \text{length} \times \text{width}^2$ . For bilateral tumors, C57BL/6 were inoculated with 100K and 40K LLC-JSP cells in right and left flank, respectively. At 12 days post inoculation, the aforementioned treatments were administered intratumorally to the right tumor every 3 days for 3 doses total. For both single flank and bilateral flank tumor models, mice were sacrificed when total tumor burden exceeded 2000 mm<sup>3</sup>. For metastatic lung tumor model, LLC-JSP (200K) were injected intravenously (i.v.) to 6 week old C57BL/6 mice. At 3 days post cancer cell

injection, mice were randomly grouped and treated with i.v. saline, p-iPLK1-NP (25 mg/kg NP), or i.p. PD-L1 antibody (5 mg/kg) and volasertib (1.25 mg/kg) every 3 days for a total of 4 doses. All studies were reviewed and approved by Institutional Animal Care and Use Committee (IACUC) at Oregon Health and Science University (OHSU).

### **3.2.7 Statistical analysis**

GraphPad Prism 8.0 (GraphPad Software Inc.) was used for all statistical analysis. Comparison between two groups was performed with Student's *t* test. Tumor growth was analyzed using two-way repeated measures ANOVA with Tukey's correction for multiple comparisons. Kaplan Meier survival curve was analyzed using the log-rank (Mantel-Cox) method. Significance was set at  $p < 0.05$ . *In vitro* data are expressed as mean  $\pm$  SD; *in vivo* data are expressed as mean  $\pm$  SEM.

### 3.3 RESULTS

#### 3.3.1 PLK1 knock-down induces expression of PD-L1

We and others have previously reported that PLK1 inhibition or knock-down results in cell cycle arrest in G2/M.<sup>156,191</sup> PLK1 knockdown resulted in an increase in PD-L1 surface expression in both human (A549) and murine (LLC-JSP) lung cancer cell lines. As shown in Fig. 3.1A, 85% knockdown of PLK1 mRNA (by siRNA against PLK1) resulted in 2.5-fold increase in PD-L1 mRNA expression in A549 cell line compared with control treated cells. This was then confirmed at the surface protein level in A549 (Fig. 3.1B) and LLC-JSP (Fig. 3.1C) lung cancer cell lines at 3 days post siRNA treatments.

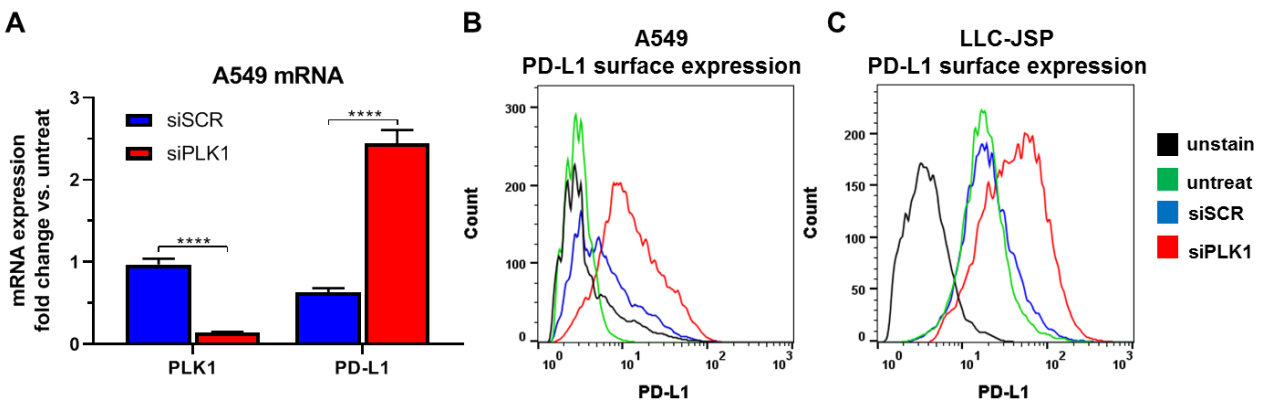


**Figure 3.1. PLK1 siRNA knock-down induces PD-L1 expression.** (A) PLK1 and PD-L1 mRNA expression in A549 (human NSCLC) at 48 hr post treatment with PLK1 siRNA (siPLK1) or scrambled siRNA (siSCR) normalized to HPRT housekeeping gene. Data presented as mean  $\pm$  SD from triplicates; \*\*\*\*P<0.0001. (B) PD-L1 surface expression of A549 (B) and LLC-JSP (C) at 72 hr post treatments assessed by flow cytometry (10,000 events per sample).

### 3.3.2 Combination of PLK1 inhibition with PD-L1 blockade enhances tumor control *in vivo*

Based on our finding that PLK1 reduction results in PD-L1 increase, we sought to investigate whether PLK1 inhibition and PD-L1 blockade would synergize *in vivo*. We used LLC-JSP cell line to develop flank tumor model in immune-competent mice.<sup>192</sup> Established tumors (>60 mm<sup>3</sup>) at day 8 post tumor inoculation were treated i.p. with the PLK1 inhibitor volasertib (20 mg/kg) and PD-L1 monoclonal antibody (10 mg/kg) every 5 days for a total of 3 doses (Fig. 3.2A). As shown in Fig. 3.2B, the combination treatment significantly reduced tumor growth compared with single drug administrations. Moreover, the combination significantly prolonged survival of mice (Fig. 3.2C).

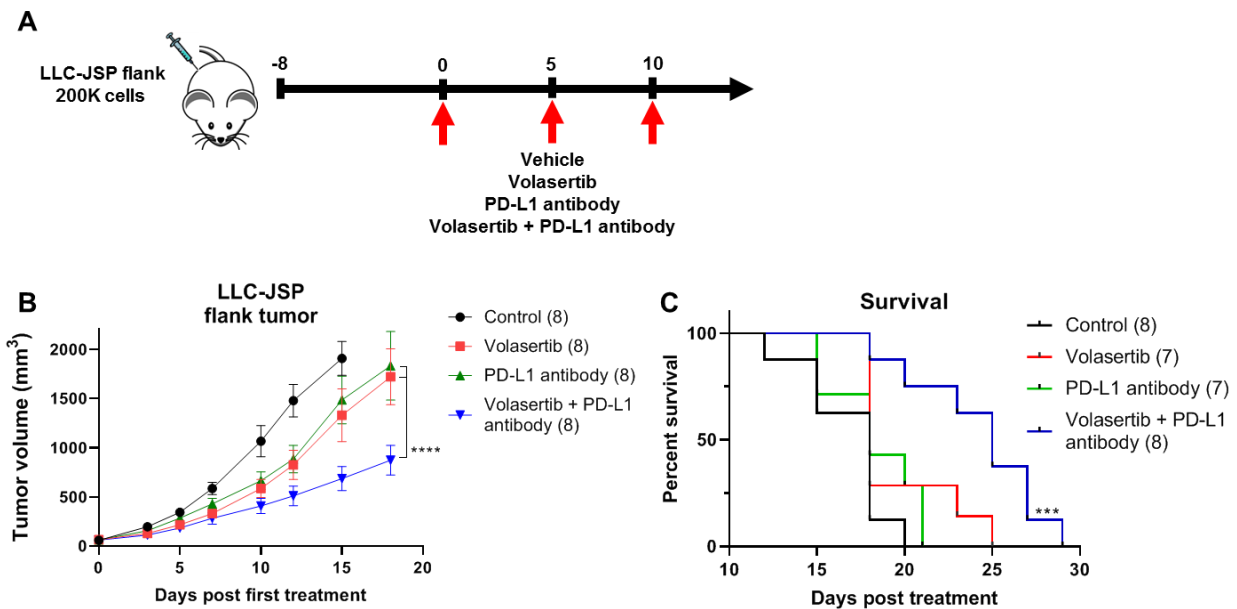


**Figure 3.2. PD-L1 blockade potentiates the effect of PLK1 inhibition in syngenic lung tumors.** (A) C57BL/6 mice were injected with 200K LLC-JSP cells in right flank. On day 8 post tumor inoculation, mice were grouped (n=7-8) and received i.p. treatments of control vehicles (PBS and HCl/saline), PLK1 inhibitor volasertib (20 mg/kg), PD-L1 antibody (200 µg), or combination of PLK1 inhibitor and PD-L1 antibody. Treatments were administered every 5 days for 3 doses. (B) Tumor growth of mice. (C) Kaplan-Meier Survival curve. Data presented as mean ± SEM; \*\*\*P<0.001, \*\*\*\*P<0.0001.



### **3.3.3 Nanoparticle delivery of PLK1 inhibitor volasertib (iPLK1-NP)**

Despite the promise of PLK1 as a therapeutic target, clinical trials with current small molecule inhibitors have been disappointing. To reduce toxicity and improve tumor bioavailability of PLK1 inhibitor, we investigated whether our MSNP platform could improve the efficacy of a clinically available PLK1 inhibitor. In our prior work,<sup>119,151,156</sup> we demonstrated the promise of this MSNP platform to target and deliver siRNA to breast tumors including those metastasized to lungs. In this research, we utilized the platform to deliver the small molecule inhibitor volasertib, which is the most advanced inhibitor of PLK1. Volasertib was loaded onto mesoporous silica (Fig. 3.3A) prior to surface modification with polyethylene imine (PEI) and polyethylene glycol (PEG). The final nanoparticle (referred to as iPLK1-NP) size is 90 nm (Fig. 3.3B) which is in the appropriate range to take advantage of the EPR effect, and contains 0.5 wt.% PLK1 inhibitor volasertib. As shown in Fig. 3.3C, treatment of LLC-JSP cells with volasertib or iPLK1-NP significantly reduced cell viability compared with vehicle treated cells in a dose-dependent manner. Further, treatment with iPLK1-NP reduced cell viability more than the free PLK1 inhibitor. In agreement with previous finding using PLK1 siRNA (Fig. 3.1), treatment with iPLK1-NP resulted in significant increase in PD-L1 cell surface expression (Fig. 3.3D).

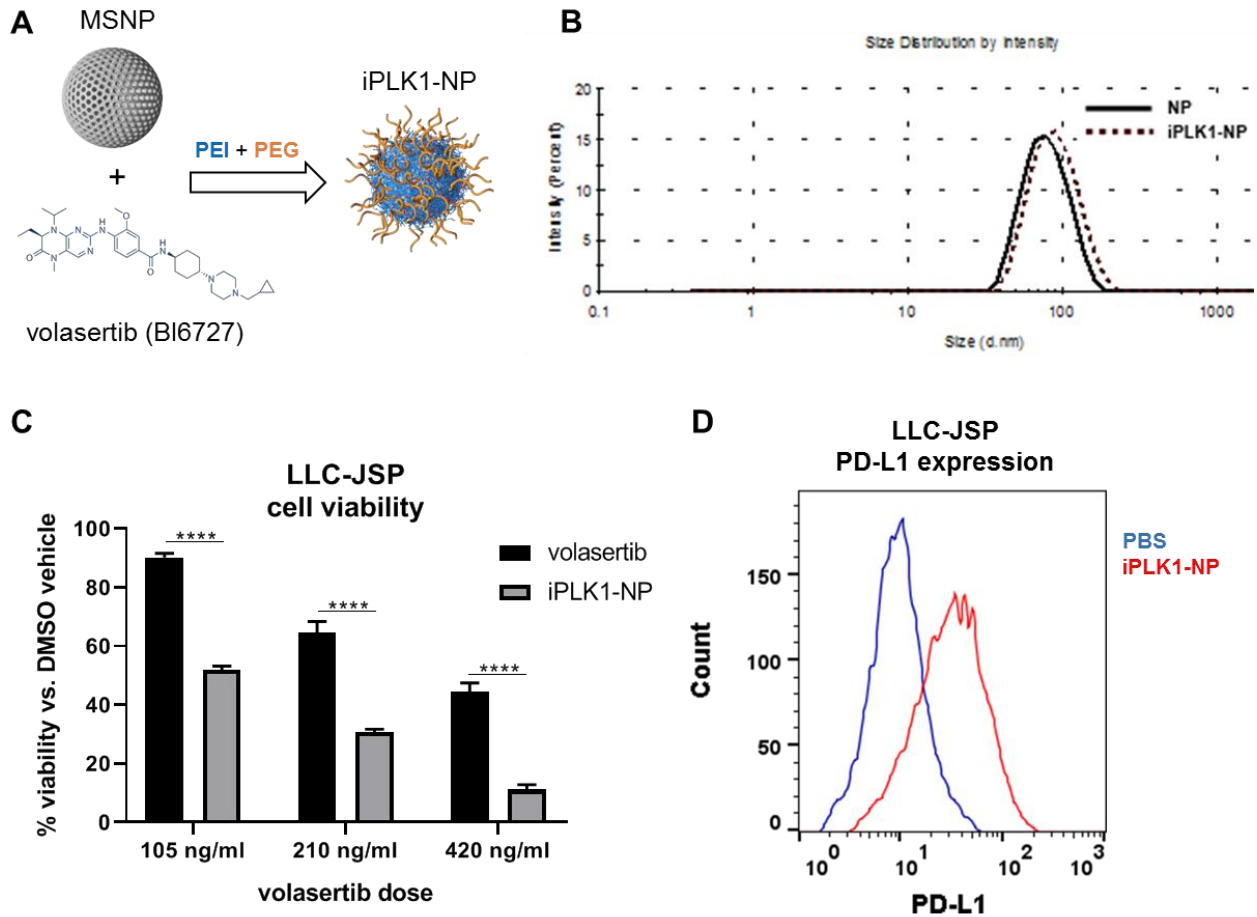


**Figure 3.3. Nanoparticle delivery of PLK1 inhibitor volasertib (iPLK1-NP).** (A) Schematic of synthesis of iPLK1-NP. (B) Hydrodynamic size of NP (with no inhibitor) and iPLK1-NP measured with Zetasizer. (C) Viability of LLC-JSP cells treated with volasertib (in 1%DMSO/PBS), iPLK1 (in PBS), or 1%DMSO/PBS for 4 days. Data presented as mean  $\pm$  SD from 4 independent samples; \*\*\*\* $P < 0.0001$ . (D) PD-L1 surface expression of LLC-JSP cells treated with PBS or iPLK1-NP (42  $\mu$ g/ml NP, 210 ng/ml volasertib) for 3 days.

### **3.3.4 PD-L1 targeted nanoparticle for iPLK1 delivery (p-iPLK1-NP)**

To evade immune response, many tumors overexpress PD-L1, thus PD-L1 can be utilized for tumor targeting of therapeutics. As iPLK1-NP could effectively kill cancer cells and simultaneously upregulate PD-L1 of the surviving cells, we aimed to utilize this as an advantage to target PD-L1+ cancer cells by conjugating PD-L1 antibody on iPLK1-NP. In this sense, a feed-forward loop can be generated where repeated administrations of PD-L1 targeted iPLK1-NP (referred to as p-iPLK1-NP) would upregulate PD-L1 expression and allow for superior tumor targeting to induce both apoptosis (via PLK1 inhibition) and anti-tumor immune responses (via PD-L1 blockade). This would be particularly advantageous for treating tumors with low PD-L1 expression, and may ultimately allow for higher response rates of immune checkpoint blockade. As illustrated in Fig. 3.4A, PD-L1 antibody was conjugated to PEG on NPs, and antibody amount was determined by BCA assay to be 4 wt.%. The hydrodynamic size of the construct is shown in Fig. 3.4B to be about 90 nm. As with iPLK1-NP, treatment with p-iPLK1-NP significantly reduced cell viability in LLC-JSP cell line (Fig. 3.4C). Furthermore, LLC-JSP cells incubated for 2 hours with p-iPLK1-NP blocked PD-L1 surface receptors as much as free PD-L1 antibody delivered at 25-fold higher dose. This is likely due to the high local concentration of antibody the cell experienced when antibody was delivered with nanoparticles (Fig. 3.4D). The iPLK1-NP had no effect on PD-L1 level at this short time point (Fig. 3.4D). Treatment of cells for 2 days with iPLK1-NP increased PD-L1 level as anticipated, which was reduced to normal level (see untreated) upon treatment with nanoparticle containing PD-L1 antibody (p-iPLK1-NP) (Fig. 3.4E). This demonstrates the nanoparticle targeting and blockade of PD-L1 receptors, which are induced by PLK1 inhibition.

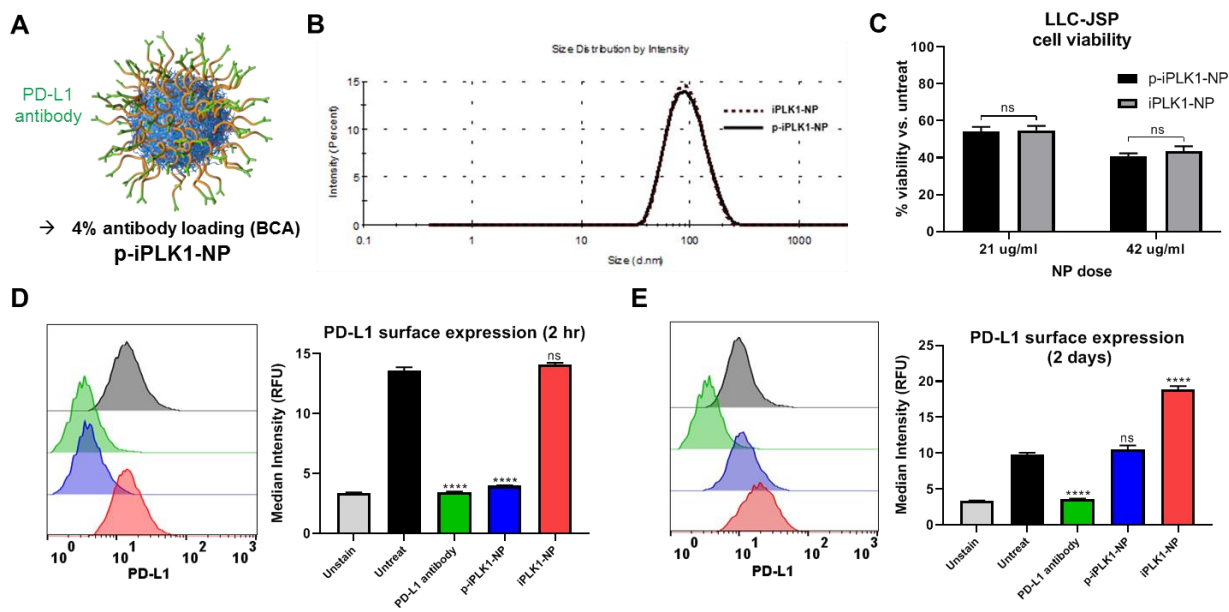


**Figure 3.4. PD-L1 targeted nanoparticle for iPLK1 delivery (p-iPLK1-NP).** (A) Schematic and (B) hydrodynamic size of p-iPLK1-NP containing 4 wt.% of PD-L1 antibody and 0.5 wt.% of PLK1 inhibitor. (C) 5 day cell viability of LLC-JSP cells treated with iPLK1-NP or p-iPLK1-NP. Data presented as mean  $\pm$  SD from 4 independent samples; ns – not significant. PD-L1 surface expression assessed by flow cytometry after LLC-JSP cells were incubated with various treatments as specified for (D) 2 hrs and (E) 2 days. Doses: free PD-L1 antibody (50  $\mu$ g/ml), iPLK1-NP (50  $\mu$ g/ml), and p-iPLK1-NP (50  $\mu$ g/ml, containing 2  $\mu$ g/ml PD-L1 antibody). Left: representative histograms, right: median intensity (RFU). Data presented as mean  $\pm$  SD from independent duplicates (10,000 events per sample); \*P<0.05, \*\*P<0.01, \*\*\*P<0.001, \*\*\*\*P<0.0001.

### 3.3.5 Local delivery of p-iPLK1-NP reduces local and distant tumor growth

To assess the anti-tumor immune response of p-iPLK1-NP, we utilized a bilateral flank tumor model. C57BL/6 mice were injected with 100K and 40K LLC-JSP cells on the right and left flank, respectively. At day 12 post injection, the right flank (local) tumors were injected with PBS, p-NP, iPLK1-NP, or p-iPLK1-NP (0.5 mg NP, 2.5  $\mu$ g iPLK1, 20  $\mu$ g PD-L1) every 3 days for a total of 3 injections (Fig.3.5A). Tumor growth of local (treated) and distant (untreated) tumors were monitored. Treatments with p-iPLK1-NP significantly reduced tumor growth of local tumor compared with nanoparticle containing a single drug (p-NP or iPLK1-NP) (Fig. 3.5B). Importantly, a delay in the onset of distant tumors was also observed for p-iPLK1-NP treated mice (Fig. 3.5C), which illustrates that an anti-tumor immune response was generated. Furthermore, treatment of p-iPLK1-NP significantly prolonged survival of mice compared with saline control or single drug NPs (Fig. 3.5D). Additionally, in a separate study, mice were injected with saline or p-iPLK1-NP as illustrated in Fig. 3.5A and tumors were harvested one day after last treatment to assess T cell infiltration. As shown in Fig. 3.5E, tumors treated with p-iPLK1-NP had significantly higher CD3<sup>+</sup> and CD8<sup>+</sup> tumor infiltrating lymphocytes (TILs), while CD4<sup>+</sup> TILs were not enhanced compared with the control tumors.

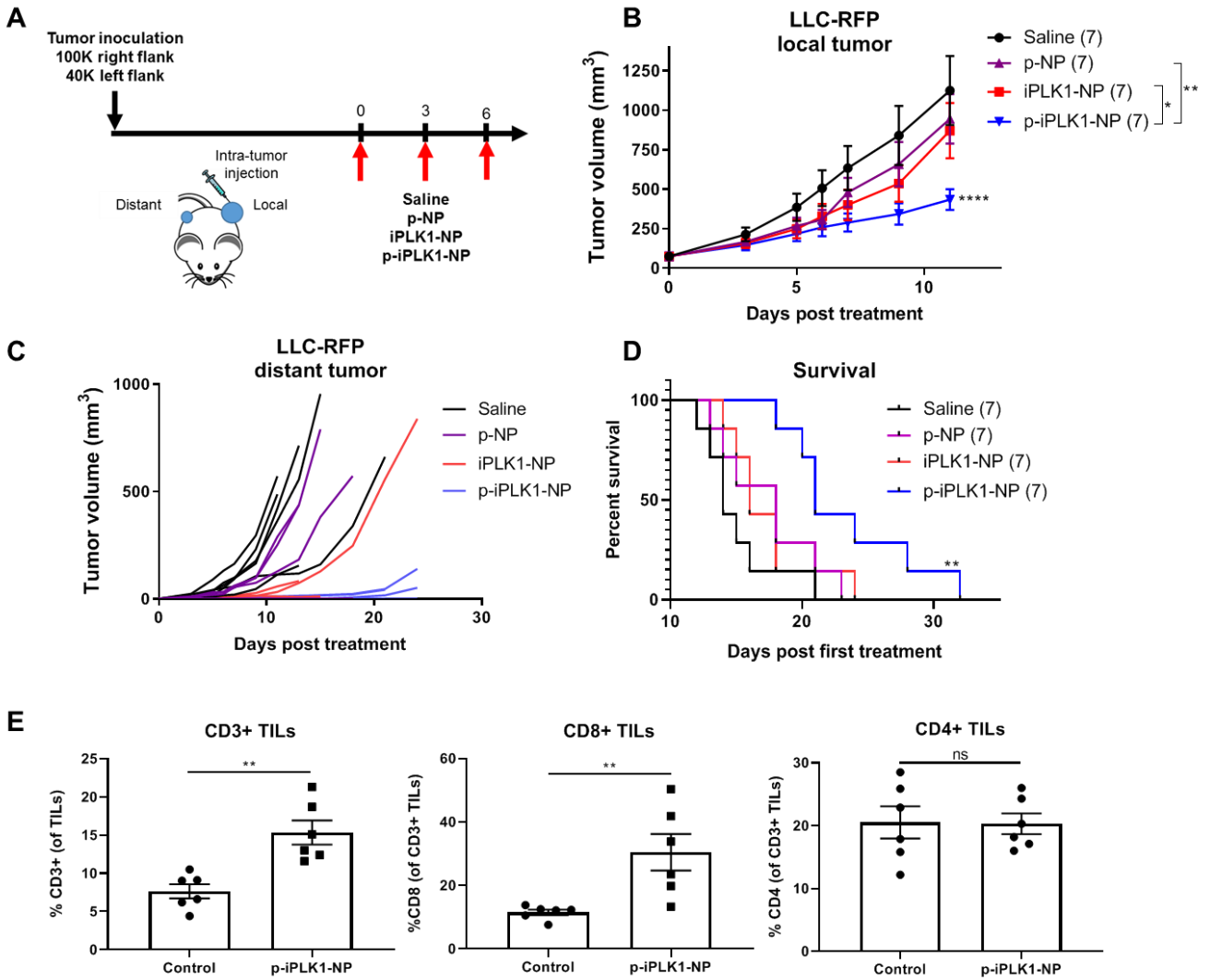


**Figure 3.5. p-iPLK1-NP elicits anti-tumor immune effects.** (A) 100K LLC-JSP cells were injected in right flank and 40K cells were injected in left flank of C57BL/6 mice. On day 12 post tumor inoculation, mice received intratumoral treatments of saline, p-NP, iPLK1-NP, or p-iPLK1-NP to the right (local) tumor. 0.5 mg NP in 50  $\mu$ l per dose for 3 doses total. (B) Local tumor growth. (C) Distant (untreated) tumor growth of individual mice. (D) Kaplan Meier Survival curve. (E) Mice were injected with tumors as described in (A) and received treatments of saline or p-iPLK1-NP. One day after last treatment, tumors were harvested to assess tumor infiltrating lymphocytes (TILs) with flow (50,000 events per sample). Data presented as mean  $\pm$  SEM; \* $P$ <0.05, \*\* $P$ <0.01, \*\*\* $P$ <0.001, \*\*\*\* $P$ <0.0001.

### **3.3.6 Systemic administration of p-iPLK1-NP prolongs survival of mice with experimental metastatic tumors**

To demonstrate the clinical potential of p-iPLK1-NP for lung cancer, we developed an experimental metastatic lung tumor model by intravenous injection of LLC-JSP cells (200K cells). Three days post cell injection, mice were randomly grouped and treated with saline, p-iPLK1-NP, or free drugs (volasertib + PD-L1 antibody) every 3 days for 4 doses total, as shown in Fig. 3.6A. The free drugs were administered at 5-fold higher dose than the amounts on NP. Mice treated with p-iPLK1-NP survived significantly longer than those treated with saline (Fig. 3.6B). The presence of lung tumor was confirmed visually for each deceased mouse. Data indicate that p-iPLK1-NP was as effective as the free drugs administered at 5-fold higher dose owing to the ability of nanoparticles for tumor targeting and co-localizing the therapeutic effects. Furthermore, treatment with p-iPLK1-NP did not cause any weight loss, demonstrating the safety of the construct (Fig. 3.6C).

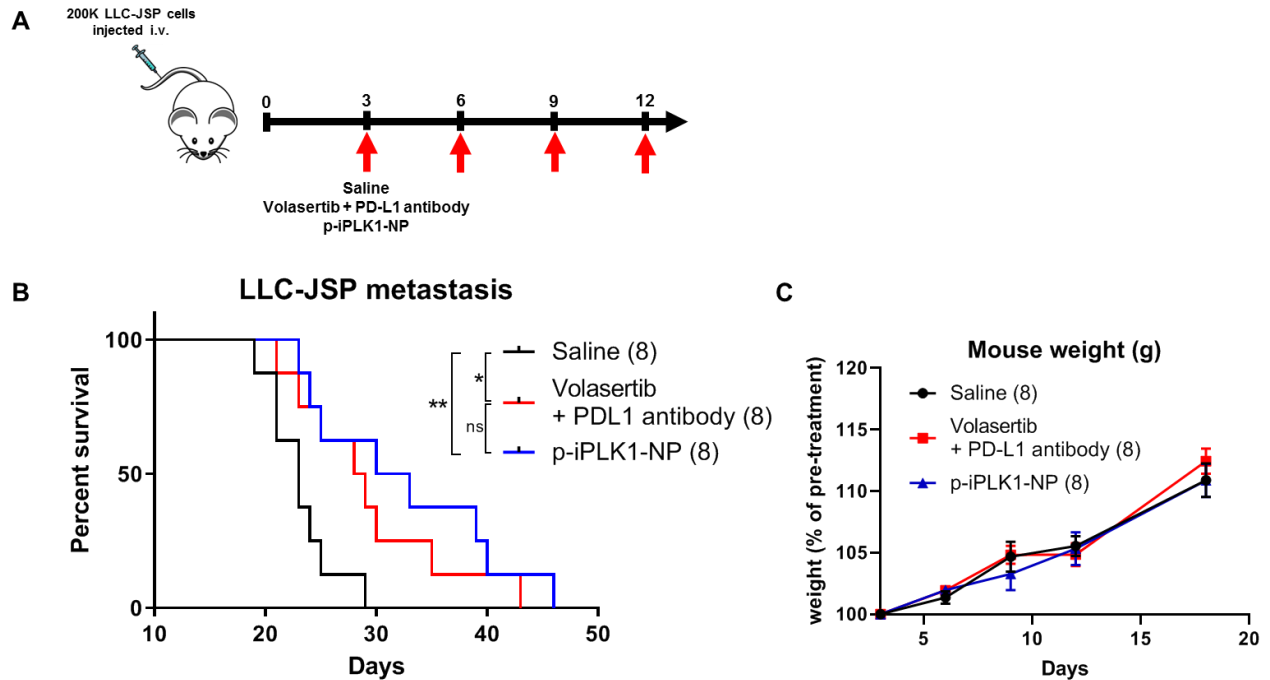


**Figure 3.6. p-iPLK1-NP improves survival of mice bearing metastatic lung tumors.** (A) C57BL/6 mice were injected with 200K LLC-JSP cells intravenously. After 3 days, mice were randomly assigned systemic treatments of saline, free drugs (12.5  $\mu$ g volasertib and 100  $\mu$ g PD-L1 antibody), or p-iPLK1-NP (containing 2.5  $\mu$ g volasertib and 20  $\mu$ g PD-L1) for a total of 4 doses. (B) Kaplan-Meier Survival curve. \* $P < 0.05$ , \*\* $P < 0.01$  (Log-rank Mantel-Cox test). (C) Mice weight change post first treatment.



### 3.4 DISCUSSION

In this research, I report for the first time that PLK1 inhibition results in an increase of immune checkpoint PD-L1 expression in human and mouse NSCLC cells. This suggests that avoiding the immune response is a mechanism exploited by NSCLC cells that survive PLK1 inhibition. Previous studies have also shown roles of PLK1 in regards to immunity. For instance, PLK1 has been shown to be a regulator of STAT3 activation,<sup>111</sup> which promotes an immune suppressive microenvironment, and inhibiting PLK1 resulted in loss of phosphorylated STAT3 in NSCLC cells.<sup>112</sup> Further, PLK1 was found to associate with the MAVS and negatively controls its activity in inducing type I interferons.<sup>113,114</sup> Intriguingly, PLK1 inhibition has also been shown to significantly increase HLA mRNA which encode MHC class I protein, the antigen presenting surface receptors.<sup>109</sup> These studies suggest that PLK1 inhibition may be promising to augment immunotherapy. However, to the best of our knowledge, this is the first study to report the effectiveness of the combination of PLK1 inhibition with immunotherapy.

I show that PLK1 inhibition induces PD-L1 upregulation and that PD-L1 blockade significantly potentiates the effect of PLK1 inhibition in NSCLC treatment. Other cytotoxic agents have also been shown to increase PD-L1 expression, including paclitaxel in ovarian cancer,<sup>193</sup> CDK4/6 inhibitors,<sup>190</sup> and PARP inhibitors<sup>194</sup> in breast cancer. Therefore, it is logical that these drugs are now in clinical investigations in combination with PD-L1 checkpoint blockade.<sup>195</sup> My findings also suggest that PLK1 inhibitors should be combined with PD-L1 immune checkpoint blockade to facilitate effective therapy in clinics.

To overcome the efficacy and toxicity limitations of current PLK1 inhibitors that have not advanced beyond clinical trials, I developed a PLK1 inhibitor nanoparticle platform and conjugated it to PD-L1 antibody to synergize combination effects of PLK1 inhibition and PD-L1 blockade. In our prior works, we reported on the efficacy and safety profile of this platform in delivering siRNA to mediate gene knockdown of breast and lung tumors *in vivo*.<sup>119,151,156</sup> In this research, I demonstrate that the platform can also improve delivery of small molecule inhibitors (i.e. volasertib) as treatment with PLK1 inhibitor on nanoparticles significantly reduced cell viability compared with free PLK1 inhibitor. Further, the therapeutic benefit of nanoparticle delivery was demonstrated in an experimental metastatic lung tumor model, where administration of the drugs on nanoparticles improved survival as much as the free drugs at 5-fold higher dose. This suggests that nanoparticle can overcome dose limiting toxicity issues of PLK1 inhibitors.

Our research herein focused on lung cancer, the leading cancer killer.<sup>1</sup> Like melanoma, where immunotherapy has been the most promising, lung cancer is a disease with a high mutational load which drives the expression of various neo-epitopes which can be recognized by host immune system.<sup>196,197</sup> Consequently, immunotherapy is a promising approach to treat lung cancer. However, objective response rates are much lower for lung cancer patients than melanoma. The research described here illustrates how superior responses can be achieved for lung cancers when combining PLK1 inhibition with PD-L1 blockade. Further, as the increase of PD-L1 is not specific to PLK1 inhibitors, other cytotoxic agents that induce upregulation of PD-L1 can be explored to synergize with current immune checkpoint blockade agents. Additionally, by co-localizing therapeutic effects with our MSNP platform, the dose of the drugs required can be reduced by 5-fold.

This suggests that nanoparticles can improve efficacy and reduce systemic toxicities of free drugs. This is key to improving outcomes as current combination therapy strategies with immune checkpoint blockade can lead to higher rates of adverse events. Lastly, due to the versatility of the MSNP platform, siRNA can also be loaded to target any gene identified as a regulator of cancer progression or immune evasion, in addition to the targeting antibody (e.g. PD-L1) and PLK1 inhibitor. In this regard, the platform may ultimately allow for patient-specific combination therapies to be delivered as a single drug agent, which can localize therapeutic effects in tumors and mitigate toxicity.

## Chapter 4: Summary, conclusions, and future directions

### 4.1 Summary and conclusions

In this dissertation, polymer modified mesoporous silica nanoparticles (NP) were developed as targeted therapies to augment radiation and immunotherapy for NSCLC. As discussed in **Chapter 1**, radiation therapy and immunotherapy are critical treatments in the management of NSCLC. Radiation is currently administered to over half of all NSCLC cancer patients, in both early and late disease stages. The ultimate goal of radiation therapy is to provide curative outcomes with minimal toxicity. Consequently, radiation sensitizers that can escalate radiation effects selectively to cancer cells hold great promise for patients receiving radiation. However, despite the efforts, there is no targeted therapy currently approved for use with radiation in NSCLC. Immunotherapy, specifically immune checkpoint blockade, is a new treatment strategy that has advanced rapidly to FDA approval due to the promising durable responses observed for some patients. For metastatic NSCLC, four immunotherapy drugs are now routinely administered either as first line or second line therapy. However, the majority of patients still do not respond to these therapies. Auto-immune disorders from systemic distribution of the drugs are also a concern that must be closely managed by clinicians.

Due to the heterogeneity and plasticity of cancer cells, it is now generally accepted that monotherapy will be ineffective in providing curative outcomes, especially for difficult to treat cancers such as lung cancer. Identifying rationale combination strategies can provide superior outcomes for patients, and may ultimately lead to cures. PLK1 is a promising molecular target to improve existing therapies. PLK1 is involved in almost every

aspect of mitosis and also regulates a variety of genes involved in cancer progression and survival. Nanoparticles provide a means to integrate multiple therapies and co-localize their anti-cancer killing effects, while improving tumor bioavailability. Our group has extensively optimized a MSNP platform to overcome limitations of traditional cancer therapies. I utilized this platform to combine rationale therapies into a single drug agent in an effort to improve radiation and immunotherapy for NSCLC, the deadliest form of cancer.

In **Chapter 2**, the MSNP platform was developed as a molecular targeted radiation sensitizer. By conjugating EGFR monoclonal antibody cetuximab to MSNP and delivering siRNA against PLK1, I showed that this nanoparticle construct (C-siPLK1-NP) effectively targets EGFR+ cells and reduces PLK1 expression at the mRNA and protein levels. This led to G2/M arrest, reduced DNA repair capacity, and cell death in NSCLC cells. Furthermore, I showed a synergistic combination between C-siPLK1-NP and radiation that significantly enhances cell death, which was confirmed *in vivo* in flank A549 lung tumors. The translational potential of the platform as a systemic lung cancer therapeutic was also demonstrated in an orthotopic lung tumor model, where systemic administration of C-siPLK1-NP reduced tumor growth and led to prolonged survival of mice. Further, C-siPLK1-NP had excellent reproducibility between various synthesized batches. My findings in this study demonstrate that C-siPLK1-NP is effective as a targeted therapy and as a potent radiation sensitizer for EGFR+ NSCLC. Since EGFR is overexpressed in 50% of NSCLC patients, C-siPLK1-NP will be applicable to many patients. Importantly, EGFR is also a mediator of DNA repair following radiation and thus EGFR antibody on the C-siPLK1-NP serves as dual roles in tumor homing and radiation sensitizer. . EGFR

is also overexpressed in other cancer types including subtypes of breast cancer, colon, glioblastoma, and head and neck cancer, and the level is low in normal human tissues, thus C-siPLK1-NP also has promise as an EGFR+ targeted therapy and radiation sensitizer beyond lung cancer.

In **Chapter 3**, I discovered that PLK1 inhibition results in significant increase in PD-L1 surface expression in human and mouse lung cancer cells. I then show that the combination of PLK1 inhibitor and PD-L1 antibody significantly reduced tumor growth and prolonged survival of mice compared with single drug administration. However, PLK1 inhibitor volasertib alone has shown great toxicity in clinical trials, which will likely increase when combined with PD-L1 antibody. Therefore, I used our nanoparticle platform to deliver the PLK1 small molecule inhibitor volasertib in an effort to increase efficacy and reduce systemic toxicities. I found that delivery of volasertib with nanoparticles significantly reduced lung cancer cell viability better than free volasertib at two-fold higher concentration. Further, to co-localize therapeutic effects of PLK1 inhibition and PD-L1 blockade, I conjugated PD-L1 antibody on the nanoparticles loaded with volasertib to create p-iPLK1-NP construct. Upon intratumoral administration of the p-iPLK1-NP, significant control of tumor growth was observed for both local (treated) tumors and distant (untreated) tumors compared with nanoparticles delivering a single drug or saline treated tumors. An increase of CD3+ and CD8+ T cells was also observed in tumors treated with p-iPLK1-NP versus saline treated tumors, illustrating the activation of anti-tumor immune responses. Lastly, the therapeutic benefit of the nanoparticles in delivering the drugs was demonstrated in an aggressive experimental metastatic lung tumor model. Systemic administration of p-iPLK1-NP was as effective in prolonging survival of mice as

the free drugs, which were delivered at a 5-fold higher dose than dose on NP. In conclusion, this study introduces a rationale combination therapy strategy in targeting PLK1 and PD-L1 to elicit cell death and generate an immune response. As PD-L1 antibodies are already an FDA approved treatment for patients (as second line therapy) and the PLK1 inhibitor volasertib has been under investigation in several clinical trials, the findings are highly impactful and suggest that clinical trials with this combination should be investigated. Furthermore, our MSNP platform can co-localize the therapeutics to achieve efficacy at lower dose and overcome toxicity issues of the free drugs.

## **4.2 Future directions**

In this work, I developed our nanoparticle platform into an effective radiation sensitizer for EGFR+ lung cancer, and as an immuno-nanoparticle to improve existing immunotherapies. My findings demonstrated the promise of PLK1 inhibition to improve radiation therapy (Chapter 2) or immunotherapy (Chapter 3) with the NP platform. Future studies should investigate whether targeting PLK1 in combination with both radiation and immune checkpoint blockade would further enhance the therapeutic efficacy. As discussed in Chapter 1, radiation damage can alter the immunosuppressive microenvironment established by cancer cells which may augment immune checkpoint blockade. Indeed, the combination of radiation and immunotherapy in efforts to improve the abscopal effect is a hot area in cancer research, with many preclinical and clinical studies investigating this combination in several cancers.

My research suggests that PLK1 is a very promising target to combine with radio-immunotherapy to improve local tumor control and generate abscopal effects, which have

so far only been minimally observed in patients. For example, in a clinical trial investigating the combination of CTLA-4 antibodies (immune checkpoint blockade agents) with radiation, only 3 out of 31 patients showed a partial response in abscopal (un-irradiated) tumors.<sup>198</sup> By inducing mitotic arrest, PLK1 inhibition will render cancer cells more susceptible to radiation damage, while causing an increase in PD-L1 expression. Treatment with PD-L1 targeted therapies would then release the tumor brakes on the immune system and allow for priming of adaptive immunity. In this way, systemic anti-tumor immune (abscopal) effects can be generated.

Due to the versatility of the nanoparticle platform that has been demonstrated in this dissertation, another future direction is incorporation of other therapeutic agents to facilitate a more robust therapy. For instance, as p-iPLK1-NP can also deliver oligonucleotides (Fig. 4.1), incorporating siRNA or miRNA against genes that regulate immune evasion or radiation resistance can further improve the efficacy. Adjuvant oligos can also be incorporated to enhance vaccination effect. To this end, I investigated whether the adjuvant CpG could further stimulate anti-tumor immunity and improve tumor control in bilateral tumor model shown in Fig. 3.5. Indeed, I found that incorporation of CpG on p-iPLK1-NP (referred to as p-iPLK1-NP-CpG) significantly improved survival of 2 out of 7 mice, and one mouse was completely free from tumors (Fig. 4.2). CpG oligodeoxynucleotides act as a danger associated molecular pattern (DAMP) to stimulate PRR, specifically the toll-like receptor 9 (TLR9). As discussed in Chapter 1, this serves as a danger signal for the activation of antigen presenting cells and subsequent priming of T cells. Thus, by releasing antigens (via cancer killing by PLK1 inhibition), delivering CpG adjuvant, and blocking PD-L1 immune checkpoints, this therapeutic tackles various



strategies by which cancer cells evade the immune response. My work in Chapter 3 also suggests that PLK1 inhibition itself enhanced antitumor immunity, which may owe to reduction of STAT3 phosphorylation<sup>111,112</sup> or regulation of type I interferon (IFN) production,<sup>113,114</sup> which should be further elucidated. Whether this therapeutic will lead to sustained immune responses and curative outcomes should also be investigated.

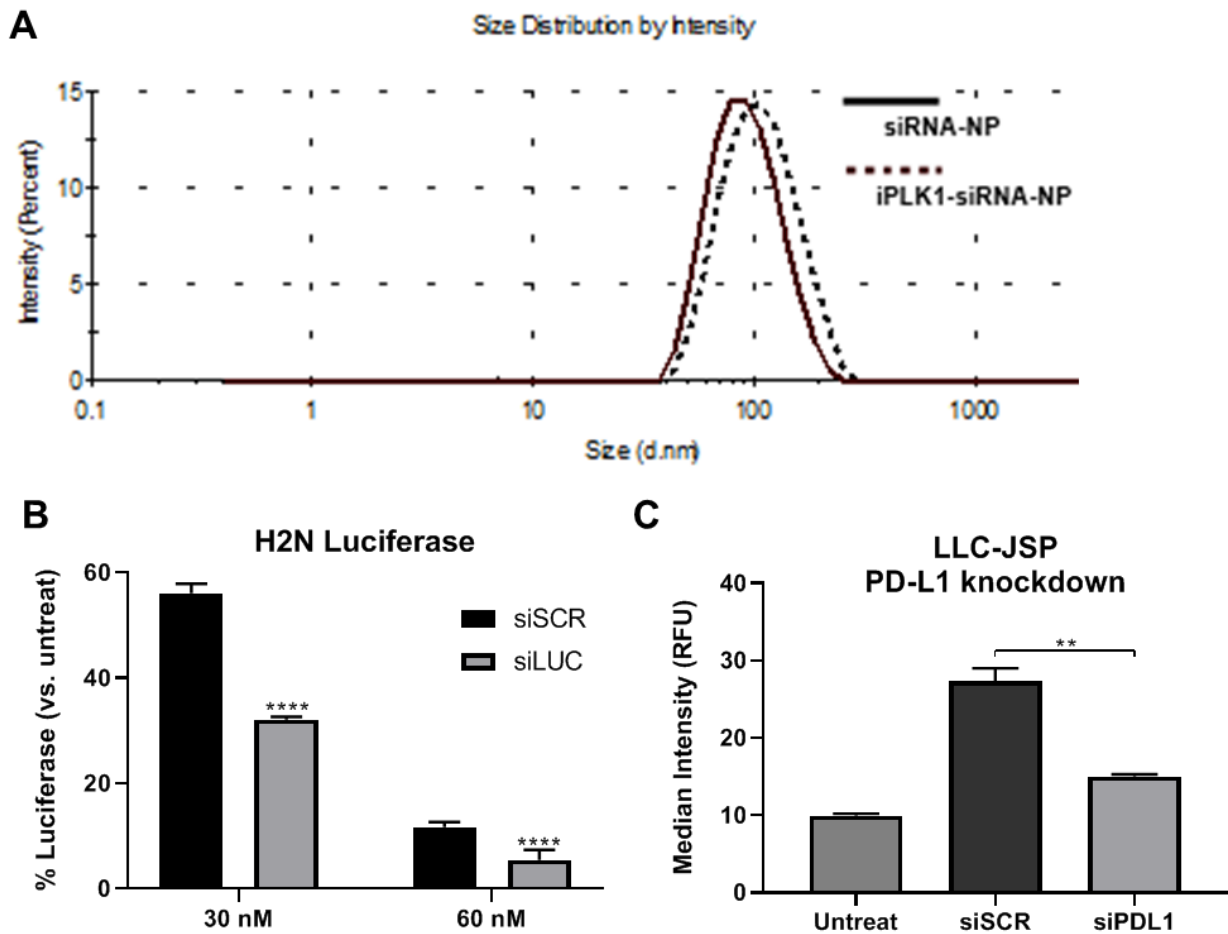


**Figure 4.1. siRNA knock-down with iPLK1-NP.** (A) Hydrodynamic size of siRNA bound NP and iPLK1-NP (2 wt.% siRNA). (B) Luciferase expression of LM2-4luc+/H2N treated with iPLK-NP loaded with luciferase siRNA (siLUC) or scrambled siRNA (siSCR) (48 hr treatment, 30 and 60 nM dose siRNA (2 wt.%). Data presented as mean  $\pm$  SD from 3 independent replicates. (C) PD-L1 surface protein expression of LLC-JSP were treated with 60 nM siSCR or PD-L1 siRNA (siPDL1) on iPLK1-NP for 3 days, assessed by flow cytometry. Data presented as mean  $\pm$  SD from independent replicates; \*\*P<0.01, \*\*\*\*P<0.0001 vs. siSCR control.

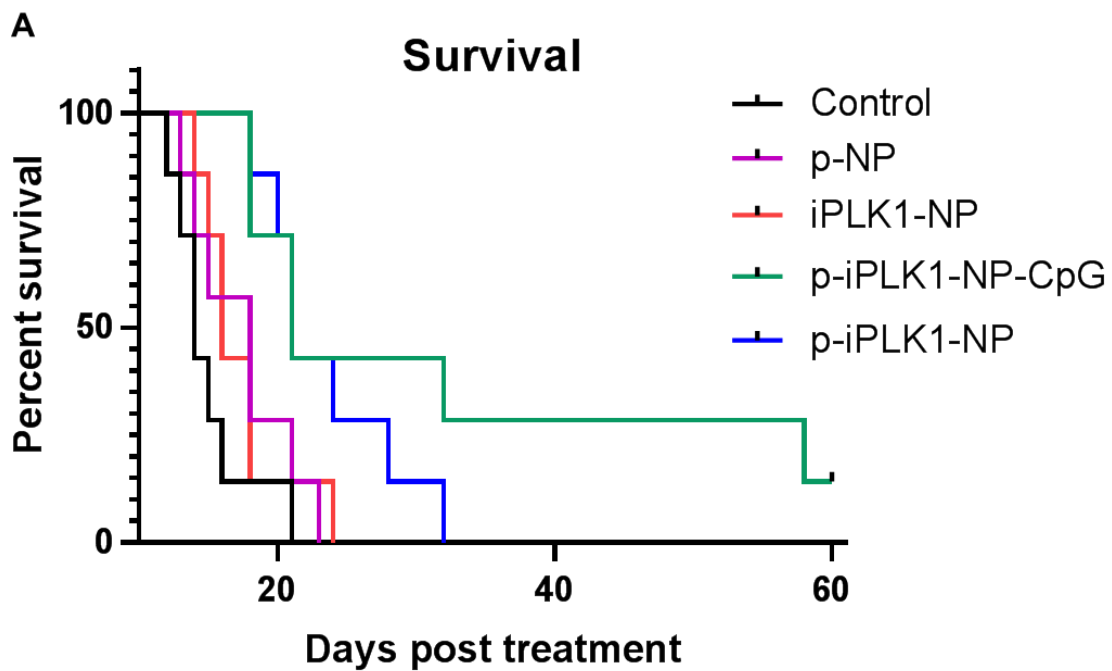


**Figure 4.2. Adding CpG to p-iPLK1-NP enhances therapeutic benefit as demonstrated by Kaplan Meier Survival curve.** 100K LLC-JSP cells were injected in right flank and 40K cells were injected in left flank of C57BL/6 mice. On day 12 post tumor inoculation, mice received intratumoral treatments of saline, p-NP, iPLK1-NP, p-iPLK1-NP, or p-iPLK1-NP-CpG to the right (local) tumor. 0.5 mg NP (2.5  $\mu$ g iPLK1, 20  $\mu$ g PD-L1 antibody, 20  $\mu$ g CpG) in 50  $\mu$ l was administered every 3 days for a total of 3 doses.

While this dissertation focused on NSCLC cancer treatment, the therapies developed herein are also applicable to many other cancers, which warrants investigation. Ultimately, the goal is to advance our novel therapeutics to clinical trials. To this end, more extensive toxicological studies will need to be conducted. So far, the nanoparticle platform has demonstrated excellent safety profile in mouse models as demonstrated in our prior works. We have also demonstrated the reproducibility, scalability, and long-term stabilization and storage of the nanoparticles. Thus, the platform is well positioned to make the leap to the clinical setting. By identifying novel combination therapies to deliver with the platform, as has been demonstrated in this dissertation, our nanoparticle platform may garner significant benefits for cancer patients and improve outcomes and quality of life.

## References

1. American Cancer Society. Cancer Facts & Figures. 2018.
2. Hirsch FR, Scagliotti GV, Mulshine JL, et al. Lung cancer: current therapies and new targeted treatments. *Lancet* 2017; **389**(10066): 299-311.
3. Wang ZX, Xue D, Liu ZL, et al. Overexpression of polo-like kinase 1 and its clinical significance in human non-small cell lung cancer. *The international journal of biochemistry & cell biology* 2012; **44**(1): 200-10.
4. Liu Z, Sun Q, Wang X. PLK1, A Potential Target for Cancer Therapy. *Translational oncology* 2016; **10**(1): 22-32.
5. Zitouni S, Nabais C, Jana SC, Guerrero A, Bettencourt-Dias M. Polo-like kinases: structural variations lead to multiple functions. *Nat Rev Mol Cell Biol* 2014; **15**(7): 433-52.
6. Zhang Z, Zhang G, Gao Z, et al. Comprehensive analysis of differentially expressed genes associated with PLK1 in bladder cancer. *BMC Cancer* 2017; **17**(1): 861.
7. Fu Z, Wen D. The Emerging Role of Polo-Like Kinase 1 in Epithelial-Mesenchymal Transition and Tumor Metastasis. *Cancers (Basel)* 2017; **9**(10).
8. Mai WX, Meng H. Mesoporous silica nanoparticles: A multifunctional nano therapeutic system. *Integrative biology : quantitative biosciences from nano to macro* 2013; **5**(1): 19-28.
9. Chen Y, Chen H, Shi J. In vivo bio-safety evaluations and diagnostic/therapeutic applications of chemically designed mesoporous silica nanoparticles. *Advanced materials (Deerfield Beach, Fla)* 2013; **25**(23): 3144-76.
10. Tarn D, Ashley CE, Xue M, Carnes EC, Zink JI, Brinker CJ. Mesoporous silica nanoparticle nanocarriers: biofunctionality and biocompatibility. *Acc Chem Res* 2013; **46**(3): 792-801.

11. Ngamcherdtrakul W, Sangvanich T, Reda M, Gu S, Bejan D, Yantasee W. Lyophilization and stability of antibody-conjugated mesoporous silica nanoparticle with cationic polymer and PEG for siRNA delivery. *Int J Nanomedicine* 2018; **13**: 4015-27.
12. Tang F, Li L, Chen D. Mesoporous silica nanoparticles: synthesis, biocompatibility and drug delivery. *Advanced materials (Deerfield Beach, Fla)* 2012; **24**(12): 1504-34.
13. Wang J-s, Wang H-j, Qian H-l. Biological effects of radiation on cancer cells. *Military Medical Research* 2018; **5**(1): 20.
14. Diwanji TP, Mohindra P, Vyfhuis M, et al. Advances in radiotherapy techniques and delivery for non-small cell lung cancer: benefits of intensity-modulated radiation therapy, proton therapy, and stereotactic body radiation therapy. *Translational Lung Cancer Research* 2017; **6**(2): 131-47.
15. Bradley JD, Paulus R, Komaki R, Masters G, Blumenschein G, Schild S. Standard-dose versus high-dose conformal radiotherapy with concurrent and consolidation carboplatin plus paclitaxel with or without cetuximab for patients with stage IIIA or IIIB non-small-cell lung cancer (RTOG 0617): a randomized, two-by-two factorial phase 3 study. *The Lancet Oncology* 2015; **16**.
16. Oehler C, Dickinson DJ, Broggin-Tenzer A, et al. Current concepts for the combined treatment modality of ionizing radiation with anticancer agents. *Current pharmaceutical design* 2007; **13**(5): 519-35.
17. Steel GG, McMillan TJ, Peacock JH. The 5Rs of radiobiology. *International journal of radiation biology* 1989; **56**(6): 1045-8.
18. Pajonk F, Vlashi E, McBride WH. Radiation resistance of cancer stem cells: the 4 R's of radiobiology revisited. *Stem cells (Dayton, Ohio)* 2010; **28**(4): 639-48.
19. Ewing D. The oxygen fixation hypothesis: a reevaluation. *American journal of clinical oncology* 1998; **21**(4): 355-61.

20. Ogawa Y, Kubota K, Ue H, et al. Safety and effectiveness of a new enzyme-targeting radiosensitization treatment (KORTUC II) for intratumoral injection for low-LET radioresistant tumors. *International journal of oncology* 2011; **39**(3): 553-60.
21. Wang H, Mu X, He H, Zhang XD. Cancer Radiosensitizers. *Trends Pharmacol Sci* 2018; **39**(1): 24-48.
22. Golden EB, Formenti SC, Schiff PB. Taxanes as radiosensitizers. *Anti-cancer drugs* 2014; **25**(5): 502-11.
23. Kvols LK. Radiation sensitizers: a selective review of molecules targeting DNA and non-DNA targets. *Journal of nuclear medicine : official publication, Society of Nuclear Medicine* 2005; **46 Suppl 1**: 187s-90s.
24. Schaefer D, McBride WH. Opportunities and challenges of radiotherapy for treating cancer. *Nat Rev Clin Oncol* 2015; **12**(9): 527-40.
25. Ahmad SS, Crittenden MR, Tran PT, et al. Clinical Development of Novel Drug-Radiotherapy Combinations. *Clin Cancer Res* 2019; **25**(5): 1455-61.
26. Morris ZS, Harari PM. Interaction of radiation therapy with molecular targeted agents. *J Clin Oncol* 2014; **32**(26): 2886-93.
27. Seshacharyulu P, Ponnusamy MP, Haridas D, Jain M, Ganti AK, Batra SK. Targeting the EGFR signaling pathway in cancer therapy. *Expert opinion on therapeutic targets* 2012; **16**(1): 15-31.
28. Lee HC, An S, Lee H, et al. Activation of epidermal growth factor receptor and its downstream signaling pathway by nitric oxide in response to ionizing radiation. *Molecular cancer research : MCR* 2008; **6**(6): 996-1002.
29. Chen DJ, Nirodi CS. The epidermal growth factor receptor: a role in repair of radiation-induced DNA damage. *Clin Cancer Res* 2007; **13**(22 Pt 1): 6555-60.

30. Bonner JA, Harari PM, Giralt J, et al. Radiotherapy plus Cetuximab for Squamous-Cell Carcinoma of the Head and Neck. *New England Journal of Medicine* 2006; **354**(6): 567-78.
31. Bradley JD, Paulus R, Komaki R, et al. Standard-dose versus high-dose conformal radiotherapy with concurrent and consolidation carboplatin plus paclitaxel with or without cetuximab for patients with stage IIIA or IIIB non-small-cell lung cancer (RTOG 0617): a randomised, two-by-two factorial phase 3 study. *The Lancet Oncology* 2015; **16**(2): 187-99.
32. Lesueur P, Chevalier F, Austry J-B, et al. Poly-(ADP-ribose)-polymerase inhibitors as radiosensitizers: a systematic review of pre-clinical and clinical human studies. *Oncotarget* 2017; **8**(40): 69105-24.
33. Kunz-Schughart LA, Dubrovskaja A, Peitzsch C, et al. Nanoparticles for radiooncology: Mission, vision, challenges. *Biomaterials* 2017; **120**: 155-84.
34. Lord CJ, Ashworth A. PARP inhibitors: Synthetic lethality in the clinic. *Science (New York, NY)* 2017; **355**(6330): 1152-8.
35. Bi Y, Verginadis II, Dey S, et al. Radiosensitization by the PARP inhibitor olaparib in BRCA1-proficient and deficient high-grade serous ovarian carcinomas. *Gynecologic Oncology* 2018; **150**(3): 534-44.
36. Li Y, Seto E. HDACs and HDAC Inhibitors in Cancer Development and Therapy. *Cold Spring Harbor perspectives in medicine*; **6**(10): a026831.
37. Konsoula Z, Velena A, Lee R, Dritschilo A, Jung M. Histone deacetylase inhibitor: antineoplastic agent and radiation modulator. *Advances in experimental medicine and biology* 2011; **720**: 171-9.
38. Seo SK, Jin HO, Woo SH, et al. Histone deacetylase inhibitors sensitize human non-small cell lung cancer cells to ionizing radiation through acetyl p53-mediated c-myc

- down-regulation. *Journal of thoracic oncology : official publication of the International Association for the Study of Lung Cancer* 2011; **6**(8): 1313-9.
39. Chinnaiyan P, Vallabhaneni G, Armstrong E, Huang SM, Harari PM. Modulation of radiation response by histone deacetylase inhibition. *Int J Radiat Oncol Biol Phys* 2005; **62**(1): 223-9.
  40. Tsai CL, Liu WL, Hsu FM, et al. Targeting histone deacetylase 4/ubiquitin-conjugating enzyme 9 impairs DNA repair for radiosensitization of hepatocellular carcinoma cells in mice. *Hepatology (Baltimore, Md)* 2017.
  41. Kachhap SK, Rosmus N, Collis SJ, et al. Downregulation of homologous recombination DNA repair genes by HDAC inhibition in prostate cancer is mediated through the E2F1 transcription factor. *PloS one* 2010; **5**(6): e11208.
  42. Ren J, Chu Y, Ma H, et al. Epigenetic interventions increase the radiation sensitivity of cancer cells. *Current pharmaceutical design* 2014; **20**(11): 1857-65.
  43. Thurn KT, Thomas S, Raha P, Qureshi I, Munster PN. Histone deacetylase regulation of ATM-mediated DNA damage signaling. *Molecular cancer therapeutics* 2013; **12**(10): 2078-87.
  44. Shabason JE, Tofilon PJ, Camphausen K. Grand rounds at the National Institutes of Health: HDAC inhibitors as radiation modifiers, from bench to clinic. *Journal of cellular and molecular medicine* 2011; **15**(12): 2735-44.
  45. Johnstone RW. Histone-deacetylase inhibitors: novel drugs for the treatment of cancer. *Nature reviews Drug discovery* 2002; **1**(4): 287-99.
  46. Decker RH, Gettinger SN, Glazer PM, Wilson LD. Vorinostat, a Histone Deacetylase Inhibitor, in Combination with Thoracic Radiotherapy in Advanced Non-small Cell Lung Cancer: A Dose Escalation Study. *International Journal of Radiation Oncology • Biology • Physics* 2011; **81**(2): S574-S5.



47. Wang EC, Min Y, Palm RC, et al. Nanoparticle formulations of histone deacetylase inhibitors for effective chemoradiotherapy in solid tumors. *Biomaterials* 2015; **51**: 208-15.
48. Maréchal A, Zou L. DNA damage sensing by the ATM and ATR kinases. *Cold Spring Harbor perspectives in biology*; **5**(9): a012716.
49. Weber AM, Ryan AJ. ATM and ATR as therapeutic targets in cancer. *Pharmacol Ther* 2015; **149**: 124-38.
50. Taylor AMR, Harnden DG, Arlett CF, et al. Ataxia telangiectasia: a human mutation with abnormal radiation sensitivity. *Nature* 1975; **258**(5534): 427-9.
51. Teng P-n, Bateman NW, Darcy KM, et al. Pharmacologic inhibition of ATR and ATM offers clinically important distinctions to enhancing platinum or radiation response in ovarian, endometrial, and cervical cancer cells. *Gynecologic oncology* 2015; **136**(3): 554-61.
52. Dillon MT, Barker HE, Pedersen M, et al. Radiosensitization by the ATR Inhibitor AZD6738 through Generation of Acentric Micronuclei. *Molecular cancer therapeutics* 2017; **16**(1): 25-34.
53. Fresno Vara JA, Casado E, de Castro J, Cejas P, Belda-Iniesta C, Gonzalez-Baron M. PI3K/Akt signalling pathway and cancer. *Cancer treatment reviews* 2004; **30**(2): 193-204.
54. Schuurbiens OC, Kaanders JH, van der Heijden HF, Dekhuijzen RP, Oyen WJ, Bussink J. The PI3-K/AKT-pathway and radiation resistance mechanisms in non-small cell lung cancer. *Journal of thoracic oncology : official publication of the International Association for the Study of Lung Cancer* 2009; **4**(6): 761-7.
55. Li H-F, Kim J-S, Waldman T. Radiation-induced Akt activation modulates radioresistance in human glioblastoma cells. *Radiation oncology (London, England)* 2009; **4**: 43-.

56. Plastaras JP, Vapiwala N, Ahmed MS, et al. Validation and toxicity of PI3K/Akt pathway inhibition by HIV protease inhibitors in humans. *Cancer biology & therapy* 2008; **7**(5): 628-35.
57. Rengan R, Mick R, Pryma DA, et al. Long-term Results of a Phase I/II Trial of Nelfinavir with Concurrent Chemoradiotherapy for Locally Advanced Non-Small Cell Lung Cancer. *International Journal of Radiation Oncology • Biology • Physics* 2018; **102**(3): S19.
58. Porta C, Paglino C, Mosca A. Targeting PI3K/Akt/mTOR Signaling in Cancer. *Frontiers in oncology* 2014; **4**: 64-.
59. Nagata Y, Takahashi A, Ohnishi K, et al. Effect of rapamycin, an mTOR inhibitor, on radiation sensitivity of lung cancer cells having different p53 gene status. *International journal of oncology* 2010; **37**(4): 1001-10.
60. Schiewer MJ, Den R, Hoang DT, et al. mTOR is a selective effector of the radiation therapy response in androgen receptor-positive prostate cancer. *Endocrine-related cancer*, **19**(1): 1-12.
61. Deutsch E, Le Pechoux C, Faivre L, et al. Phase I trial of everolimus in combination with thoracic radiotherapy in non-small-cell lung cancer. *Annals of oncology : official journal of the European Society for Medical Oncology / ESMO* 2015; **26**(6): 1223-9.
62. Goel S, Duda DG, Xu L, et al. Normalization of the vasculature for treatment of cancer and other diseases. *Physiological reviews* 2011; **91**(3): 1071-121.
63. Willett CG, Kozin SV, Duda DG, et al. Combined vascular endothelial growth factor-targeted therapy and radiotherapy for rectal cancer: theory and clinical practice. *Seminars in oncology* 2006; **33**(5 Suppl 10): S35-S40.
64. Schmidt B, Lee H-J, Ryeom S, Yoon SS. Combining Bevacizumab with Radiation or Chemoradiation for Solid Tumors: A Review of the Scientific Rationale, and Clinical Trials. *Current angiogenesis* 2012; **1**(3): 169-79.

65. Chinot OL, Wick W, Mason W, et al. Bevacizumab plus Radiotherapy–Temozolomide for Newly Diagnosed Glioblastoma. *New England Journal of Medicine* 2014; **370**(8): 709-22.
66. Wozniak AJ, Moon J, Thomas CR, Jr., et al. A Pilot Trial of Cisplatin/Etoposide/Radiotherapy Followed by Consolidation Docetaxel and the Combination of Bevacizumab (NSC-704865) in Patients With Inoperable Locally Advanced Stage III Non-Small-Cell Lung Cancer: SWOG S0533. *Clinical lung cancer* 2015; **16**(5): 340-7.
67. Murata R, Nishimura Y, Hiraoka M. An antiangiogenic agent (TNP-470) inhibited reoxygenation during fractionated radiotherapy of murine mammary carcinoma. *Int J Radiat Oncol Biol Phys* 1997; **37**(5): 1107-13.
68. Zou W, Wolchok JD, Chen L. PD-L1 (B7-H1) and PD-1 pathway blockade for cancer therapy: Mechanisms, response biomarkers, and combinations. *Science Translational Medicine* 2016; **8**(328): 328rv4-rv4.
69. Buchbinder EI, Desai A. CTLA-4 and PD-1 Pathways: Similarities, Differences, and Implications of Their Inhibition. *American journal of clinical oncology* 2016; **39**(1): 98-106.
70. Patel SA, Minn AJ. Combination Cancer Therapy with Immune Checkpoint Blockade: Mechanisms and Strategies. *Immunity* 2018; **48**(3): 417-33.
71. Asna N, Livoff A, Batash R, et al. Radiation therapy and immunotherapy-a potential combination in cancer treatment. *Current oncology (Toronto, Ont)* 2018; **25**(5): e454-e60.
72. Vinay DS, Ryan EP, Pawelec G, et al. Immune evasion in cancer: Mechanistic basis and therapeutic strategies. *Seminars in cancer biology* 2015; **35 Suppl**: S185-98.
73. Wu AA, Drake V, Huang H-S, Chiu S, Zheng L. Reprogramming the tumor microenvironment: tumor-induced immunosuppressive factors paralyze T cells. *Oncoimmunology* 2015; **4**(7): e1016700-e.

74. Zou W. Immunosuppressive networks in the tumour environment and their therapeutic relevance. *Nature reviews Cancer* 2005; **5**(4): 263-74.
75. Joyce JA, Fearon DT. T cell exclusion, immune privilege, and the tumor microenvironment. *Science (New York, NY)* 2015; **348**(6230): 74-80.
76. Schiavoni G, Gabriele L, Mattei F. The tumor microenvironment: a pitch for multiple players. *Front Oncol* 2013; **3**: 90.
77. Whiteside TL. The tumor microenvironment and its role in promoting tumor growth. *Oncogene* 2008; **27**(45): 5904-12.
78. Ohaegbulam KC, Assal A, Lazar-Molnar E, Yao Y, Zang X. Human cancer immunotherapy with antibodies to the PD-1 and PD-L1 pathway. *Trends in molecular medicine* 2015; **21**(1): 24-33.
79. Shrimali RK, Janik JE, Abu-Eid R, Mkrtychyan M, Khleif SN. Programmed death-1 & its ligands: promising targets for cancer immunotherapy. *Immunotherapy* 2015; **7**(7): 777-92.
80. Reck M, Rodríguez-Abreu D, Robinson AG, et al. Pembrolizumab versus Chemotherapy for PD-L1–Positive Non–Small-Cell Lung Cancer. *New England Journal of Medicine* 2016; **375**(19): 1823-33.
81. Scott Gettinger M. Immunotherapy of advanced non-small cell lung cancer with immune checkpoint inhibition. Uptodate.com; 2018.
82. Jenkins RW, Barbie DA, Flaherty KT. Mechanisms of resistance to immune checkpoint inhibitors. *British journal of cancer* 2018; **118**: 9.
83. La-Beck NM, Jean GW, Huynh C, Alzghari SK, Lowe DB. Immune Checkpoint Inhibitors: New Insights and Current Place in Cancer Therapy. *Pharmacotherapy: The Journal of Human Pharmacology and Drug Therapy* 2015; **35**(10): 963-76.
84. Reynolds KL, Cohen JV, Ryan DP, et al. Severe immune-related adverse effects (irAE) requiring hospital admission in patients treated with immune checkpoint inhibitors for

- advanced malignancy: Temporal trends and clinical significance. *Journal of Clinical Oncology* 2018; **36**(15\_suppl): 3096-.
85. Moya-Horno I, Viteri S, Karachaliou N, Rosell R. Combination of immunotherapy with targeted therapies in advanced non-small cell lung cancer (NSCLC). *Therapeutic advances in medical oncology* 2018; **10**: 1758834017745012-.
86. Barr FA, Sillje HH, Nigg EA. Polo-like kinases and the orchestration of cell division. *Nat Rev Mol Cell Biol* 2004; **5**(6): 429-40.
87. Gutteridge RE, Ndiaye MA, Liu X, Ahmad N. Plk1 Inhibitors in Cancer Therapy: From Laboratory to Clinics. *Molecular cancer therapeutics* 2016; **15**(7): 1427-35.
88. Wang Y, Singh R, Wang L, et al. Polo-like kinase 1 inhibition diminishes acquired resistance to epidermal growth factor receptor inhibition in non-small cell lung cancer with T790M mutations. *Oncotarget* 2016; **7**(30): 47998-8010.
89. Francescangeli F, Patrizii M, Signore M, et al. Proliferation state and polo-like kinase1 dependence of tumorigenic colon cancer cells. *Stem cells (Dayton, Ohio)* 2012; **30**(9): 1819-30.
90. Danovi D, Folarin A, Gogolok S, et al. A high-content small molecule screen identifies sensitivity of glioblastoma stem cells to inhibition of polo-like kinase 1. *PloS one* 2013; **8**(10): e77053.
91. Hu K, Law JH, Fotovati A, Dunn SE. Small interfering RNA library screen identified polo-like kinase-1 (PLK1) as a potential therapeutic target for breast cancer that uniquely eliminates tumor-initiating cells. *Breast cancer research : BCR* 2012; **14**(1): R22.
92. Ando K, Ozaki T, Yamamoto H, et al. Polo-like kinase 1 (Plk1) inhibits p53 function by physical interaction and phosphorylation. *The Journal of biological chemistry* 2004; **279**(24): 25549-61.
93. McKenzie L, King S, Marcar L, et al. p53-dependent repression of polo-like kinase-1 (PLK1). *Cell cycle (Georgetown, Tex)* 2010; **9**(20): 4200-12.

94. Li Z, Li J, Bi P, et al. Plk1 phosphorylation of PTEN causes a tumor-promoting metabolic state. *Molecular and cellular biology* 2014; **34**(19): 3642-61.
95. Choi BH, Pagano M, Dai W. Plk1 protein phosphorylates phosphatase and tensin homolog (PTEN) and regulates its mitotic activity during the cell cycle. *The Journal of biological chemistry* 2014; **289**(20): 14066-74.
96. Dang CV. MYC on the path to cancer. *Cell* 2012; **149**(1): 22-35.
97. Chen H, Liu H, Qing G. Targeting oncogenic Myc as a strategy for cancer treatment. *Signal Transduction and Targeted Therapy* 2018; **3**(1): 5.
98. Tan J, Li Z, Lee PL, et al. PDK1 Signaling Toward PLK1–MYC Activation Confers Oncogenic Transformation, Tumor-Initiating Cell Activation, and Resistance to mTOR-Targeted Therapy. *Cancer Discovery* 2013; **3**(10): 1156-71.
99. Padmanabhan A, Li X, Bieberich CJ. Protein kinase A regulates MYC protein through transcriptional and post-translational mechanisms in a catalytic subunit isoform-specific manner. *The Journal of biological chemistry* 2013; **288**(20): 14158-69.
100. Gemenetzidis E, Elena-Costea D, Parkinson EK, Waseem A, Wan H, Teh M-T. Induction of Human Epithelial Stem/Progenitor Expansion by FOXM1. *Cancer research* 2010; **70**(22): 9515-26.
101. Liao G-B, Li X-Z, Zeng S, et al. Regulation of the master regulator FOXM1 in cancer. *Cell communication and signaling : CCS* 2018; **16**(1): 57-.
102. Fu Z, Malureanu L, Huang J, et al. Plk1-dependent phosphorylation of FoxM1 regulates a transcriptional programme required for mitotic progression. *Nature Cell Biology* 2008; **10**: 1076.
103. Chabaliere-Taste C, Brichese L, Racca C, Canitrot Y, Calsou P, Larminat F. Polo-like kinase 1 mediates BRCA1 phosphorylation and recruitment at DNA double-strand breaks. *Oncotarget* 2016; **7**(3): 2269-83.

104. Yata K, Lloyd J, Maslen S, et al. Plk1 and CK2 act in concert to regulate Rad51 during DNA double strand break repair. *Molecular cell* 2012; **45**(3): 371-83.
105. Ayob AZ, Ramasamy TS. Cancer stem cells as key drivers of tumour progression. *Journal of Biomedical Science* 2018; **25**(1): 20.
106. Kim Y, Joo KM, Jin J, Nam D-H. Cancer stem cells and their mechanism of chemo-radiation resistance. *International journal of stem cells* 2009; **2**(2): 109-14.
107. Rycaj K, Tang DG. Cancer stem cells and radioresistance. *International journal of radiation biology* 2014; **90**(8): 615-21.
108. Yao D, Gu P, Wang Y, et al. Inhibiting polo-like kinase 1 enhances radiosensitization via modulating DNA repair proteins in non-small-cell lung cancer. *Biochemistry and cell biology = Biochimie et biologie cellulaire* 2018; **96**(3): 317-25.
109. Li M, Liu Z, Wang X. Exploration of the Combination of PLK1 Inhibition with Immunotherapy in Cancer Treatment. *Journal of oncology* 2018; **2018**: 3979527-.
110. Kortylewski M, Yu H. Role of Stat3 in suppressing anti-tumor immunity. *Current opinion in immunology* 2008; **20**(2): 228-33.
111. Zhang Y, Du XL, Wang CJ, et al. Reciprocal activation between PLK1 and Stat3 contributes to survival and proliferation of esophageal cancer cells. *Gastroenterology* 2012; **142**(3): 521-30.e3.
112. Yan W, Yu H, Li W, et al. Plk1 promotes the migration of human lung adenocarcinoma epithelial cells via STAT3 signaling. *Oncology letters* 2018; **16**(5): 6801-7.
113. Gringhuis SI, Hertoghs N, Kaptein TM, et al. HIV-1 blocks the signaling adaptor MAVS to evade antiviral host defense after sensing of abortive HIV-1 RNA by the host helicase DDX3. *Nature immunology* 2017; **18**(2): 225-35.
114. Vitour D, Dabo S, Ahmadi Pour M, et al. Polo-like kinase 1 (PLK1) regulates interferon (IFN) induction by MAVS. *The Journal of biological chemistry* 2009; **284**(33): 21797-809.

115. Gjertsen BT, Schoffski P. Discovery and development of the Polo-like kinase inhibitor volasertib in cancer therapy. *Leukemia* 2015; **29**(1): 11-9.
116. Raab M, Kappel S, Krämer A, et al. Toxicity modelling of Plk1-targeted therapies in genetically engineered mice and cultured primary mammalian cells. *Nature Communications* 2011; **2**: 395.
117. Ingelheim B. Results of Phase III study of volasertib for the treatment of acute myeloid leukemia presented at European Hematology Association Annual Meeting. Ridgefield, Conn.; 2016.
118. Ellis PM, Leighl NB, Hirsh V, et al. A Randomized, Open-Label Phase II Trial of Volasertib as Monotherapy and in Combination With Standard-Dose Pemetrexed Compared With Pemetrexed Monotherapy in Second-Line Treatment for Non-Small-Cell Lung Cancer. *Clinical lung cancer* 2015; **16**(6): 457-65.
119. Gu S, Hu Z, Ngamcherdtrakul W, et al. Therapeutic siRNA for drug-resistant HER2-positive breast cancer. *Oncotarget* 2016; **7**(12): 14727-41.
120. Gu S, Ngamcherdtrakul W, Reda M, Hu Z, Gray JW, Yantasee W. Lack of acquired resistance in HER2-positive breast cancer cells after long-term HER2 siRNA nanoparticle treatment. *PloS one* 2018; **13**(6): e0198141.
121. Arbutus. Arbutus Reports Topline Results from TKM-PLK1 HCC Clinical Trial. VANCOUVER, BC and DOYLESTOWN, PA: GLOBE NEWSWIRE 2016.
122. Demeure MJ, Armaghany T, Ejadi S, et al. A phase I/II study of TKM-080301, a PLK1-targeted RNAi in patients with adrenocortical cancer (ACC). *Journal of Clinical Oncology* 2016; **34**(15\_suppl): 2547-.
123. Rosenblum D, Joshi N, Tao W, Karp JM, Peer D. Progress and challenges towards targeted delivery of cancer therapeutics. *Nature communications* 2018; **9**(1): 1410.
124. Golombek SK, May J-N, Theek B, et al. Tumor targeting via EPR: Strategies to enhance patient responses. *Advanced drug delivery reviews* 2018; **130**: 17-38.



125. Thakor AS, Gambhir SS. Nanooncology: The future of cancer diagnosis and therapy. *CA: A Cancer Journal for Clinicians* 2013; **63**(6): 395-418.
126. Zhang X-D, Luo Z, Chen J, et al. Ultrasmall Glutathione-Protected Gold Nanoclusters as Next Generation Radiotherapy Sensitizers with High Tumor Uptake and High Renal Clearance. *Scientific reports* 2015; **5**: 8669.
127. Liang G, Jin X, Zhang S, Xing D. RGD peptide-modified fluorescent gold nanoclusters as highly efficient tumor-targeted radiotherapy sensitizers. *Biomaterials* 2017; **144**: 95-104.
128. Bobo D, Robinson KJ, Islam J, Thurecht KJ, Corrie SR. Nanoparticle-Based Medicines: A Review of FDA-Approved Materials and Clinical Trials to Date. *Pharmaceutical research* 2016; **33**(10): 2373-87.
129. Karve S, Werner ME, Sukumar R, et al. Revival of the abandoned therapeutic wortmannin by nanoparticle drug delivery. *Proc Natl Acad Sci U S A* 2012; **109**(21): 8230-5.
130. Kievit FM, Wang K, Ozawa T, et al. Nanoparticle-mediated knockdown of DNA repair sensitizes cells to radiotherapy and extends survival in a genetic mouse model of glioblastoma. *Nanomedicine : nanotechnology, biology, and medicine* 2017; **13**(7): 2131-9.
131. Kranz LM, Diken M, Haas H, et al. Systemic RNA delivery to dendritic cells exploits antiviral defence for cancer immunotherapy. *Nature* 2016; **534**(7607): 396-401.
132. Kuai R, Ochyl LJ, Bahjat KS, Schwendeman A, Moon JJ. Designer vaccine nanodiscs for personalized cancer immunotherapy. *Nature Materials* 2016; **16**: 489.
133. Zhu G, Mei L, Vishwasrao HD, et al. Intertwining DNA-RNA nanocapsules loaded with tumor neoantigens as synergistic nanovaccines for cancer immunotherapy. *Nature communications* 2017; **8**(1): 1482.

134. Schmid D, Park CG, Hartl CA, et al. T cell-targeting nanoparticles focus delivery of immunotherapy to improve antitumor immunity. *Nature communications* 2017; **8**(1): 1747.
135. Mi Y, Smith CC, Yang F, et al. A Dual Immunotherapy Nanoparticle Improves T-Cell Activation and Cancer Immunotherapy. *Advanced materials (Deerfield Beach, Fla)* 2018; **30**(25): e1706098.
136. Kosmidis AK, Sidhom JW, Fraser A, Bessell CA, Schneck JP. Dual Targeting Nanoparticle Stimulates the Immune System To Inhibit Tumor Growth. *ACS Nano* 2017; **11**(6): 5417-29.
137. Chiang C-S, Lin Y-J, Lee R, et al. Combination of fucoidan-based magnetic nanoparticles and immunomodulators enhances tumour-localized immunotherapy. *Nature Nanotechnology* 2018; **13**(8): 746-54.
138. Meir R, Shamalov K, Sadan T, et al. Fast Image-Guided Stratification Using Anti-Programmed Death Ligand 1 Gold Nanoparticles for Cancer Immunotherapy. *ACS Nano* 2017; **11**(11): 11127-34.
139. Xu S, Cui F, Huang D, et al. PD-L1 monoclonal antibody-conjugated nanoparticles enhance drug delivery level and chemotherapy efficacy in gastric cancer cells. *International journal of nanomedicine* 2018; **14**: 17-32.
140. Emami F, Banstola A, Vatanara A, et al. Doxorubicin and Anti-PD-L1 Antibody Conjugated Gold Nanoparticles for Colorectal Cancer Photochemotherapy. *Mol Pharm* 2019; **16**(3): 1184-99.
141. Schmid P, Adams S, Rugo HS, et al. Atezolizumab and Nab-Paclitaxel in Advanced Triple-Negative Breast Cancer. *N Engl J Med* 2018; **379**(22): 2108-21.
142. Lorenzer C, Dirin M, Winkler AM, Baumann V, Winkler J. Going beyond the liver: progress and challenges of targeted delivery of siRNA therapeutics. *Journal of controlled release : official journal of the Controlled Release Society* 2015; **203**: 1-15.

143. Ngamcherdtrakul W, Castro DJ, Gu S, et al. Current development of targeted oligonucleotide-based cancer therapies: Perspective on HER2-positive breast cancer treatment. *Cancer treatment reviews* 2016; **45**: 19-29.
144. Zuckerman JE, Davis ME. Clinical experiences with systemically administered siRNA-based therapeutics in cancer. *Nature Reviews Drug Discovery* 2015; **14**: 843.
145. Ozcan G, Ozpolat B, Coleman RL, Sood AK, Lopez-Berestein G. Preclinical and clinical development of siRNA-based therapeutics. *Advanced drug delivery reviews* 2015; **87**: 108-19.
146. Ehlerding EB, Chen F, Cai W. Biodegradable and Renal Clearable Inorganic Nanoparticles. *Advanced science (Weinheim, Baden-Wurttemberg, Germany)* 2016; **3**(2).
147. Kempen PJ, Greasley S, Parker KA, et al. Theranostic Mesoporous Silica Nanoparticles Biodegrade after Pro-Survival Drug Delivery and Ultrasound/Magnetic Resonance Imaging of Stem Cells. *Theranostics* 2015; **5**(6): 631-42.
148. Sripanyakorn S, Jugdaohsingh R, Thompson RPH, Powell JJ. Dietary silicon and bone health. *Nutrition Bulletin* 2005; **30**(3): 222-30.
149. Phillips E, Penate-Medina O, Zanzonico PB, et al. Clinical translation of an ultrasmall inorganic optical-PET imaging nanoparticle probe. *Science Translational Medicine* 2014; **6**(260): 260ra149-260ra149.
150. Stern JM, Kibanov Solomonov VV, Sazykina E, Schwartz JA, Gad SC, Goodrich GP. Initial Evaluation of the Safety of Nanoshell-Directed Photothermal Therapy in the Treatment of Prostate Disease. *International journal of toxicology* 2016; **35**(1): 38-46.
151. Ngamcherdtrakul W, Morry J, Gu S, et al. Cationic Polymer Modified Mesoporous Silica Nanoparticles for Targeted SiRNA Delivery to HER2+ Breast Cancer. *Advanced functional materials* 2015; **25**(18): 2646-59.

152. Ngamcherdtrakul W, Sangvanich T, Reda M, Gu S, Bejan D, Yantasee W. Lyophilization and stability of antibody-conjugated mesoporous silica nanoparticle with cationic polymer and PEG for siRNA delivery. *International journal of nanomedicine* 2018; **13**: 4015-27.
153. Yantasee W, Gray JW, Ngamcherdtrakul W. Novel siRNA-nanoparticle platform for treating drug resistant HER2 positive breast cancer. Final Report to the National Cancer Institute (NCI) for the Phase II SBIR Contract # HHSN261201300078C to PDX Pharmaceuticals in collaboration with the BME of OHSU; September 9, 2016.
154. Miller KD, Siegel RL, Lin CC, et al. Cancer treatment and survivorship statistics, 2016. *CA: A Cancer Journal for Clinicians* 2016; **66**(4): 271-89.
155. Baker S, Dahele M, Lagerwaard FJ, Senan S. A critical review of recent developments in radiotherapy for non-small cell lung cancer. *Radiation Oncology* 2016; **11**(1): 115.
156. Morry J, Ngamcherdtrakul W, Gu S, et al. Targeted treatment of metastatic breast cancer by PLK1 siRNA delivered by an antioxidant nanoparticle platform. *Molecular cancer therapeutics* 2017: DOI: 10.1158/535-7163.mct-16-0644.
157. Cheng MW, Wang BC, Weng ZQ, Zhu XW. Clinicopathological significance of Polo-like kinase 1 (PLK1) expression in human malignant glioma. *Acta histochemica* 2012; **114**(5): 503-9.
158. Knecht R, Elez R, Oechler M, Solbach C, von Ilberg C, Strebhardt K. Prognostic significance of polo-like kinase (PLK) expression in squamous cell carcinomas of the head and neck. *Cancer research* 1999; **59**(12): 2794-7.
159. Inoue M, Yoshimura M, Kobayashi M, et al. PLK1 blockade enhances therapeutic effects of radiation by inducing cell cycle arrest at the mitotic phase. *Scientific reports* 2015; **5**: 15666.
160. Selvaggi G, Novello S, Torri V, et al. Epidermal growth factor receptor overexpression correlates with a poor prognosis in completely resected non-small-cell lung cancer.

*Annals of oncology : official journal of the European Society for Medical Oncology / ESMO* 2004; **15**(1): 28-32.

161. Gonzalez-Conchas GA, Rodriguez-Romo L, Hernandez-Barajas D, et al. Epidermal growth factor receptor overexpression and outcomes in early breast cancer: A systematic review and a meta-analysis. *Cancer treatment reviews* 2018; **62**: 1-8.
162. Alterio D, Marvaso G, Maffini F, et al. Role of EGFR as prognostic factor in head and neck cancer patients treated with surgery and postoperative radiotherapy: proposal of a new approach behind the EGFR overexpression. *Medical oncology (Northwood, London, England)* 2017; **34**(6): 107.
163. Galizia G, Lieto E, Ferraraccio F, et al. Prognostic significance of epidermal growth factor receptor expression in colon cancer patients undergoing curative surgery. *Annals of surgical oncology* 2006; **13**(6): 823-35.
164. Nakamura H, Kawasaki N, Taguchi M, Kabasawa K. Survival impact of epidermal growth factor receptor overexpression in patients with non-small cell lung cancer: a meta-analysis. *Thorax* 2006; **61**(2): 140-5.
165. Fujino S, Enokibori T, Tezuka N, et al. A comparison of epidermal growth factor receptor levels and other prognostic parameters in non-small cell lung cancer. *European Journal of Cancer* 1996; **32**(12): 2070-4.
166. Nyati MK, Morgan MA, Feng FY, Lawrence TS. Integration of EGFR inhibitors with radiochemotherapy. *Nature reviews Cancer* 2006; **6**(11): 876-85.
167. Bonner JA, Harari PM, Giralt J, et al. Radiotherapy plus cetuximab for locoregionally advanced head and neck cancer: 5-year survival data from a phase 3 randomised trial, and relation between cetuximab-induced rash and survival. *The Lancet Oncology* 2010; **11**(1): 21-8.
168. Bradley JD, Paulus R, Komaki R, et al. Standard-dose versus high-dose conformal radiotherapy with concurrent and consolidation carboplatin plus paclitaxel with or without

- cetuximab for patients with stage IIIA or IIIB non-small-cell lung cancer (RTOG 0617): a randomised, two-by-two factorial phase 3 study. *The Lancet Oncology*; **16**(2): 187-99.
169. Franken NA, Rodermond HM, Stap J, Haveman J, van Bree C. Clonogenic assay of cells in vitro. *Nature protocols* 2006; **1**(5): 2315-9.
170. Altemeier WA, Matute-Bello G, Gharib SA, Glenn RW, Martin TR, Liles WC. Modulation of lipopolysaccharide-induced gene transcription and promotion of lung injury by mechanical ventilation. *Journal of immunology (Baltimore, Md : 1950)* 2005; **175**(5): 3369-76.
171. Pawlik TM, Keyomarsi K. Role of cell cycle in mediating sensitivity to radiotherapy. *Int J Radiat Oncol Biol Phys* 2004; **59**(4): 928-42.
172. Chou TC. Drug combination studies and their synergy quantification using the Chou-Talalay method. *Cancer Res* 2010; **70**(2): 440-6.
173. Sharma A, Singh K, Almasan A. Histone H2AX phosphorylation: a marker for DNA damage. *Methods in molecular biology (Clifton, NJ)* 2012; **920**: 613-26.
174. Wang H, Mu X, He H, Zhang X-D. Cancer Radiosensitizers. *Trends in Pharmacological Sciences* 2018; **39**(1): 24-48.
175. Ahmad SS, Crittenden MR, Tran PT, et al. Clinical Development of Novel Drug-Radiotherapy Combinations. *Clinical Cancer Research* 2018: clincanres.2466.018.
176. Fennell DA, Summers Y, Cadranel J, et al. Cisplatin in the modern era: The backbone of first-line chemotherapy for non-small cell lung cancer. *Cancer treatment reviews* 2016; **44**: 42-50.
177. Maione P, Sacco PC, Sgambato A, Casaluce F, Rossi A, Gridelli C. Overcoming resistance to targeted therapies in NSCLC: current approaches and clinical application. *Therapeutic advances in medical oncology* 2015; **7**(5): 263-73.
178. Reck M, Rodríguez-Abreu D, Robinson AG, et al. Pembrolizumab versus Chemotherapy for PD-L1–Positive Non–Small-Cell Lung Cancer. 2016; **375**(19): 1823-33.

179. Cancer Genome Atlas Research N. Comprehensive molecular profiling of lung adenocarcinoma. *Nature* 2014; **511**(7511): 543-50.
180. Yewale C, Baradia D, Vhora I, Patil S, Misra A. Epidermal growth factor receptor targeting in cancer: A review of trends and strategies. *Biomaterials* 2013; **34**(34): 8690-707.
181. Cenicerros L, Aristu J, Castanon E, et al. Stereotactic body radiotherapy (SBRT) for the treatment of inoperable stage I non-small cell lung cancer patients. *Clinical & translational oncology : official publication of the Federation of Spanish Oncology Societies and of the National Cancer Institute of Mexico* 2016; **18**(3): 259-68.
182. de Braud F, Cascinu S, Spitaleri G, et al. A phase I, dose-escalation study of volasertib combined with nintedanib in advanced solid tumors. *Annals of oncology : official journal of the European Society for Medical Oncology / ESMO* 2015; **26**(11): 2341-6.
183. Schoffski P, Awada A, Dumez H, et al. A phase I, dose-escalation study of the novel Polo-like kinase inhibitor volasertib (BI 6727) in patients with advanced solid tumours. *European journal of cancer (Oxford, England : 1990)* 2012; **48**(2): 179-86.
184. Lin CC, Su WC, Yen CJ, et al. A phase I study of two dosing schedules of volasertib (BI 6727), an intravenous polo-like kinase inhibitor, in patients with advanced solid malignancies. *British journal of cancer* 2014; **110**(10): 2434-40.
185. Frost A, Mross K, Steinbild S, et al. Phase i study of the Plk1 inhibitor BI 2536 administered intravenously on three consecutive days in advanced solid tumours. *Current oncology (Toronto, Ont)* 2012; **19**(1): e28-35.
186. Blanco E, Shen H, Ferrari M. Principles of nanoparticle design for overcoming biological barriers to drug delivery. *Nature biotechnology* 2015; **33**(9): 941-51.
187. Gutteridge REA, Ndiaye MA, Liu X, Ahmad N. Plk1 Inhibitors in Cancer Therapy: From Laboratory to Clinics. *Molecular cancer therapeutics* 2016; **15**(7): 1427-35.

188. Malhotra J, Jabbour SK, Aisner J. Current state of immunotherapy for non-small cell lung cancer. *Translational lung cancer research* 2017; **6**(2): 196-211.
189. Kanwal B, Biswas S, Seminara RS, Jeet C. Immunotherapy in Advanced Non-small Cell Lung Cancer Patients: Ushering Chemotherapy Through the Checkpoint Inhibitors? *Cureus* 2018; **10**(9): e3254-e.
190. Zhang J, Bu X, Wang H, et al. Cyclin D-CDK4 kinase destabilizes PD-L1 via cullin 3-SPOP to control cancer immune surveillance. *Nature* 2018; **553**(7686): 91-5.
191. McCarroll JA, Dwarte T, Baigude H, et al. Therapeutic targeting of polo-like kinase 1 using RNA-interfering nanoparticles (iNOPs) for the treatment of non-small cell lung cancer. *Oncotarget* 2015; **6**(14): 12020-34.
192. Chen L, Gibbons DL, Goswami S, et al. Metastasis is regulated via microRNA-200/ZEB1 axis control of tumour cell PD-L1 expression and intratumoral immunosuppression. *Nature communications* 2014; **5**: 5241.
193. Peng J, Hamanishi J, Matsumura N, et al. Chemotherapy Induces Programmed Cell Death-Ligand 1 Overexpression via the Nuclear Factor-kappaB to Foster an Immunosuppressive Tumor Microenvironment in Ovarian Cancer. *Cancer research* 2015; **75**(23): 5034-45.
194. Jiao S, Xia W, Yamaguchi H, et al. PARP Inhibitor Upregulates PD-L1 Expression and Enhances Cancer-Associated Immunosuppression. *Clin Cancer Res* 2017; **23**(14): 3711-20.
195. Esteva FJ, Hubbard-Lucey VM, Tang J, Pusztai L. Immunotherapy and targeted therapy combinations in metastatic breast cancer. *The Lancet Oncology* 2019; **20**(3): e175-e86.
196. Campbell JD, Alexandrov A, Kim J, et al. Distinct patterns of somatic genome alterations in lung adenocarcinomas and squamous cell carcinomas. *Nature genetics* 2016; **48**(6): 607-16.



197. Rizvi NA, Hellmann MD, Snyder A, et al. Mutational landscape determines sensitivity to PD-1 blockade in non–small cell lung cancer. *Science (New York, NY)* 2015; **348**(6230): 124-8.
198. Tang C, Welsh JW, de Groot P, et al. Ipilimumab with Stereotactic Ablative Radiation Therapy: Phase I Results and Immunologic Correlates from Peripheral T Cells. *Clin Cancer Res* 2017; **23**(6): 1388-96.